AD_____

Award Number: DAMD17-00-1-0319

TITLE: Isolation of Estrogen-Responsive Genes in Human Breast Cancer Cells

PRINCIPAL INVESTIGATOR: James R. Davie, Ph.D.

CONTRACTING ORGANIZATION: University of Manitoba
Winnipeg, Manitoba, Canada R3E-OW3

REPORT DATE: October 2003

TYPE OF REPORT: Final

PREPARED FOR: U.S. Army Medical Research and Materiel Command
Fort Detrick, Maryland 21702-5012

DISTRIBUTION STATEMENT: Approved for Public Release;
Distribution Unlimited

The views, opinions and/or findings contained in this report are those of the author(s) and should not be construed as an official Department of the Army position, policy or decision unless so designated by other documentation.

REPORT DOCUMENTATION PAGE

Form Approved
OMB No. 074-0188

1. AGENCY USE ONLY (Leave blank)	2. REPORT DATE	3. REPORT TYPE AND DATES COVERED
	October 2003	Final (1 Sep 2000 - 1 Sep 2003)

4. TITLE AND SUBTITLE
Isolation of Estrogen-Responsive Genes in Human Breast Cancer Cells

5. FUNDING NUMBERS
DAMD17-00-1-0319

6. AUTHOR(S)
James R. Davie, Ph.D.

7. PERFORMING ORGANIZATION NAME(S) AND ADDRESS(ES)
University of Manitoba
Winnipeg, Manitoba, Canada R3E-OW3

E-Mail: davie@cc.umanitoba.ca

8. PERFORMING ORGANIZATION REPORT NUMBER

9. SPONSORING / MONITORING AGENCY NAME(S) AND ADDRESS(ES)
U.S. Army Medical Research and Materiel Command
Fort Detrick, Maryland 21702-5012

10. SPONSORING / MONITORING AGENCY REPORT NUMBER

11. SUPPLEMENTARY NOTES
Original contains color plates: ALL DTIC reproductions will be in black and white

12a. DISTRIBUTION / AVAILABILITY STATEMENT
Approved for Public Release; Distribution Unlimited

12b. DISTRIBUTION CODE

13. ABSTRACT (Maximum 200 Words)

The purpose of this proposal is to isolate and identify estrogen-receptor (ER)-bound DNA in human breast cancer cells using the chromatin immunoprecipitation (ChIP) protocol. Two cross-linking reagents were tested in ChIP. Cisplatin cross-links protein to DNA, and formaldehyde cross-links protein to DNA and protein to protein. ER-bound DNA has been isolated using ChIP from formaldehyde cross-linked human breast cancer MCF7 (T5) cells (ER positive and hormone dependent). Southern blotting analysis shows that ER-DNA contains ER-responsive genes (ER, PR, pS2 and *c-myc*). ER-bound DNA from T5 cells treated with estradiol (E2) for 30, 60 and 120 min were isolated and analyzed by PCR. PCR analysis demonstrated that ER-DNA contains pS2 gene promoter, which is expressed in ER positive cells. An ER-bound DNA library from formaldehyde cross-linked T5 cells has been constructed. ChIP-ER-DNA were cloned, sequenced after pre-screening, and blast searched in GenBank. Approximately two thousand positive colonies were collected from this library, and 100 more cloned DNA were sequenced. A ½(ERE)-Sp1 sequence has been identified in PACE4 (pro-protein convertase) and EWS (Ewing's sarcoma) genes. Northern blotting and RT-PCR analyses show that PACE4 is down-regulated, but EWS is not, by estradiol.

14. SUBJECT TERMS
Estrogen-responsive genes, Estrogen Receptor, Chromatin Immunoprecipitation, Molecular Biology

15. NUMBER OF PAGES
95

16. PRICE CODE

17. SECURITY CLASSIFICATION OF REPORT	18. SECURITY CLASSIFICATION OF THIS PAGE	19. SECURITY CLASSIFICATION OF ABSTRACT	20. LIMITATION OF ABSTRACT
Unclassified	Unclassified	Unclassified	Unlimited

Table of Contents

INTRODUCTION

The goal of this research is to isolate and identify the estrogen receptor (ER) associated genes in human breast cancer cells. Approximately 60% of ER positive human breast tumors need estrogen to grow, and the need for estrogen corresponds to the presence of the estrogen receptor in the tumor. ER is a transcription factor that binds directly or indirectly to regulatory regions of estrogen responsive genes. In the presence of estradiol (E2), ER dimerizes and binds to estrogen response elements (ERE) to turn on or turn off the expression of the genes, which are required in order for breast cancer cells to proliferate (Luqmani et al., 1989; Berry et al., 1989). A number of estrogen-inducible genes, such as cathepsin D and c-fos genes, have ER binding to DNA with help from another transcription factor Sp1 (Krishnan et al., 1994; Safe, 2001; Duan et al., 1998). In some cases, ER operates through Sp1 without binding to DNA (Xie et al., 1999; Duan et al., 1998; Dubik and Shiu, 1992).

Recently, a number of ER responsive genes in breast cancer cells and carcinoma have been identified by cDNA microarrays, suppression subtractive hybridization (SSH), serial analysis of gene expression (SAGE) and cDNA subtraction analysis (Kuang et al., 1998; Yang et al., 1999; Charpentier et al., 2000). However, all of the reported ER-responsive genes are based on the observed increase of their respective mRNA levels, a result of transcriptional activation directly or indirectly by ER. In this study, we used a chromatin immunoprecipitation (ChIP) strategy to isolate ER-bound genomic DNA fragments *in situ*, where ER plays a role not only as an activator or a repressor, but perhaps also in chromatin structure.

Two different procedures were used to cross-link ER to DNA. Cis-diamminedichloroplatinum (cisplatin) can directly cross-link ER to DNA (Zamble and Lippard, 1995; Olinski et al., 1987; Samuel et al., 1998), while formaldehyde can directly and indirectly cross-link ER to DNA (Wrenn and Katzenellenbogen, 1990; Dedon et al., 1991; Orlando et al., 1997). ER-DNA from ChIP was ligated into a vector and was used to construct an ER-bound genomic DNA library. Approximately two thousand ChIP's DNA clones were obtained, over seven hundred clones were pre-screened for previously sequenced clones and one hundred clones were sequenced. Blast search from GenBank was performed to identify DNA sequences that were bound to ER *in situ*. Several genes in the ER-bound DNA library have been identified and listed.

Two clones contained a sequence approximately 1000 base pairs downstream of exon 17 of PACE 4 gene. A ½(ERE)-Sp1 sequence, which contains a ½(ERE) (GGTAA) and a Sp1 binding sequence (GCGGCAGGG), was found in this region. PACE 4 is a mammalian pro-protein convertase family member that plays an important role in tumorigenesis (Cheng et al., 1997; Bassi et al., 2000). An analysis of breast tumors revealed that PACE4 is primarily expressed in ER positive but not ER negative breast epithelial cancer cells (Cheng et al., 1997). The results of Northern blotting analysis and RT-PCR show that PACE4 is down regulated after 30 min treatment of estradiol in MCF7(T5) cells. EWS (Ewing's sarcoma) gene, a member of the TET family of RNA-binding proteins, is commonly involved in chromosomal translocations leading to the development of cancer (Muerhoff et al., 1995). RT-PCR shows that EWS is not induced by estrogen; however, the gene exists in high frequency in ER-bound DNA library.

5. BODY OF REPORT

A. EXPERIMENT METHODS

i. Cell culture

Human breast cancer MCF-7 (T5) cells (ER-positive and hormone-dependent) and MDA MB 231 cells (ER-negative and hormone-independent) were grown as described previously (Experiment Methods, 2001 and 2002 report). MCF-7 (T5) cells were grown in estrogen depleted or estrogen replaced conditions as described before (Sun et al., 2001). Cells cultured under E2 depleted conditions (or serum-free medium) were incubated at 37 °C for one hour with 10 nM E2.

ii. Formaldehyde and cisplatin cross-linking

Formaldehyde and cisplatin cross-linking were performed as described previously (Experiment Methods, 2001 report)(Spencer and Davie, 2002a; Spencer and Davie, 2002b). Briefly, cells treated with or without E2 were washed twice with PBS, and incubated with 1% formaldehyde in PBS for 10 min at room temperature. After washing, the formaldehyde cross-linked cells were harvested and stored at -80 °C. Cisplatin cross-linked cells were carried out as follows. After estradiol treatment, the cells were washed twice with PBS, and incubated with 1 mM cisplatin in fresh medium at 37 °C for two hours. After washing, cells were harvested and storied at -80 °C until use.

iii. Chromatin immunoprecipitation (ChIP) and PCR

Chromatin immunoprecipitation was performed as described previously (Experiment Methods, 2001 and 2002 annual reports). ChIP-DNA and library DNA were analyzed by PCR to detect

pS2 promoter: For, 5'-GACGGAATGGGCTTCATGAGC, and

Rev, 5'-GATAACATTTGCCTAAGGAGG,

ErbB2 promoter: For, 5'-GTGTTGTCCCAGTTCTGTTTA, and

Rev, 5'-GTCTTTAGTTGAGAACCCTAG

ERα promoter: For, 5'-CCTCCAGCACCTTTGTAATGC, and

Rev, 5'-AAAGAGCACAGCCCGAGGTTA,

Vimentin exon 1: For, 5'-TCTATTTTGAAACTACGGACGTCGAGTTT, and

Rev, 5'-CCAGATCACGATTGCACCGGGAAGGTTT

iv. Pre-screening of library DNA

DNA of individual clones from the library was extracted using DNA purification column (Qiagen). Restriction enzyme NotI was used to digest DNA and the positive clone DNA, that contained DNA inset with different size, were loaded on the nylon membrane HybonN+ (Ameshiam-Pharmacia) in the dot blot equipment. EWS and PACE4 fragments, which have been identified in the library, were randomly radio-labeled by ^{32}P -dCTP. The radio-labeled probes were hybridized on the slot blot membrane by Southern blotting analysis (Delcuve and Davie, 1989). The negative DNA, that did not cross reacted with the previously characterized sequences, were selected for sequencing.

v. Sequencing and Blast search of GenBank

The plasmids DNA were sequenced using ABI Prism 310 Genetic Analyzer. The DNA sequences were submitted to GenBank (NIH) database and identical or similar sequences were identified by the Blast search program.

vi. Western blotting analysis of IP efficiency for cross-linking

The cell lysate and IP-unbound fractions from formaldehyde and cisplatin cross-linked cells were reversed as described previously (Experiment Methods, 2001 report)(Sun et al., 1996). Equal volumes (10 μl) of cell lysate and IP-unbound fraction were loaded onto SDS-10% polyacrylamide gel and electrophoresed. The proteins were transferred onto nitrocellulose membrane for Western blotting analysis as described previously (Experiment Methods, 2001 report). Anti-ER mouse monoclonal antibodies (Novacastra Laboratoried Ltd) were used.

vii. Northern blotting analysis and RT-PCR

Total RNA was prepared using Trizol reagent (Invitrogen). Northern blotting analysis was performed as previously described (Sun et al., 1999). cDNA fragments were labeled using ^{32}P –dCTP and used as probes. *c-myc* cDNA fragment was EcoRI-BglII insert from pJ5, pS2 cDNA fragment was from pBRpS2/ PstI. PACE4 cDNA fragment was a purified PCR product covered PACE4 exon 16. GAPDH cDNA fragment was a purified PCR product covered GAPDH exon 7.

Primers for GAPDH exon7, For: AAGGTCATCCCTGAGCTGAAC

Rev: CCAGGAAATGAGCTTGACAAA.

RT-PCR was carried out as described before (Sun et al., 1999). The primers used in RT-PCR were as follows:

PACE4 exon 16, For: CTATGGATTTGGTTTGGTGGAC

Rev: AGGCTCCATTCTTTCAACTTCC

c-myc exon2, For: ACTGCCTCCCGCTTTGTGTGC

Rev: CTAGGGGACAGGGGCGGGGTG

B. RESULT AND DISCUSSION

The goal of this project is to isolate ER associated DNA sequences in human breast cancer cells. The chromatin immunoprecipitation protocol was designed to isolate DNA that was bound to ER in cells using formaldehyde and cisplatin cross-linking strategies. Formaldehyde produces direct and indirect protein-DNA cross-links; however, cisplatin only produces direct protein-DNA cross-links. ChIP –DNA from formaldehyde and cisplatin cross-linked human breast cancer MCF-7(T5) cells were analyzed. An ER-bound genomic DNA library from formaldehyde cross-linked MCF-7(T5) cells was constructed. Approximately two thousand clones were obtained from this library, and one hundred of these clones were sequenced. Using Blast search program, we have identified a few novel ER associated DNA sequences. Two clones contained a sequence 1 kb downstream of exon 17 of the PACE4 gene. PACE4 is a mammalian proprotein convertase that plays an important role in tumorigenesis. Northern blotting and RT-PCR analyses show that PACE4 was down regulated by estrogen in breast cancer cells. RT-PCR analysis shows that EWS gene was not regulated by estrogen. EWS gene associated with ER may play a structural function in breast cancer cells, since it contains a ½(ERE)-Sp1 sequence in exon 16 and exists in the library with high frequency. Upon sequencing all of the clones that did not cross reacted with previously sequenced DNA from ER-bound DNA library, a detailed list of ER-binding DNA sequences will be published.

1. Chromatin Immunoprecipitation using cisplatin cross-linking

a. Optimization of cisplatin cross-linking protocol

Formaldehyde cross-linking is commonly used in the ChIP protocol to identify DNA fragments directly or indirectly associated with proteins. However, comparison of the DNA directly bound to ER with that indirectly bound allow us to understand the ER regulation at the different promoters in breast cancer cells. To isolate and characterize the DNA directly bound to ER *in situ*, we developed a cisplatin cross-linking protocol. Cisplatin binds bifunctionally to DNA, directly cross-links protein to DNA. We have discovered that cisplatin cross-linked ER to nuclear DNA in human breast cancer cells.

To optimize cisplatin cross-linking conditions, we first tested the sonication conditions. From the previous formaldehyde cross-linking ChIP experiments, we believed that short DNA sizes (approximately 300-500 base pairs) was better for ChIP, since longer DNA sequences make it difficult to map site of ER binding. We optimized the sonication conditions and found that few more times of sonication pulses (15 seconds pulse) yielded the desired DNA length. Fig.1 shows that under our sonication conditions, the DNA sizes ranged from 200 to 600 base pairs (average length 300 bp) in both formaldehyde cross-linked and cisplatin cross-linked cells.

Since ER was cross-linked to DNA by cisplatin, the ER conformation may be changed which in turn might affect the binding ability of the antibody. As a result, we next tested the IP efficiency in cisplatin cross-linked cell lysate. The cisplatin cross-linked MCF7(T5) cell lysate was incubated with anti-ER antibodies, and the unbound fraction was collected and reversed by thiourea. Equal volume of thiourea reversed cell lysate and unbound fraction were electrophoresed on SDS acrylamide gel and transferred onto nitrocellulose membrane for Western blotting analysis (Fig.2 A). The agarose beads which contained ER-DNA complexes were incubated with thiourea to reverse cross-links.

DNA was released into the supernatant fraction. The proteins remained in the beads were loaded onto SDS-PAGE to carry out Western blotting analysis (Fig.2 B). The results from Western blotting analysis show that under this condition, ER antibodies could immunoprecipite ER in cisplatin cross-linked cells. However, the efficiency of IP was low in comparison with cells that were not cross-linked (see Fig.1, 2001 report).

b. Analysis of DNA bound directly to ER

ER-bound DNA was isolated from cisplatin cross-linked MCF7 (T5) cells by ChIP procedure. The ChIP-DNA from cisplatin cross-linked cells was analyzed by PCR using two estrogen-inducible promoters, pS2 promoter and ERα promoter. The pS2 promoter contains a consensus ERE sequence with one nucleotide alteration (AGTCACGGTGGCC) and few weak Sp1 binding sites (see Result, 2001 report). ERα is an auto-regulated gene, and the ERα promoter contains a ½ (ERE) sequence (TGACC) and few strong Sp1 binding sequences (such as GGGCCGGGG) (Castles et al., 1997).

ER-DNA isolated by ChIP or directly (as Input) from MCF7(T5) cells treated with or without estradiol (10 nM for one hour) was used as a template. PCR results showed that estradiol significantly increased the association of ER with the pS2 promoter in formaldehyde cross-linked MCF7(T5) cells that was identical with our former observation (see Fig.2, 2002 report). Surprisingly, there is no significant alteration of the association of ER with pS2 promoter after estrogen induction in cisplatin cross-linked MCF7(T5) cells (Fig.3). In ERα promoter, estradiol increased ER binding in both of formaldehyde cross-linked and cisplatin cross-linked MCF7 (T5) cells (Fig.3).

Formaldehyde is a very reactive dipolar compound and cross-links protein to DNA and protein to protein in 2 Å distance (Orlando v 1997). However, cisplatin has a sequence preference for purine N7, and it cross-links guanine and thymidine to protein in 4 Å distance. We do not know why cisplatin poorly cross-linked ER to ERE sequence in pS2 promoter, it maybe due to cross-linker's sequence preference.

ErbB2 was reported as an estrogen down-regulated gene in breast cancer cells (Bates and Hurst, 1997) and its promoter contains a ½(ERE)-Sp1 sequence. In cisplatin cross-linked ChIP-DNA, estrogen reduces ER bound in ErbB2 promoter (Fig.3). Vimentin exon1 that does not contain any ERE or ½(ERE) sequences was used as a negative control. PCR result showed that ER does not bind in this sequence (Fig.3 D).

Formaldehyde is commonly used as a cross-linking agent in ChIP to identify DNA fragments associated with interesting target proteins (Gerhold et al., 1999; Orlando et al., 1997; Orlando and Paro, 1993). ER-bound DNA from formaldehyde cross-linked cells contains DNA sequences directly and indirectly associated with ER *in vivo*. In this project, we developed a novel cisplatin cross-link ChIP protocol to identify DNA directly bound to ER. Based on the above experiments, we found that two major obstacles limit the application of cisplatin in ChIP. In the previous experiment, we found that at high concentration (> 1 mM) of cisplatin, the cytotoxicity of cisplatin became increasingly evident. Cross-linking protein to DNA using cisplatin under noapoptosic conditions need approximately one to two hours (Samuel et al., 1998). Recent evidence demonstrates that transcription factors dynamically associate with DNA (Shang et al., 2000; Chen et al., 1999). ChIP-DNA from cisplatin cross-linked for two hours was the DNA from

accumulated protein-DNA complexes during this time period. Since cisplatin preferentially cross-links protein to DNA sequences that are rich in guanine. PCR analysis of cisplatin cross-linking ChIP-DNA could not reflect the accurate loading of proteins in the DNA.

2. Estrogen-responsive genes library

ER-bound genomic DNA library in breast cancer MCF7 (T5) cells has been established. The strategy of construction of formaldehyde cross-link ER-bound DNA library is presented in the flowchart (Fig. 4). This strategy contains three major procedures: the isolation of ChIP-DNA, the construction of ChIP-DNA library and the identification of genes from GenBank.

MCF7(T5) cells were cross-linked with 1% formaldehyde and the cell lysate was prepared after sonication to reduce DNA to 200-600 bp. ER-associated DNA were immunoprecipitaed by anti-ER antibodies. After thiourea reversing of cross-link, ChIP-DNA was collected and ligated to a unique linker and amplified (Experimental Methods, 2002 report). PCR produced DNA was inserted into vector pGEM-Easy. After transformation, the individual colonies were cloned and cloned DNA was extracted. To avoid re-sequencing previously characterized DNA sequences we developed a pre-screening protocol which will set aside previously characterized sequences. Cloned DNA was digested by restriction enzymes NotI and the positive clones containing different size ChIP-DNA were dotted onto a Nylon membrane using a slot blot manifold. DNA fragments that have been characterized from previous batches of clones, such as EWS and PACE4, were ^{32}P radio-labeled as probes. After hybridization, the negative clones

were selected for the future sequencing as new ER targets (Fig. 5). Table I lists the clone number, prescreening clone number and sequencing clone number. Approximately 2000 clones were prepared. Only a limited number of clones have been sequenced so far. Table II lists the genes which were identified in GenBank Blast search program. All of the identified fragments were directly or indirectly binding to ER, these fragments may or may not contain (ERE) or ½(ERE). All of the sequenced clones contained ½(ERE) or ½(ERE)-Sp1 sequences.

Since only very limited number of clones from this library has been sequenced, few known estrogen-inducible genes, such as pS2, were not yet identified in this library. After sequencing more clones from this library, we will publish a list of ER-bound genes in human breast cancer cells. Interestingly, few novel genes contained ER-bound fragments were identified in this library.

3. PACE4 gene is down-regulated by estradiol in ER positive breast cancer cells

There were two clones in this library containing a sequence 1 kb downstream of exon 17 of the PACE4 gene (see Fig. 4 and Fig. 6, 2002 report). We scanned the sequence, 246 nucleotide region of exon 17 of PACE4 gene, for the presence of ERE, ½(ERE) and Sp1 binding sites. A ½(ERE)-$(N)_x$-Sp1 site was found in this region, suggesting that ER was associated with this region *in situ*.

PACE4 is a mammalian pro-protein convertase family member and plays an important role in tumorigenesis. An analysis of breast cancer tumors revealed that PACE4 is primarily expressed in ER positive but not ER negative breast epithelial cancer cells (Cheng et al., 1997). This observation is congruent with the possibility that PACE4

is an estrogen responsive gene. Northern blotting analysis and reverse-transcription (RT)-PCR were used to test if PACE4 is responsive to estrogen treatment. Total RNA extracted from MCF(T5) cells treated with 10 nM E2 for different time (0 to 150 min). The cDNA fragments of PACE4, pS2 and *c-myc* were radio-labeled as probes in Northern blotting analysis. Fig. 6 shows that the expression of pS2 and *c-myc* increase after 30 minutes of estradiol induction. However, PACE4 expression was reduced after 30 minutes of estradiol treatment. When E2 incubation is extended to 60 to 90 minutes, mRNA returned to normal levels. In one preparation, the level of PACE4 mRNA dropped again after 90 to 120 minutes. The result from RT-PCR was identical with Northern blotting analysis. Fig. 7 shows that PACE4 mRNA level declined after 30 minutes of E2 treatment. Both Northern blotting and RT-PCR analyses provided evidence that PACE4 was an estrogen down-regulated gene in breast cancer cells.

ER functions as a transcriptional activator in most of estrogen-responsive genes in ER positive and hormone dependent human breast cancer cells. So far, very few genes have been characterized as estrogen down- regulated genes, such as ErbB2. PACE4 gene is another estrogen down-regulated gene in breast cancer cells and tumors.

5. EWS gene associated with ER is not induced by estradiol in breast cancer cells

Interestingly, a DNA fragment located downstream of exon 16 of EWS gene was found in ER-bound DNA library with high frequency. A ½(ERE)-Sp1 sequence has been detected in this region (see Fig.5 and Fig.6, 2002 report). In the pre-screening dot blot analysis, a number of clones were homologous with EWS DNA fragment. We have tested EWS expression as a function of estrogen treatment. Preliminary RT-PCR results

show that EWS was expressed in breast cancer cells; however, it was not induced by estradiol (Fig.8).

EWS gene is commonly involved in chromosomal translocations that lead to the development of cancer. EWS may have a role in coupling transcription and RNA processing (Arvand and Denny, 2001). It will be interesting to understand the mechanism and significance of ER binding to EWS gene in breast cancer cells. From this preliminary experiment, we suggest that ER bound to EWS gene may play a structural rather than a functional role.

D. RECOMMENDATIONS

In the three years' study, we have established an ER-bound genomic DNA library from breast cancer cells. ER-bound DNA was isolated by chromatin immunoprecipitation protocol from formaldehyde cross-linked breast cancer MCF7 (T5) cells. ChIP-DNA should contain all ER-bound DNA sequences that are not only responsible for transcription but also may have a structural role. Two thousand more clones have been isolated, and seven hundred of these clones have been tested by a developed pre-screening procedure. A limited number of clones have been sequenced and blast searched in GenBank. Few genes containing ½(ERE) or ½(ERE)-Sp1 were found in the ER-bound DNA library and listed. We will publish a list of ER-associated genes in breast cancer cells after we sequence all of the clones selected from the pre-screening procedure.

A mammalian pro-protein convertase PACE4 gene was detected in the library. Northern blotting analysis and RT-PCR revealed that PACE4 was down-regulated by estradiol in 30 to 60 minutes. PACE4 plays a role in tumorgenesis and is expressed only

in ER positive breast cancer cells. Characterization of PACE4 regulation in breast cancer cells and tumors may have a clinic and diagnostic significance.

Another frequently repeated EWS fragment is found in ER-DNA library but is not estrogen inducible. EWS gene is involved in oncogenesis in a number of cancer cells and tumors. ER bound to EWS DNA may play a structural role in breast cancer cells.

6. KEY RESEARCH ACCOMPLISHMENTS

- Analysis of ChIP-DNA from formaldehyde cross-linked and cisplatin cross-linked breast cancer MCF7 (T5) cells.
- Establishment of a genomic DNA library of ER-associated genes in breast cancer cells by formaldehyde cross-linking.
- A list of ER-associated genes from ER-DNA library of MCF(T5) cells.
- PACE4 gene containing ½(ERE)-Sp1 sequence at the downstream of Exon 17.
- PACE4 is down-regulated by estrogen in breast cancer cells.
- EWS gene is not estrogen inducing gene. ER bound to EWS DNA may play a role in chromatin structure.

7. REPORTABLE OUTCOMES

A. Pulications:

1. Sun JM, Spencer VA, Chen HY, Li L, Davie JR. Measurement of histone acetyltransferase and histone deacetylase activities and kinetics of histone acetylation.
Methods. 2003 Sep;31(1):12-23.

2. Spencer VA, Sun JM, Li L, Davie JR. Chromatin immunoprecipitation: a tool for studying histone acetylation and transcription factor binding.
Methods. 2003 Sep;31(1):67-75.

3. Davie JR. Inhibition of histone deacetylase activity by butyrate.
J Nutr. 2003 Jul;133(7 Suppl):2485S-2493S

4. Sun JM, Chen HY, Moniwa M, Litchfield DW, Seto E, Davie JR. The transcriptional repressor Sp3 is associated with CK2-phosphorylated histone deacetylase 2.

J Biol Chem. 2002 Sep 27;277(39):35783-6. Epub 2002 Aug 09.

5. Sun JM, Chen HY, Davie JR. Isolation of transcriptionally active chromatin from human breast cancer cells using Sulfolink coupling gel chromatography.

J Cell Biochem. 2002;84(3):439-46.

6. Sun JM, Chen HY, Davie JR. Effect of estradiol on histone acetylation dynamics in human breast cancer cells.

J Biol Chem. 2001 Dec 28;276(52):49435-42. Epub 2001 Oct 26.

7. Spencer VA and Davie JR, Isolation of proteins cross-linked to DNA by cisplatin, The protein protocol handbook

8. Spencer VA and Davie JR, Isolation of proteins cross-linked to DNA by formaldehyde, The protein protocol handbook

B. Abstracts:

1. Differential distribution of Sp1 and Sp3 in human breast cancer cells,

2001 AACR-NCI-EORTC International Conference on Molecular Targets and Cancer Therapeutics.

2. Isolation and characterization of estrogen responsive genes in human breast cancer cells,
Era of Hope 2002 meeting

C. Presentations:

2001 FASEB Summer Research Conference on Nuclear Structure and Cancer

D. Employment or research opportunities applied for and/or received based on experience/training supported by this award

1, The following is a list of personnel receiving pay from this research effort.
Jian-Min Sun, professional associate
Xiuli Ma, technician
Charlene Bergen, dishwasher

2, Virginia Spencer, obtained Ph.D. degree in August 2003, supported by this award.

8. CONCLUSIONS

ER plays a key role in the transcription regulation of estrogen-responsive genes in breast cancer cells. A number of estrogen-responsive genes have been identified by cDNA microarrays, suppression subtractive hybridization (SSH), serial analysis of gene expression (SAGE) or cDNA subtraction assay. However, these procedures are based on mRNA expression level. We used chromatin immunoprecipitation protocol to isolate ER-bound DNA fragments *in situ*. The ER-bound DNA library should contain all of ER-bound DNA which are induced or repressed by estrogen, or may play a structural role in breast cancer cells.

Following the project schedule, we have analyzed the ChIP-DNA from formaldehyde and from cisplatin cross-linked breast cancer cells. A genomic DNA library containing ER-bound DNA fragments *in situ* was established. A list of ER-bound DNA in breast cancer cells was presented.

PACE4 gene was identified in ER-bound DNA library. Downstream of PACE4 exon 17, a ½(ERE)-Sp1 sequence has been found. PACE4 is a mammalian pro-protein convetase and may play a role in tumorigenesis. Northern blotting analysis and RT-PCR show that PACE4 is an estrogen down regulated gene.

EWS gene is involved in chromosome relocalization and tumor development. The preliminary data shows ER bound to EWS gene exon 16 and it may play a structural function in breast cancer cells.

9. REFERENCES:

Arvand,A and Denny C.T. (2001). Biology of EWS/ETS fusions in Ewing's family tumours. Oncogene *20*, 5747-5754.

Bassi,D.E., Mahloogi,H., and Klein-Szanto,A.J. (2000). The proprotein convertases furin and PACE4 play a significant role in tumor progression. Mol. Carcinog. *28*, 63-69.

Bates,N.P. and Hurst,H.C. (1997). An intron 1 enhancer element mediates oestrogen-induced suppression of ERBB2 expression. Oncogene *15*, 473-481.

Berry,M., Nunez,A.M., and Chambon,P. (1989). Estrogen-responsive element of the human pS2 gene is an imperfectly palindromic sequence. Proc. Natl. Acad. Sci. U. S. A. *86*, 1218-1222.

Castles,C.G., Oesterreich,S., Hansen,R., and Fuqua,S.A. (1997). Auto-regulation of the estrogen receptor promoter. J. Steroid Biochem. Mol. Biol. *62*, 155-163.

Charpentier,A.H., Bednarek,A.K., Daniel,R.L., Hawkins,K.A., Laflin,K.J., Gaddis,S., MacLeod,M.C., and Aldaz,C.M. (2000). Effects of estrogen on global gene expression: identification of novel targets of estrogen action. Cancer Res. *60*, 5977-5983.

Chen,H., Lin,R.J., Xie,W., Wilpitz,D., and Evans,R.M. (1999). Regulation of hormone-induced histone hyperacetylation and gene activation via acetylation of an acetylase. Cell *98*, 675-686.

Cheng,M., Watson,P.H., Paterson,J.A., Seidah,N., Chretien,M., and Shiu,R.P. (1997). Pro-protein convertase gene expression in human breast cancer. Int. J. Cancer *71*, 966-971.

Dedon,P.C., Soults,J.A., Allis,C.D., and Gorovsky,M.A. (1991). A simplified formaldehyde fixation and immunoprecipitation technique for studying protein-DNA interactions. Anal. Biochem. *197*, 83-90.

Delcuve,G.P. and Davie,J.R. (1989). Chromatin structure of erythroid-specific genes of immature and mature chicken erythrocytes. Biochem. J. *263*, 179-186.

Duan,R., Porter,W., and Safe,S. (1998). Estrogen-induced c-fos protooncogene expression in MCF-7 human breast cancer cells: role of estrogen receptor Sp1 complex formation. Endocrinology *139*, 1981-1990.

Dubik,D. and Shiu,R.P. (1992). Mechanism of estrogen activation of c-myc oncogene expression. Oncogene *7*, 1587-1594.

Gerhold,D., Rushmore,T., and Caskey,C.T. (1999). DNA chips: promising toys have become powerful tools. Trends. Biochem. Sci. *24*, 168-173.

Krishnan,V., Wang,X., and Safe,S. (1994). Estrogen receptor-Sp1 complexes mediate estrogen-induced cathepsin D gene expression in MCF-7 human breast cancer cells. J. Biol. Chem. *269*, 15912-15917.

Kuang,W.W., Thompson,D.A., Hoch,R.V., and Weigel,R.J. (1998). Differential screening and suppression subtractive hybridization identified genes differentially expressed in an estrogen receptor- positive breast carcinoma cell line. Nucleic Acids Res. *26*, 1116-1123.

Luqmani,Y., Bennett,C., Paterson,I., Corbishley,C.M., Rio,M.C., Chambon,P., and Ryall,G. (1989). Expression of the pS2 gene in normal, benign and neoplastic human stomach. Int. J. Cancer *44*, 806-812.

Muerhoff,A.S., Leary,T.P., Simons,J.N., Pilot Matias,T.J., Dawson,G.J., Erker,J.C., Chalmers,M.L., Schlauder,G.G., Desai,S.M., and Mushahwar,I.K. (1995). Genomic organization of GB viruses A and B: two new members of the Flaviviridae associated with GB agent hepatitis. J. Virol. *69*, 5621-5630.

Olinski,R., Wedrychowski,A., Schmidt,W.N., Briggs,R.C., and Hnilica,L.S. (1987). In vivo DNA-protein cross-linking by cis- and trans- diamminedichloroplatinum(II). Cancer Res. *47*, 201-205.

Orlando,V. and Paro,R. (1993). Mapping polycomb-repressed domains in the bithorax complex using in vivo formaldehyde cross-linked chromatin. Cell *75*, 1187-1198.

Orlando,V., Strutt,H., and Paro,R. (1997). Analysis of chromatin structure by in vivo formaldehyde cross- linking. Methods *11*, 205-214.

Safe,S. (2001). Transcriptional activation of genes by 17 beta-estradiol through estrogen receptor-Sp1 interactions. Vitam. Horm. *62*, 231-252.

Samuel,S.K., Spencer,V.A., Bajno,L., Sun,J.-M., Holth,L.T., Oesterreich,S., and Davie,J.R. (1998). *In situ* cross-linking by cisplatin of nuclear matrix-bound transcription factors to nuclear DNA of human breast cancer cells. Cancer Res. *58*, 3004-3008.

Shang,Y., Hu,X., DiRenzo,J., Lazar,M.A., and Brown,M. (2000). Cofactor dynamics and sufficiency in estrogen receptor-regulated transcription. Cell *103*, 843-852.

Spencer,V.A. and Davie,J.R. (2002a). Isolation of proteins cross-linked to DNA by cisplatin. In The Protein Protocols Handbook, J.M.Walker, ed. (Totowa: Humana press), pp. 747-752.

Spencer,V.A. and Davie,J.R. (2002b). Isolation of proteins cross-linked to DNA by formaldehyde. In The Proteins Protocol Handbook, J.M.Walker, ed. (Totowa: Humana Press), pp. 753-760.

Sun,J.-M., Chen,H.Y., and Davie,J.R. (2001). Effect of estradiol on histone acetylation dynamics in human breast cancer cells. J. Biol. Chem. *276*, 49435-49442.

Sun,J.-M., Chen,H.Y., Litchfield,D.W., and Davie,J.R. (1996). Developmental changes in transcription factors associated with the nuclear matrix of chicken erythrocytes. J. Cell. Biochem. *62*, 454-466.

Sun,J.-M., Chen,H.Y., Moniwa,M., Samuel,S., and Davie,J.R. (1999). Purification and characterization of chicken erythrocyte histone deacetylase 1. Biochemistry *38*, 5939-5947.

Wrenn,C.K. and Katzenellenbogen,B.S. (1990). Cross-linking of estrogen receptor to chromatin in intact MCF-7 human breast cancer cells: optimization and effect of ligand. Mol. Endocrinol. *4*, 1647-1654.

Xie,W., Duan,R., and Safe,S. (1999). Estrogen induces adenosine deaminase gene expression in MCF-7 human breast cancer cells: role of estrogen receptor-Sp1 interactions. Endocrinology *140*, 219-227.

Yang,G.P., Ross,D.T., Kuang,W.W., Brown,P.O., and Weigel,R.J. (1999). Combining SSH and cDNA microarrays for rapid identification of differentially expressed genes. Nucleic Acids Res. *27*, 1517-1523.

Zamble,D.B. and Lippard,S.J. (1995). Cisplatin and DNA repair in cancer chemotherapy. Trends Biochem. Sci. *20*, 435-439.

APPENDIX COVER SHEET

10. APPENDICES

Table 1

Formaldehyde cross-link ER-bound ChIP-DNA library

Clone number	2068
Plasmid number	1757
Pre-screening clones	705
Sequencing clones	124

Table 2

List of ER-bound DNA from ChIP-DNA library

Gene	Binding site	Sequence	Clone numbers
PACE4	½(ERE)-Sp1	GGTAAGCGGCAGGG	2
EWS	½(ERE)-Sp1	ACTGGAAAGCGGGC	5
Human normal cartilase (HNC)	½(ERE)-Sp1	ACTGGGAAAACCCTGGCGTTA	1
Carboxypeptidase (CPE)	½(ERE)	GGTCA	2
Telomeric DNA Clone 10PTEL19	½(ERE)-Sp1	GGTAAGCGGCAGGG	1
Beta-lactamase (tumor protein ?)			5

B. FIGURES

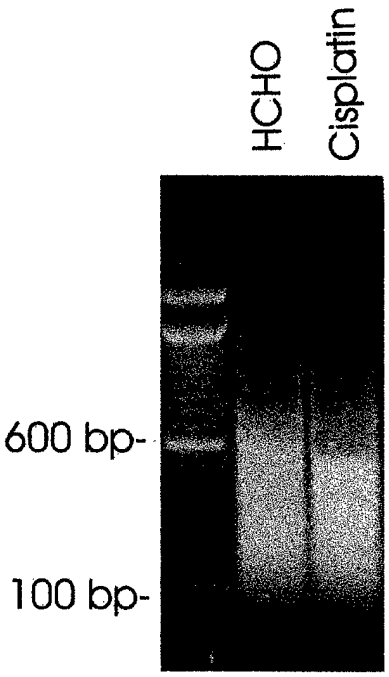

Fig.1. T5 cells cross-linked by 1% formaldehyde for 10 min and 1mM cisplatin for 2 hours were lysed by sonication. DNA was extracted from chromatin by phenol/chloroform, loaded on 1% agarose gel, and stained with ethidium bromide.

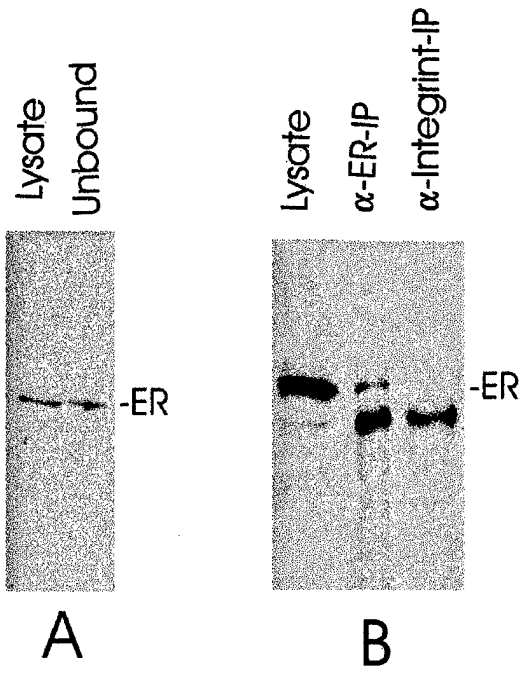

Fig.2. Western blot analysis of cisplatin cross-linked T5 cell fractions using anti-ERα monoclonal antibodies. Ten microliter of cell lysate and ChIP's unbound fraction was reversed by thiourea from cisplatin cross-linking were loaded on 10% SDS polyacrylamide gel and immunochemically stained with anti- ERα monoclonal antibodies (A). Thiourea reversed cell lysate and protein A-Sephorose beads were loaded onto 10% SDS polyacrylamide gel and immunochemically stained with anti- ERα monoclonal antibodies (B).

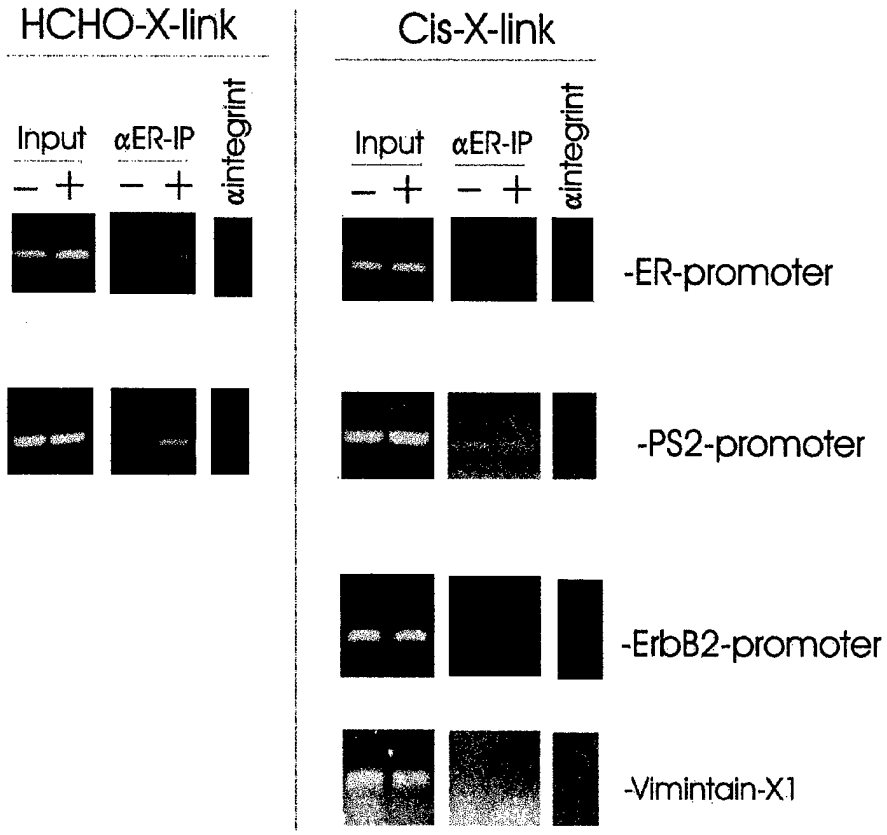

Fig.3. PCR analysis of chromatin immunoprecipitated DNA anti-ERα monoclonal antibodies from formaldehyde (HCHO-X-link) and cisplatin cross-linked (Cis-X-link) MCF7 (T5) cells. Equal volume (1 μl) of ChIP-DNA was used in each PCR reaction as template and 1 pM of primers of pS2 promoter, ERα promoter, ErbB2 promoter and vimenten exon1 were added in 25 μl of reaction. Ten μl of reaction was loaded on 1% agarose gel and stained with ethidium bromide.

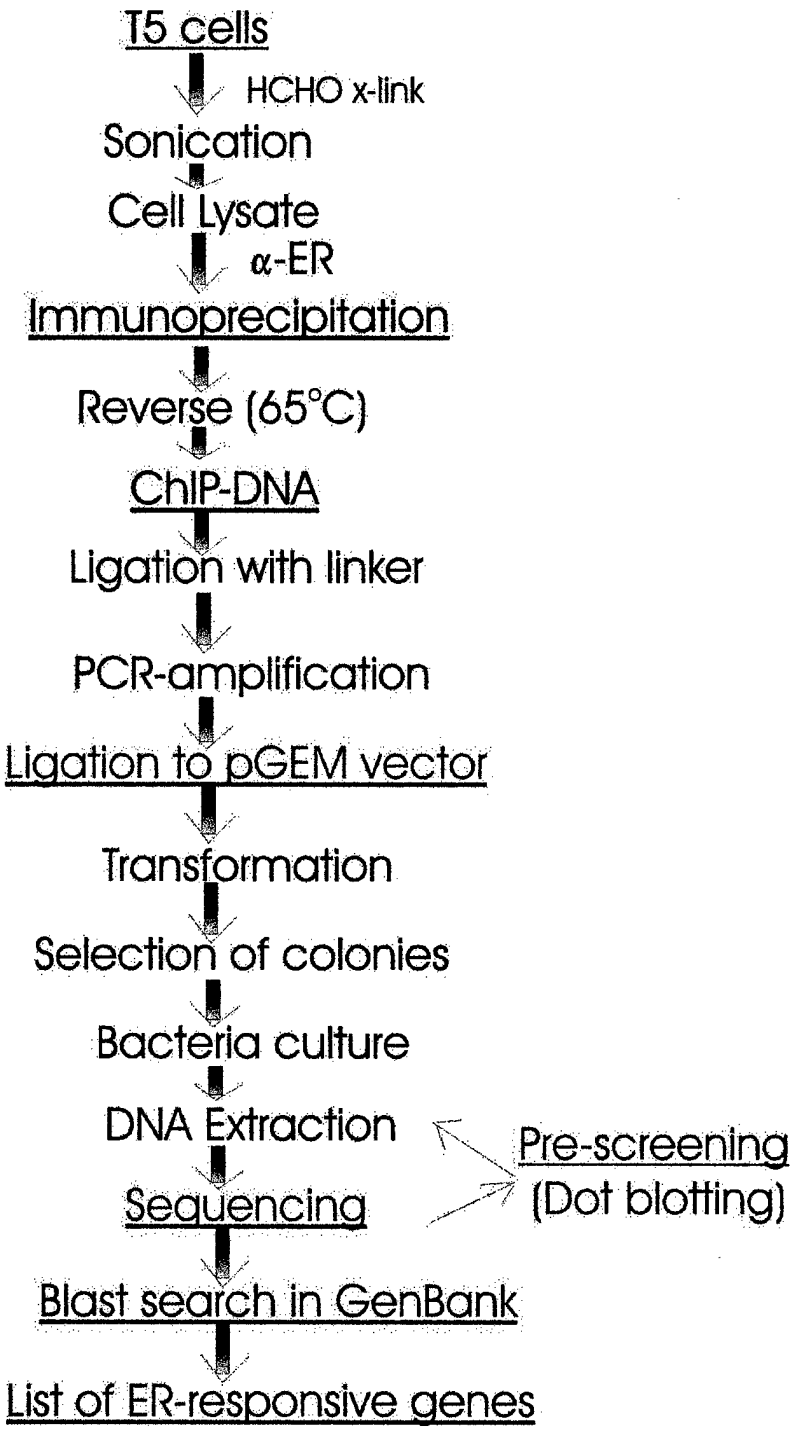

Fig.4. Strategy for construction of ER-DNA library using ChIP procedure.

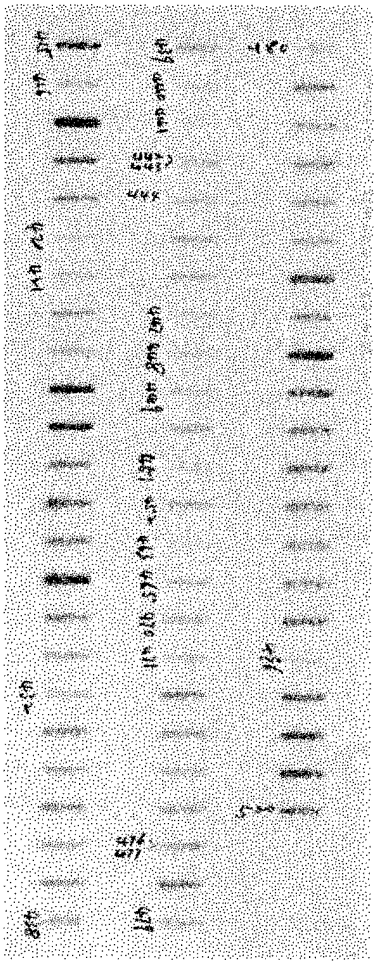

Fig.5. Dot blot analysis of pre-screening clone DNA from ER-DNA library. Individual clones were grown in 2 ml of LB and DNA was extracted using plasmid purification column (Quagen). Equal volumes (5 µl) of DNA were dotted onto a nylon HybondN+ membrane (Amesham-Pharmacia). DNA fragments of EWS and PACE4 were labeled using ^{32}P-dCTP and hybridized. The membrane was exposed to X-ray film.

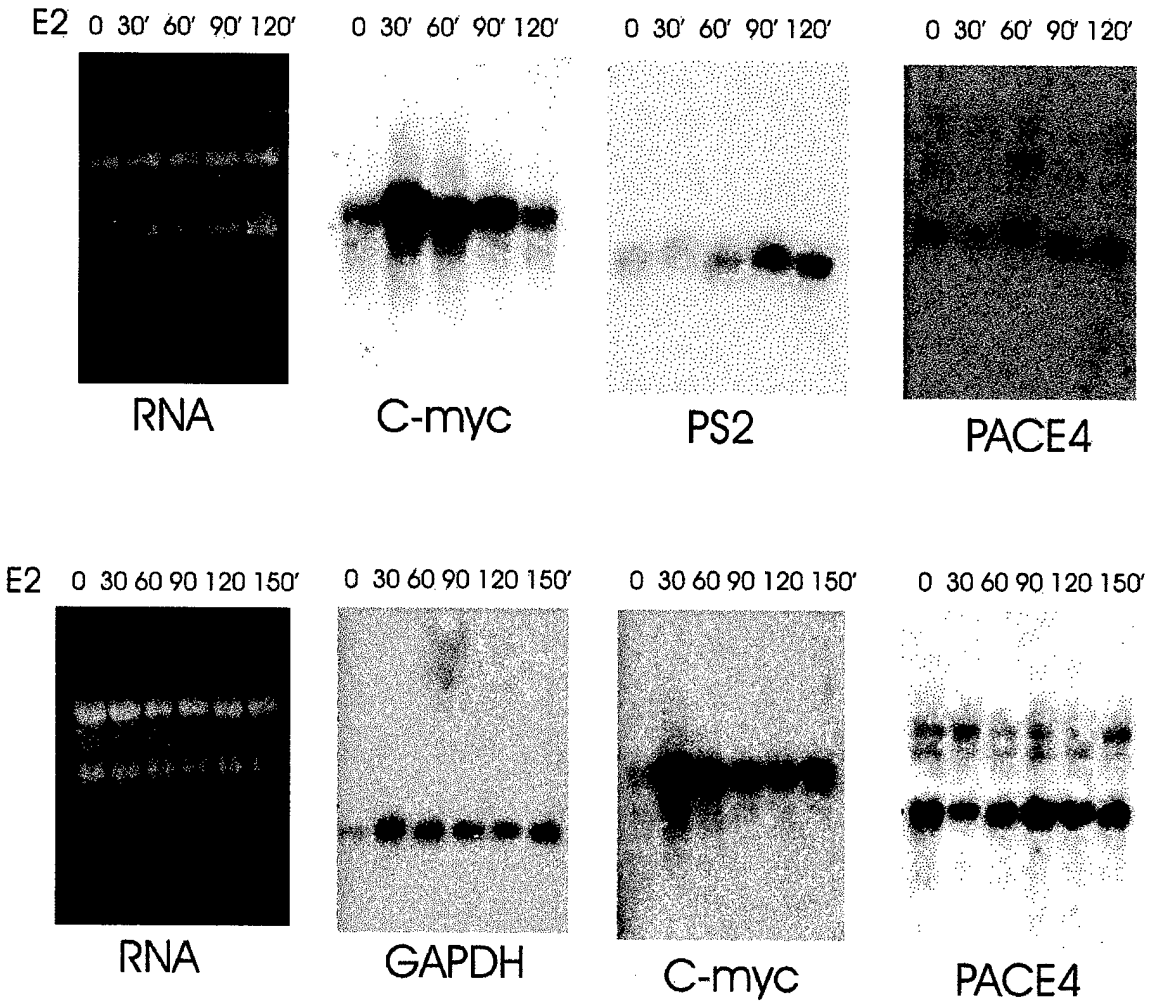

Fig.6. Northern blotting analysis of PACE4 in MCF7 (T5) cells. MCF7 (T5) cells were incubated with 10 nM E2 for 0 to 150 min, and RNA was extracted using Trizol reagent. Twenty μg of total RNA were loaded onto 1% agarose gel and stained by ethidium bromide. RNA was transferred onto a nylon HyboundN+ membrane and hybridized with cDNA fragments, *c-myc*, pS2, GAPDH and PACE4. The membranes were exposed to X-ray films.

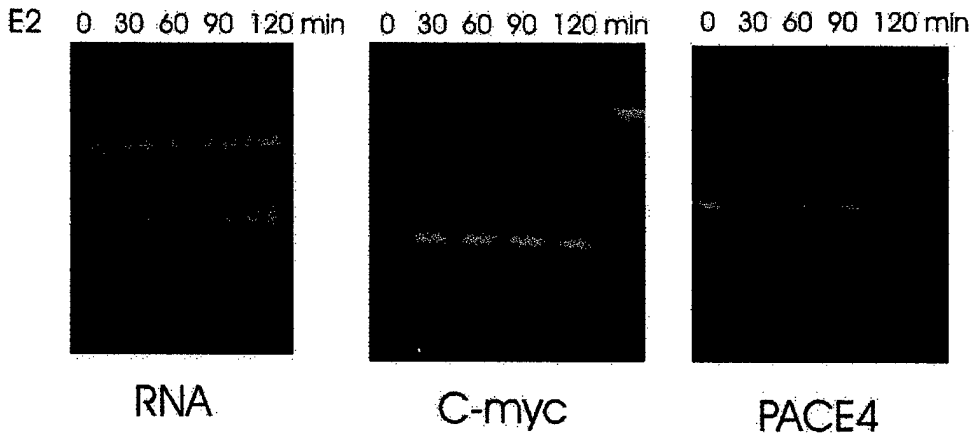

Fig.7. RT-PCR analysis of PACE4 in T5 cells. cDNA was prepared by reverse transcription of RNA extracted from 10 nM E2 induced T5 cells. Equal volumes (5 µl) of cDNA and 1 pM primers, *c-myc* exon 2 and PACE4 exon , were used in PCR. Equal volumes (10 µl) of PCR reaction were loaded onto 1% agarose gel and stained by ethidium bromide.

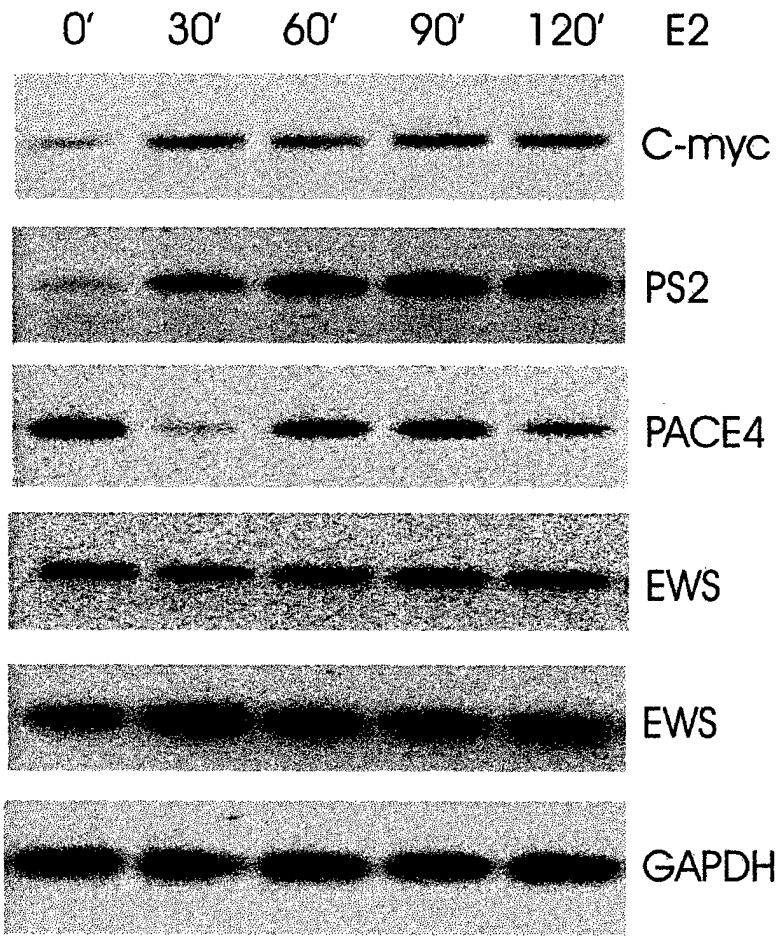

Fig.8. RT-PCR analysis of EWS in MCF7 (T5) cells. cDNA was prepared by reverse transcription (see Fig.7). 1 pM of EWS exon primer was used in PCR and 10 µl of PCR reaction was loaded onto 1% agarose gel.

Available online at www.sciencedirect.com
SCIENCE DIRECT®
ACADEMIC PRESS
Methods 31 (2003) 12–23
METHODS
www.elsevier.com/locate/ymeth

Measurement of histone acetyltransferase and histone deacetylase activities and kinetics of histone acetylation

Jian-Min Sun, Virginia A. Spencer, Hou Yu Chen, Lin Li, and James R. Davie*

Manitoba Institute of Cell Biology, University of Manitoba, 675 McDermot Avenue, Winnipeg, Man., Canada R3E 0V9

Accepted 19 February 2003

Abstract

Dynamic histone acetylation has a role in chromatin remodeling and in the regulation of transcription. Histone deacetylases (HDACs) and histone acetyltransferases (HATs) catalyze reversible histone acetylation. HATs and HDACs exist as multiprotein complexes that have coactivator and corepressor activities, respectively. The steady-state level of acetylation at a chromatin site is determined by the local net activities of these enzymes. Here we describe methods to isolate different subcellular fractions (cytosol, nuclei, tightly bound nuclear, loosely bound nuclear, immunoprecipitated multiprotein complexes, and nuclear matrix) to determine the subcellular distribution of HAT and HDAC activities. Procedures to assay the activities of these enzymes and to measure the kinetics of histone acetylation and deacetylation are presented.

Keywords: Histone acetyltransferase; Histone deacetylase; Kinetics of histone acetylation; Subcellular fractionation

1. Introduction

1.1. Histone modification and chromatin structure remodeling

Chromatin structure has a central role in the regulation of gene expression [1]. The core particle of chromatin, the nucleosome, contains four core histones (H2A, H2B, H3, H4) around which is wrapped 146 bp of DNA. The amino-terminal tails of the core histones are modified by several processes, including acetylation, phosphorylation, methylation, and ADP-ribosylation [2]. In the 1960s, it was observed that transcription was linked to histone acetylation [3]. Recent studies demonstrate that the H3 and H4 N-terminal tails participate in chromatin fiber folding and intermolecular fiber–fiber interaction [4–6]. Acetylation of the core histone tails disrupts higher-order chromatin folding and interactions with nonhistone chromosomal proteins. Condensed heterochromatin regions are generally poorly acetylated, while decondensed euchromatin regions containing transcriptionally competent and active genes are associated with acetylated histones [7,8].

The histone N-terminal domains can be acetylated at various lysine residues (5 in H3; 4 in H4; 4 in H2B; and 1 or 2 in H2A). Thus, H3, H2B, and H4 can be mono-, di-, tri-, and tetra-acetylated (Fig. 1A). Dynamically acetylated histones attaining high levels of acetylation are associated with transcribed and transcriptionally competent chromatin [9].

1.2. Dynamic histone acetylation

Histones are dynamically acetylated by histone deacetylases (HDACs) and histone acetyltransferases (HATs) (Fig. 1B). In mammalian and avian cells, one population of histones is rapidly hyperacetylated ($t_{1/2} = 7$ min for monoacetylated H4) and rapidly deacetylated ($t_{1/2} = 3$–7 min) [10–12]. This population of rapidly acetylated and deacetylated histone is limited to approximately 10% (in human breast cancer MCF-7 (T5) and MDA MB 231 cells) to 15% (in hepatoma tissue culture cells) of the core histones. A second population of histones is slowly acetylated ($t_{1/2} = 200$–

* Corresponding author. Fax: +204-787-2190.
E-mail address: davie@cc.umanitoba.ca (J.R. Davie).

1046-2023/$ - see front matter © 2003 Published by Elsevier Science (USA).
doi:10.1016/S1046-2023(03)00083-5

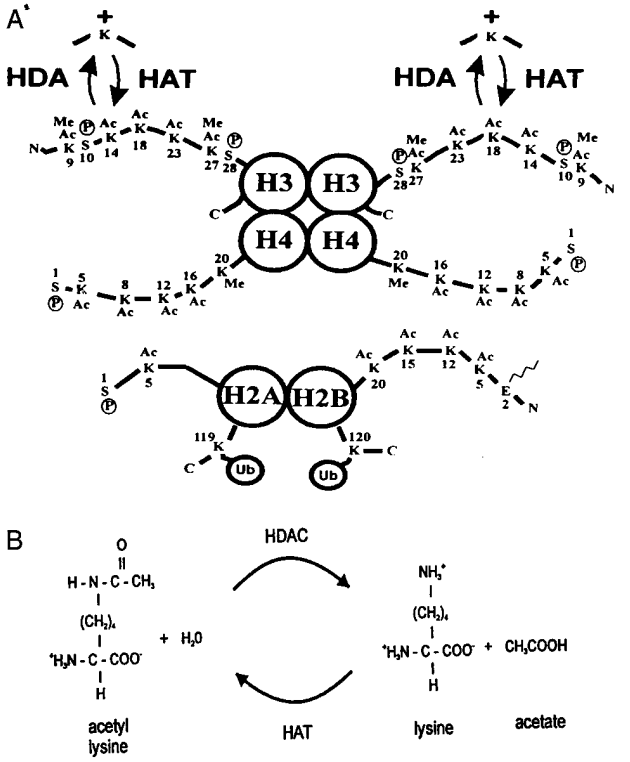

Fig. 1. (A) N-terminal tails of core histones are modified by several postsynthetic modifications: acetylation (Ac), methylation (Me), and phosphorylation (P). These modifications are reversible with the possible exception of methylation. (B) Dynamic histone acetylation occurs on lysine residues and is catalyzed by histone deacetylases (HDACs) and histone acetyltransferases (HATs).

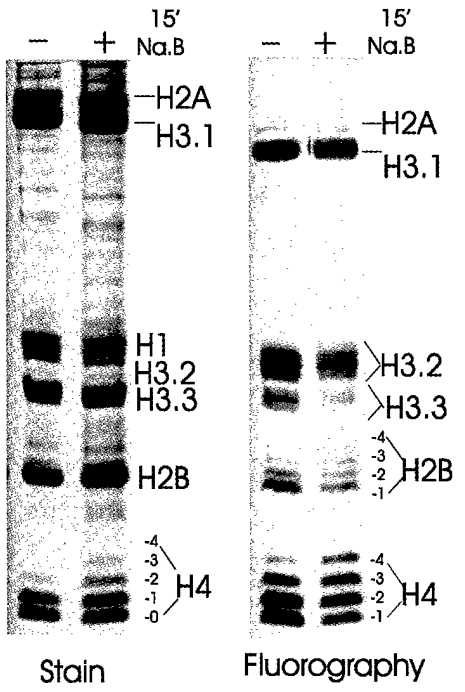

Fig. 2. Radiolabeling of histones. Histones from human breast cancer MDA MB 231 cells incubated without or with 10 mM sodium butyrate for 15 min were separated on an acetic acid–urea–Triton X-100 (AUT)–15% polyacrylamide gel, and the gel was stained with Coomassie blue and fluorographed. 0, 1, 2, 3, and 4 correspond to un-, mono-, di-, tri-, and tetra-acetylated histone isoforms, respectively.

300 min for monoacetylated H4) and deacetylated ($t_{1/2} = 30$ min) [10,12]. In avian immature erythrocytes only 2% of the core histones are engaged in dynamic acetylation. The slow rate of histone acetylation is not present. When cells are exposed to [^{3}H]acetate for a brief time (5–15 min) in the presence of sodium butyrate (an HDAC inhibitor), the radiolabel becomes incorporated predominantly into lower acetylated species (e.g., diacetylated H4) (Fig. 2). However, longer labeling times (e.g., more than 60 min) in the presence of butyrate result in the labeling of higher acetylated histone isoforms [12].

1.3. HATs and HDACs in gene regulation

Multiple HATs have been identified, with many of the HATs having coactivator activity [13–15]. Acetylation of histone tails by HATs disrupts higher-order chromatin folding and promotes the solubility of chromatin at physiological ionic strength. The coactivators, CBP, p300, PCAF, and Tip60, are potent HATs. In addition to their HAT activity, these multiprotein complexes recruit the general transcription factors and RNA polymerase II. In contrast to HATs, the recruitment of HDACs causes the removal of acetyl groups from histone tails, stabilizing nucleosome structure, promoting fiber–fiber interactions, and forming a chromatin state hampering transcription and elongation processes [1,7,16]. Three classes of HDACs in mammalian cells and their homologues in yeast have been identified [1]. HDACs are multiprotein complexes that also interfere with the formation of a functional preinitiation complex. It should be noted that both HATs and HDACs are recruited to the transcriptionally active chromatin region [12]. When the balance of HDACs and HATs favors deacetylation, the chromatin region takes on a repressive higher-order structure. However, when the balance favors acetylation, the chromatin region is in an unfolded state capable of undergoing transcription [17].

HDACs and HATs are recruited to specific regions of the genome by transcription factors. For example, the general transcription factor Sp1 recruits HDAC1, which, in turn, represses the thymidine kinase promoter [18]. Transcription factors existing as multimers, such as Sp1 and p53, are capable of simultaneously recruiting HATs and HDACs. Other factors like ligand-activated transcription factors (e.g., estrogen receptor) and modified factors (e.g., NF-κB) have their recruitment of HATs or HDACs governed by the ligand or modifying enzyme. HDAC and HAT activity assays discern which activity is associated with a specific transcription factor.

In the in vitro assay, HDAC releases acetate from the histone's acetyl lysine (Fig. 1B). For HDAC activity

assay, the lysine residues in histones may be labeled with tritium, biotin, or fluorescent dye [19,20]. Release of the acetate labeled with tritium, biotin, or fluorescence is then monitored. Some commercially available HDAC substrates are peptides derived from N-terminal tails of H3 or H4. Individual histones and nonhistone chromosomal proteins may be used in the HDAC assay to determine substrate specificity. Tritium acetate-labeled core histones are generally used as substrates in the HDAC assay. Here, we describe the procedures to prepare radiolabeled histone substrates for the HDAC assay. Next we describe HDAC and HAT activity assays. Procedures to isolate subcellular fractions to investigate the location of HAT and HDAC activities are presented. The last section describes methods to determine the rates of histone acetylation and histone deacetylation.

2. Description of method

2.1. Tritium acetate radiolabeling of histones in cultured mammalian cells

Mammalian cells cultured on plastic dishes to 80 to 90% confluency are incubated with the protein synthesis inhibitor cycloheximide, which is directly added into the medium to a final concentration of 10 μg/ml. Cycloheximide prevents the incorporation of radiolabel into newly synthesized histones. After 30 min incubation with cycloheximide, cells are washed with prewarmed 1× PBS, and then incubated with fresh medium, containing [^{3}H]acetate (0.1 mCi/ml; specific activity >10 Ci/mmol from ICN or NEN), sodium butyrate (final concentration of 10 mM), and cycloheximide (10 μg/ml) for 60 min at 37 °C. Sodium butyrate inhibits HDAC activity, allowing the HATs to drive up the acetylated histone levels.

After labeling, the medium is removed and the cells are washed twice with ice-cold 1× PBS containing 10 mM sodium butyrate. The labeled cells are then harvested by scraping using a plastic or rubber cell lifter. After centrifugation at 4000 rpm (SS-34 rotor) for 10 min, the pelleted cells are either directly processed to isolate radiolabeled histones or stored at −80 °C.

Since histone deacetylation may be active, sodium butyrate should be present in all labeling media and wash buffers to inhibit deacetylation of radiolabeled hyperacetylated histones. The absence of sodium butyrate (or other HDAC inhibitors) in the labeling and washing buffers may decrease the specific activity of the radiolabeled acetylated histone substrate.

2.2. Tritium acetate radiolabeling of histones in avian erythrocytes

Radiolabeled acetylated histones from avian erythrocytes are excellent substrates for HDAC assays [21,22]. The following sections describe the isolation of avian immature erythrocytes, the incubation of cells with radiolabeled acetate, and the isolation of radiolabeled histones. In contrast to cultured mammalian cells and avian mature erythrocytes, avian immature erythrocytes have only the fast rate of histone acetylation [23].

2.2.1. Isolation of avian immature erythrocytes

Adult white Leghorn chickens (3 months old) are made anemic by injections of 2.5% (w/v) 1-acetyl 2-phenylhydrazine dissolved in 60% ethanol applying the following injection schedule. Each chicken (approximately 1 kg) is injected with 0.7 ml (at Day 1), 0.7 ml (Day 2), 0.6 ml (Day 3), 0.4 ml (Day 4), 0.7 ml (Day 5), and 0.8 ml (Day 6) of the drug into the breast muscle. After each injection, the chicken horn gradually becomes discolored to pink. After this treatment, the anemic chicken blood contains approximately 95% reticulocytes (early, mid-, and late polychromatic erythrocytes) and 3% mature erythrocytes [24]. On the seventh day, blood, which is obtained by severing or syringing the vein, is collected into 1 to 2 vol of ice-cold blood collection buffer (75 mM NaCl, 25 mM Tris–HCl, pH 7.5, 25 mM EDTA). The blood is filtered through four layers of cheesecloth to remove any debris. The cells are then collected by centrifugation at 3500 rpm (SS-34 rotor) for 10 min at 4 °C. The white buffy coat layer which contains white blood cells is removed by aspiration. The chicken erythrocytes are washed twice in Blood Collection Buffer, and then twice with Swim's S-77 Medium pH 7.2 (Sigma).

2.2.2. Incubation of avian immature erythrocytes with radiolabeled acetate

The packed chicken immature erythrocytes are resuspended in 2 vol of Swim's S-77 Medium containing 10 μg/ml cycloheximide in a large flask, and incubated for 30 min at 37 °C in a water bath with shaking. [^{3}H]Acetate (sodium salt) is then added into the flask to a final concentration of 0.1 mCi/ml. To inhibit histone deacetylation, sodium butyrate is added to a final concentration of 10 mM after 10 min incubation, and the cells are incubated for another 50 min. Following this treatment, erythrocytes are collected by centrifugation at 3500 rpm (SS-34 rotor) for 10 min. The cell pellet is then washed twice with 5 to 10 vol of Swim's S-77 Medium to remove unincorporated free isotope. The cells can be processed for histone isolation or stored at −80 °C for future use.

2.3. Isolation of radiolabeled histones

2.3.1. Small-scale preparation of radiolabeled acetylated histones from cultured mammalian cells

Approximately 10^6 mammalian cells (frozen or fresh) that are labeled with [^{3}H]acetate are resuspended in 5 ml

of TNM buffer (10 mM Tris–HCl, pH 8.0, 100 mM NaCl, 2 mM $MgCl_2$, 0.3 M sucrose) with 0.25% NonidetP-40 and 1 mM PMSF. The cells are homogenized with a glass homogenizer. The nuclei are collected by centrifugation at 4000 rpm (SS-34 rotor) for 10 min at 4 °C, and then washed with 10 ml of TNM buffer containing 1 mM PMSF. The nuclei are resuspended in 1 ml of TNM buffer containing 1 mM PMSF and mixed well with a pipet. Sulfuric acid stock (4 N) is added to the nuclei to a final concentration of 0.4 N while the suspension is mixed. The nuclei are then placed on ice for at least 30 min. After centrifugation at 10,000 rpm (SS-34 rotor) for 20 min at 4 °C, the supernatant containing the acid-extracted histones is collected and transferred to a dialysis bag (6000–8000 MW cutoff). The supernatant is dialyzed against 20 vol of 0.1 M acetic acid for 2 h at 4 °C, and then against 20 vol of deionized distilled water overnight at 4 °C with one change of water. The dialyzed acid extract is then lyophilized to a powder and resuspended in water, and the protein concentration and radioactivity are determined.

2.3.2. Large-scale preparation of radiolabeled acetylated histones from chicken immature erythrocytes

The procedure for large-scale preparation of histones from avian immature erythrocytes is similar to the preceding method. Approximately 20 ml of frozen packed chicken immature erythrocytes is washed twice in 100 ml of reticulocyte standard buffer (RSB: 10 mM Tris–HCl, pH 7.5, 10 mM NaCl, 3 mM $MgCl_2$, 5 mM sodium butyrate) and 1 mM PMSF. After centrifugation at 3500 rpm (SS-34 rotor) for 10 min at 4 °C, cells are resuspended in 40 ml of RSB containing 0.25% NonidetP-40 and 1 mM PMSF. The cells are homogenized with glass tissue grinder five times, and the nuclei are collected by centrifugation at 3500 rpm (SS-34 rotor) for 10 min at 4 °C. After being washed with 100 ml RSB, the nuclei are resuspended into 20 ml of RSB, and extracted with 0.4 N sulfuric acid by dropping 4 N stock into the suspension while mixing. The acid-extracted supernatant is collected by centrifugation at 10,000 rpm for 20 min at 4 °C, and then dialyzed against a large volume (4 liters) of 0.1 M acetic acid for 2 h, and then against deionized distilled water with one change of water overnight. The dialysate is then lyophilized and resuspended in deionized distilled water.

2.3.3. Preparation of H2A-H2B and H3-H4 histones

Different HDAC complexes may preferentially catalyze the deacetylation of different histones. For example, chicken erythrocyte HDAC1 associated with the nuclear matrix preferred H2A and H2B as substrates, while soluble HDAC1 in large complexes preferred H3 and H4 as substrates (Fig. 3) [25]. Here, we describe how to isolate H2A-H2B dimers and H3-H4 tetramers from chicken immature erythrocytes. The procedure includes preparation of nuclei and soluble chromatin, isolation of H2A-H2B dimers and H3-H4 tetramers, and extraction of histones.

The preparation of erythrocyte nuclei is the same as previously described. Briefly, cells are washed twice in RSB with 1 mM PMSF, and homogenized in RSB containing 0.25% NonidetP-40 and 1 mM PMSF. After centrifugation at 3500 rpm (SS-34 rotor) for 10 min at 4 °C, the nuclei are resuspended in W&S buffer (1 M hexylene glycol, 10 mM Pipes, pH 7.0, 2 mM $MgCl_2$, 1% thiodiglycol, 30 mM sodium butyrate, 1 mM $CaCl_2$). To determine the concentration of the preparation of nuclei, 10 μl of the sample of nuclei is introduced into 990 μl cell lysis solution (5 M urea, 2 M NaCl), and the absorbance at OD_{260} is measured. The concentration of nuclei is adjusted with W&S buffer to a final concentration of $50A_{260}$/ml. The nuclei are prewarmed for 10 min at 37 °C in a water bath with stirring. Micrococcal nuclease is then added to a final concentration of $15A_{260}$ units/ml, and the suspension of nuclei is incubated at 37 °C for 10 min. The digestion is stopped by adding 10 mM EGTA. After centrifugation at 10,000 rpm (SS-34 rotor) for 10 min, the pellet is resuspended in 10 mM EDTA with 5 mM sodium butyrate, and incubated on ice for at least 30 min to release the EDTA-soluble chromatin fraction. After centrifugation at 10,000 rpm for 10 min, the supernatant (SE) and pellet (PE) chromatin fractions are collected. The soluble chromatin fraction SE may be used to isolate the H2A-H2B dimers and H3-H4 tetramers, in some cases we used the S150 fraction, which is enriched in highly acetylated histones [26]. Further, radiolabeled acetylated histones from the S150 fraction will have a greater specific activity than those from the SE fraction. For preparation of S150, the SE chromatin fraction is diluted with 10 mM EDTA to a final concentration of $30A_{260}$/ml. The SE fraction is made 150 mM NaCl by slowly adding a 4 M NaCl stock solution. The supernatant fraction (S150) is collected by centrifugation at 10,000 rpm (SS-34 rotor) for 10 min. Hydroxylapatite (HTP) powder (Bio-Rad) is added to the SE or S150 chromatin fraction (1 g HTP/$80A_{260}$ of chromatin), and the HTP is packed into a column. The unbound fraction is allowed to flow out and the HTP column is washed with 10 vol of low-salt buffer (0.63 M NaCl, 1 mM DTT, 0.1 M potassium phosphate buffer, pH 6.7) to remove linker histones (H1 and H5) and other nonhistone chromosomal proteins. The HTP column is then eluted with salt gradient from low-salt buffer to high-salt buffer (2 M NaCl, 1 mM DTT, 0.1 M potassium phosphate buffer, pH 6.7). The eluted fractions are collected. The order of elution is H2A-H2B dimers followed by H3-H4 tetramers (Fig. 3). Sulfuric acid is then added to the chromatin fractions to a final concentration of 0.4 N to extract histones as mentioned above.

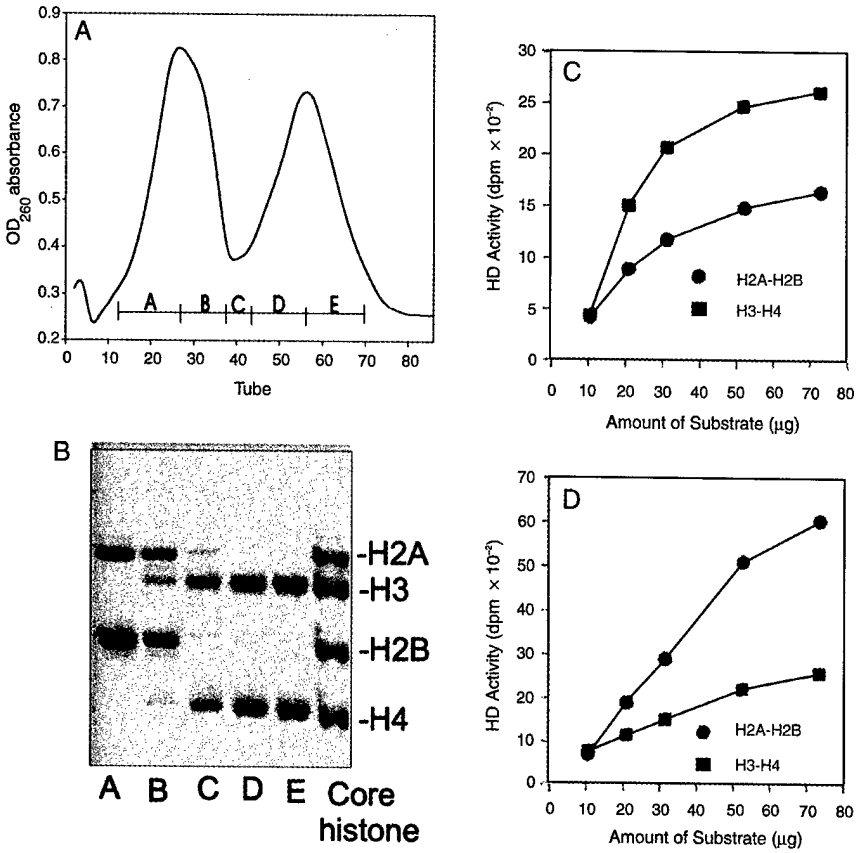

Fig. 3. Isolation of H2A-H2B dimers and H3-H4 tetramers as substrates in the HDAC assay. The chicken erythrocyte chromatin fraction (S150) was incubated with hydroxylapatite (HTP) and eluted by a salt gradient elution (0.63 M NaCl buffer to 2 M NaCl buffer). (A) Elution of histones from the HTP-bound chromatin. The histones from fractions (A–E) in the two peaks were acid extracted and separated onto a SDS–15% polyacrylamide gel, and the gel was stained with Coomassie blue. The Coomassie blue-stained gel shows the histones in the two peaks. The first peak contains H2A and H2B, and the second peak contains H3 and H4 (B). HDAC associated with nuclear matrices in chicken erythrocytes prefers H2A and H2B as a substrate (D), while HDAC in soluble high-molecular-mass complexes from chicken erythrocytes prefers H3 and H4 (C). Adapted, with permission, from Li et al. [25].

2.4. HDAC activity assay

HDAC catalyzes the removal of acetyl groups from lysine residues at the N-terminal tails of histones. Nonhistone chromosomal proteins, such as HMG proteins and transcription factors, are also substrates of HDACs [27,28]. In describing the assay, radiolabeled acetylated histone substrates are used. However, histone may be replaced with radiolabeled acetylated HMG or transcription factor substrates in this assay.

The test sample is incubated in a 1.5-ml tube in a final volume of 0.3 ml, containing 25 mM sodium phosphate buffer, pH 7.0, and 100 μg of [^{3}H]acetate (approximately 10,000 dpm)-labeled histones. For avian erythrocyte HDAC, 25 mM sodium phosphate buffer, pH 7.0 to 7.5, provided the highest HDAC activity [25]. Although the pH and buffer conditions may not have been maximal, we found that for total HDAC and HDAC1, two and three immunoprecipitated complexes were active in 25 mM sodium phosphate buffer, pH 7.0.

For each sample, a control reaction is included. The control reaction is identical to the test reaction except that the sample is boiled for 5 min to destroy the enzymatic activity before initiating the reaction. The reaction is incubated for 1 h at 37 °C with shaking, and then terminated by adding 30 μl of 2.5 N acetic acid/10 N HCl. The released radioactive acetate is extracted by adding 0.6 ml ethyl acetate with mixing. After centrifugation at 13,000 rpm for 1 min in a microcentrifuge, 0.3 ml of upper phase is transferred into a scintillation vial containing 5 ml scintillation liquid. Care should be taken when transferring the upper phase with a pipet tip. Touching the tip to the interphase will result in high background counts. The amount of [^{3}H]acetate released into the upper phase is determined using scintillation counting.

The enzymatic activity is calculated as follows:

$$\text{HDAC activity} = \{\text{counts (from test sample) (dpm)} - \text{counts (from control) (dpm)}\} / \{\text{time (h)/volume of sample (ml)}\}$$

The HDAC activity is usually plotted with the SigmaPlot program as described in Fig. 3.

2.5. Histone acetyltransferase activity assay

Commercially available ^{3}H-labeled (or ^{14}C-labeled) acetyl-coenzyme A (acetyl-CoA) and core histones are used in the HAT assay. HATs transfer [^{3}H]acetyl groups from acetyl-CoA to specific lysine residues in histones. Although the assay is described with histone substrates, the histone substrate may be replaced with another potential HAT substrate (e.g., an HMG protein or transcription factor). After the reaction, the radiolabeled acetylated histones are bound to P81 phosphocellulose paper to separate the histone from free acetyl-CoA. The radioactivity on the P81 paper is then determined by scintillation counting.

In the HAT assay, the test sample is added in a final reaction volume of 0.15 ml containing 50 mM Tris–HCl, pH 7.5, 50 mM sodium butyrate, 15 mM 2-mercaptoethanol, 100 μg of chicken histone, and 0.5 μCi acetyl CoA (>10 mCi/ml, from ICN, NEN, Sigma). The reaction is incubated at 37 °C with shaking for 1 h, and then the sample is spotted onto P81 phosphocellulose paper. The nonincorporated radiolabeled acetyl-CoA is removed by washing the P81 paper with a large volume of 50 mM sodium carbonate, pH 9.1.

We found that the variation of background, which is a consequence of incomplete washing of the P81 paper, is a serious problem in the HAT assay. Although washing P81 paper with large volumes of wash buffer with several changes is recommended, we found the background using this procedure is variable. To reduce the background counts on the P81 paper, we wash each piece of P81 paper individually using a stainless-steel vacuum filter system. Under these conditions, the variability of counts in triplicate sets of test reaction is approximately 10 to 20%. A P81 paper disk (2.5×2.5 cm^2) is assembled into the filter system and the vacuum aspiration started. The reaction is then dropped onto the disk, which is then washed with 50 ml of 50 mM sodium carbonate buffer. The P81 paper disk is removed from the unit and air-dried. The radioactivity on the P81 paper is counted in 5 ml of scintillation liquid. For all enzyme activity assays, the background is determined by measuring levels of radioactivity in boiled samples. The background counts are then subtracted from the label incorporated into the test sample.

2.6. Preparation of subcellular fractions for HDAC and HAT activity assays

2.6.1. Preparation of cellular extract

HDAC and HAT exist in the cytoplasm and nucleus. A cellular extract is used to measure the net cellular HDAC and HAT activities. Here we describe the preparation of a cellular extract from cultured mammalian cells. Cells are resuspended in TNM buffer (0.1 M NaCl, 0.3 M sucrose, 10 mM Tris–HCl, pH 7.4, 2 mM $MgCl_2$, 1% thiodiglycol) containing 1 mM PMSF, protease inhibitors, and 0.5% NonidetP-40. Cells are lysed by being passed five times through a syringe with a 22-gauge needle, and then five times through a 26-gauge needle. To extract tightly bound nuclear proteins such as HDACs, HATs, and transcription factors, the cell suspension is sonicated with 4 sets of 10-s periods at 30% output (Sonifer cell disrupter), with ice cooling. Under this condition, DNA is fragmented to an average length of 500 bp. After centrifugation at 10,000 rpm (SS-34 rotor) for 10 min, the supernatant (cellular extract) is collected. It is recommended that the quantitative release of the protein of interest be confirmed by immunoblot analyses of the supernatant and pellet fractions. In our experience the method quantitatively releases HDACs, HATs, and transcription factors such as the estrogen receptor and Sp1.

2.6.2. Fractionation of loosely bound and tightly bound nuclear proteins

We developed a procedure to isolate cytosol, nuclei, and tightly bound and loosely bound nuclear protein fractions (Fig. 4). Mammalian culture cells are suspended in TNM buffer (0.1 M NaCl, 0.3 M sucrose, 10 mM Tris–HCl, pH 7.4, 2 mM $MgCl_2$, 1% thiodiglycol) containing 1 mM PMSF and protease inhibitors, without any detergent. The nuclei are intact in this isotonic buffer and leakage of loosely bound nuclear proteins is reduced (e.g., the leakage of estrogen receptor from the nuclei of MCF-7 (T5) breast cancer cells grown under estrogen-depleted conditions was minimal). The cells (MCF-7 (T5) human breast cancer cells) are lysed by being passed through a syringe with a 22-gauge needle. For other culture cells tests should be done to decide the suitable gauge needle to lyse the cell by checking the integrity of the nuclei by microscopy. Part of the cell lysate is kept for preparation of the total cellular extract as described above. The rest of the cell lysate is centrifuged at 4500 rpm (SS34 rotor) for 10 min to collect the cytosol (supernatant) and nuclei (pellet). The nuclei are resuspended in the same volume of TNM buffer containing 1 mM PMSF and other protease inhibitors. Triton X-100 is added to a final concentration of 0.5%. The nuclei are incubated on ice for 5 min, allowing the release of loosely bound nuclear proteins. After centrifugation at 4500*g* for 10 min at 4 °C, the supernatant (Triton X-100-soluble fraction (Triton-S)) and pellet (Triton X-100-insoluble fraction (Triton-P), which contains the nuclear matrix proteins) are collected. We have used this protocol to determine the influence of estradiol on the subcellular distribution of estrogen receptor, HDACs, and HATs in human breast cancer cells [12] (Fig. 4). Fig. 4 shows the distribution of HDAC activity among the nuclear fractions, with most HDAC activity being present in the tightly bound nuclear protein fraction.

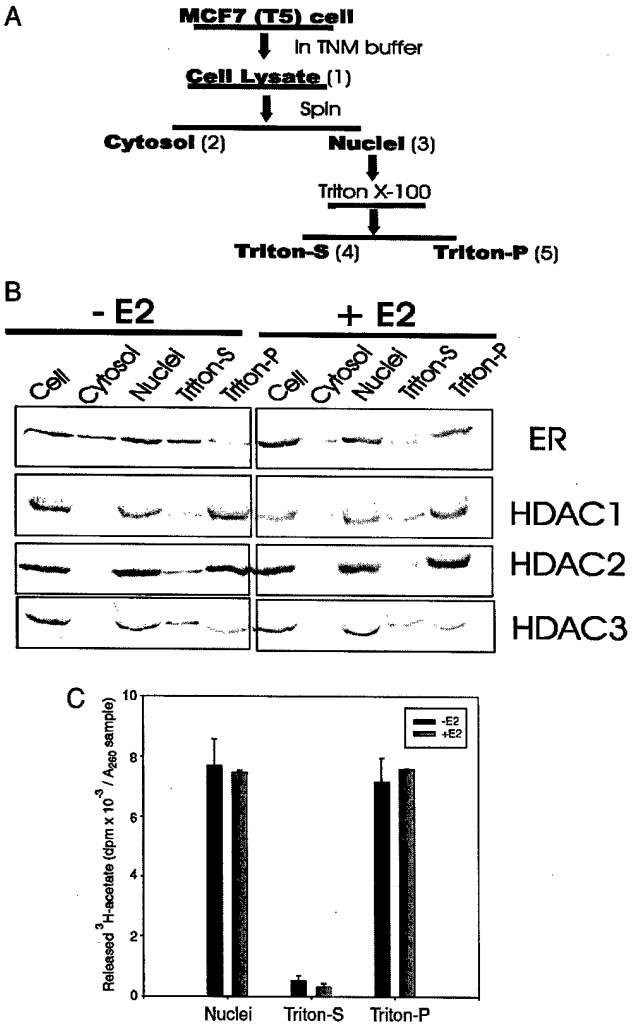

Fig. 4. Isolation of loosely bound and tightly bound nuclear proteins. MCF-7 (T5) human breast cancer cells were incubated for 20 min without (−E2) or with (+E2) 10 nM estradiol. (A) Flowchart of the protocol. (B) Immunoblot analyses showing the distribution of estrogen receptor and HDACs 1, 2, and 3 in cells incubated in the absence and presence of estradiol. (C) The HDAC assay was done on the nuclear, Triton-S, and Triton-P fractions. The assays were done in triplicate. Average counts from the test and control samples were calculated and plotted with the SigmaPlot program. Adapted, with permission, from Sun et al. [12].

2.6.3. *Isolation of protein complexes by immunoprecipitation*

Immunoprecipitation (IP) is a widely used approach to determine the protein composition of multiprotein complexes. This approach was used to demonstrate that HDACs are associated with mSin3 corepressor complex [29] and Sp1/Sp3 transcription factors [30]. The most important factor for a successful IP procedure is the antibody, which should have a high specificity and a high efficiency of precipitation.

2.6.3.1. Selection of an antibody for immunoprecipitation. To optimize the IP conditions, we first test the antibody's specificity for the antigen of interest with the cells and conditions to be applied. Next we test the efficiency of the antibody in IP. Immunoblot analysis will determine the specificity of an antibody. Fig. 5A is an example of testing the specificity of an antibody against HDAC1. This polyclonal antibody was produced using a 16-amino-acid peptide corresponding to the N terminal of mammalian HDAC1. The cell lysate or nuclear extract is loaded onto a SDS–polyacrylamide gel and transferred onto a nitrocellulose membrane. The membrane is immunochemically stained with the anti-HDAC1 antibody. Only one band was detected with this antibody. In the next step, we analyze the IP efficiency of the antibody. The ratio of cell lysate to antibodies can affect IP efficiency. To determine the optimal conditions, different amounts of cell lysate (0.5, 1, 2, and $4A_{260}$) are incubated with the same amount of antibody (2 μg) for at least 4 h at 4 °C. To the lysate is next added 50 μl of protein A:agarose (1:1) slurry and the mixture is incubated for 3 h at 4 °C. The immunodepleted (unbound) fraction and beads (bound fraction) are collected. IP efficiency is determined by immunoblot analyses of the total cell lysate (10 μl) and immunodepleted fraction (10 μl) using the anti-HDAC1 antibody. Fig. 5B shows that very little HDAC1 remains in the unbound, immunodepleted fraction, demonstrating the efficiency of this antibody in IP experiments.

2.6.3.2. Immunoprecipitation. Cellular extracts and cellular fractions can be used for immunoprecipitation to

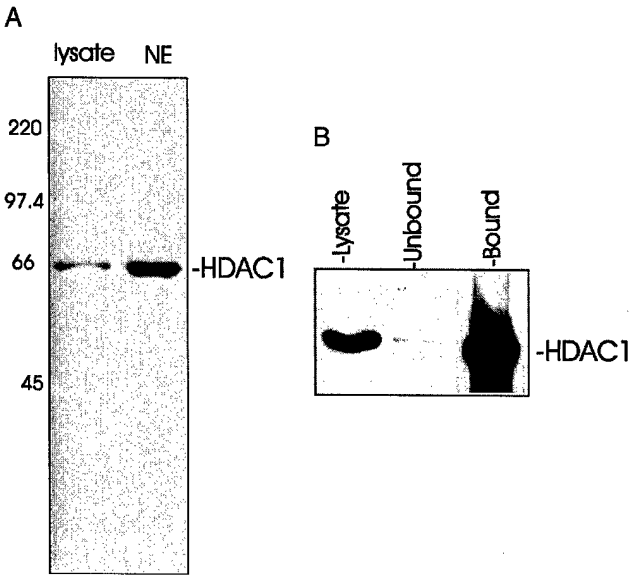

Fig. 5. Immunoblot analyses using anti-HDAC1 polyclonal antibodies. (A) Cell lysate (10 μl) and nuclear extract (10 μg) from MCF-7 (T5) cells were loaded onto a SDS–10% polyacrylamide gel and immunochemically stained with anti-HDAC1 antibodies. The cell lysate was immunoprecipitated by anti-HDAC1 antibodies. (B) Bound and unbound fractions were loaded on a SDS–10% polyacrylamide gel and immunochemically stained with anti-HDAC1 antibodies.

isolate the protein complexes of interest. When assaying the IP complex for HAT or HDAC activity, the buffers should not contain SDS which will destroy enzyme activity. To immunoprecipitate a multiprotein complex, we use either a low-stringency IP buffer (50 mM Tris–HCl, pH 8.0, 150 mM NaCl, 0.5% NonidetP-40, 1 mM EDTA, 1 mM PMSF, protease inhibitors, and phosphatase inhibitors in some experiments) or PBS buffer. The cells are resuspended in IP buffer and incubated on ice for 5 min. Cells are lysed by five passages through a 22-gauge needle. The cell lysate is then sonicated with four sets of 10-s pulses at 30% output (Sonifer cell disrupter). The cell lysate should be kept on ice between each sonication. After centrifugation at 10,000 rpm (SS34 rotor) for 10 min, the supernatant is collected and saved for IP.

The enzymatic assay and control are typically done in triplicate. Equivalent amounts of input cell lysate, antibodies, and protein A beads are used for each assay. Two A_{260} units of the cell lysate is diluted to 1 ml by adding IP buffer. The optimal amount of antibody is added to $2A_{260}$ of cell lysates. When immunoprecipitating HDAC1, we use 2 μg of anti-HDAC1 antibody with $2A_{260}$ of MCF-7 (T5) cell lysate. After incubation for at least 4 h or overnight at 4 °C, 25 μl of protein A:agarose and 25 μl of protein G:agarose (1:1) slurry are added and incubated for another 2 h. The beads are collected by a brief spin in a microcentrifuge. The beads are washed four times with 1 ml of IP buffer. Several control assays are done in parallel. First, equal amounts of cell lysate and buffer are incubated with 2 μg of preimmune serum, instead of the primary antibodies. Second, the beads with the immunoprecipitate were boiled for 5 min before adding substrate. HDAC and HAT assays may be done with the multiprotein complexes bound to the protein A/G beads.

2.6.4. Isolation of nuclear matrices

Nuclear matrix is the nuclear substructure that consists of nucleoli, nuclear pore–lamina complex, and internal nuclear matrix. The nuclear matrix is a dynamic structure that has a role in organization and function (replication, transcription) of nuclear DNA. HDACs, HATs, and transcription factors are associated with nuclear matrix.

2.6.4.1. Isolation of nuclear matrices from cultured mammalian cells. The cells are washed twice with ice-cold PBS and then harvested. The cells are resuspended in TNM buffer containing 0.25% Triton X-100 and 1 mM PMSF. The cell suspension is lysed by five passages through a 22-gauge needle. The nuclei are collected by centrifugation at 4500 rpm in a microcentrifuge for 10 min at 4 °C. The nuclei are resuspended in 0.5 ml of Penman digestion buffer (10 mM Pipes (pH 6.8 with KOH), 5 mM NaCl, 0.3 M sucrose, 3 mM $MgCl_2$, 1 mM EGTA, 0.5% Triton X-100, 1 mM PMSF (freshly added for each application)). The concentration of the sample is measured by taking the OD_{260} of a 10-μl sample diluted in 990 μl of 2 M NaCl/5 M urea. The sample is adjusted to $20A_{260}$/ml with Penman digestion buffer. The nuclei are digested by adding DNase I to a final concentration of 0.1 mg/ml and incubating the suspension of nuclei at room temperature for 1 h. The chromatin is released from the nuclei by adding ammonium sulfate from a 4 M stock to a final concentration 0.25 M with mixing. The insoluble nuclear matrix is collected by centrifugation at 6500 rpm (SS34 rotor) for 10 min at 4 °C. Small amounts of core histones may remain with this nuclear matrix fraction, and the residual chromatin may be removed by a 2 M NaCl extraction.

Avian erythrocyte nuclear matrices resuspend homogenously in a number of different buffers (e.g., TNM, RSB) and thus are suitable for the enzymatic assay. However, the nuclear matrices from mammalian culture cells tend to aggregate. To resolve this problem, the nuclear matrices are disrupted by sonication. Nuclear matrices are resuspended in 0.5 ml of IP Buffer or TNM buffer with 1 mM PMSF and protease inhibitors. The nuclear matrices, kept on ice, are sonicated twice for 15 s at 30% output (Sonifer cell disrupter). The sonicated nuclear matrices are assayed for HDAC and HAT activity.

2.6.4.2. Isolation of nuclear matrices from chicken erythrocytes. The nuclear matrix proteins of chicken erythrocytes are easily released in the presence of high salt and a reducing agent. We prepare the soluble nuclear matrix extract from chicken erythrocytes by extraction of DNase I-digested nuclei with 2 M NaCl and β-mecaptoethanol.

Approximately 5 ml of chicken erythrocyte pellets are washed twice by resuspending them in 30 ml of CKS buffer (100 mM KCl, 3 mM $MgCl_2$, 10 mM Pipes, pH 6.8, 1 mM EGTA, 0.3 M sucrose, 0.5% thiodiglycol, 1 mM PMSF) and centrifuged at 4000 rpm (SS-34 rotor) for 10 min at 4 °C. Cells are resuspended in 30 ml of CKS buffer with 0.25% Triton X-100, and homogenized with five strokes in a glass homogenizer. The nuclei are collected by centrifugation at 4000 rpm (SS34 rotor) for 10 min. The nuclei are resuspended in 10 ml of CKS buffer and passed three times through a 22-gauge needle. The nuclei are intact in this isotonic CKS buffer. The nuclei are next processed by gradient centrifugation to remove cytoplasmic contaminates. Twenty milliliters of 0.7 M sucrose–CKS buffer (same as CKS buffer except 0.7 M sucrose instead of 0.3 M sucrose) is transferred into a 40-ml centrifuge tube. Ten milliliters of the suspension of nuclei (in CKS buffer containing 0.3 M sucrose) is carefully layered on the top of the 0.7 M sucrose–CKS buffer. The tube is centrifuged at 4000 rpm (SS-34 rotor) for 10 min. The upper phase is removed and the white-gray pellet contains the isolated nuclei which are next resuspended in 5 ml of digestion buffer (10 mM Pipes, pH 6.8, 5 mM NaCl, 0.3 M sucrose,

3 mM $MgCl_2$, 1 mM EGTA, 0.5% Triton X-100, 1 mM PMSF). The absorbance at OD_{260} of the suspension of nuclei is measured by diluting 10 μl of nuclear suspension into 990 μl of 2 M NaCl/5 M urea. The nuclei are adjusted to $20A_{260}$/ml with digestion buffer. DNase I is added to the nuclei at a final concentration of 0.1 mg/ml. After incubation of the nuclei at room temperature for 60 min, ammonium sulfate is added to the DNase-digested nuclei to a final concentration of 0.25 M with mixing. After centrifugation at 6500 rpm (SS34 rotor) for 10 min, the nuclear matrices (pellet) are resuspended in 1 ml of digestion buffer. RNase A is added to a final concentration of 10 μg/ml and incubated at room temperature for 10 min. The nuclear matrices are extracted by adding β-mercaptoethanol to a final concentration of 1% (v/v) and incubating on ice for 30 min. After an equal volume of 4 M NaCl is added to the nuclear matrices, the soluble nuclear matrix proteins are isolated by centrifugation at 10,000 rpm (SS34 rotor) for 10 min. The supernatant is placed into a dialysis bag (6000–8000 MW cutoff) and dialyzed against buffer D (20 mM Hepes, pH 7.9, 20% glycerol, 0.1 M KCl, 0.2 mM EDTA, 0.5 mM PMSF, 0.5 mM DTT) at 4 °C overnight. Insoluble material is removed by centrifugation at 10,000 rpm (SS34 rotor) for 10 min.

2.7. Measurement of histone acetylation rates

There are at least three classes of acetylated histones: one is in a "frozen" state, another class is rapidly acetylated and deacetylated, and third class is slowly acetylated and deacetylated. In human breast cancer cells, approximately 60–70% histones are acetylated. In contrast, only 2% of the histones in avian immature erythrocytes are engaged in dynamic acetylation. Pulse–chase experiments to determine rates of histone acetylation are presented.

2.7.1. Pulse–chase labeling experiments with cultured mammalian cells

Mammalian cells are grown to a confluence of 70 to 80%. The medium is removed, and cells are washed with prewarmed PBS. The cells are cultured in this medium containing cycloheximide (10 μg/ml) for 30 min and then incubated at 37 °C with fresh medium containing [^{3}H]acetate (0.1 mCi/ml, special activity >10 Ci/mmol) for 15 min. We selected this labeling time as histones engaged in the fast and slow rates of histone acetylation are labeled and the extent of labeling allows detection of the radiolabeled histone by fluorography. For human breast cancer cells, the rapidly acetylated histone class is detectable following a 5- or15-min labeling period.

Following incubation of the cells with the radiolabel (the pulse), cells are washed twice with DMEM medium, without FBS, containing 10 mM sodium butyrate and 0.1 mM nonradioactive acetate. The cells are chased in the same buffer at 37 °C for various times (0, 5, 10, 20, 30, 60, 120, and 240 min). The cells are washed with ice-cold PBS containing 10 mM butyrate and harvested for histone isolation.

2.7.2. AUT–polyacrylamide gel electrophoresis and fluorography

Histones are resolved on AUT–15% polyacrylamide gels which resolve histones according to their size, charge, and hydrophobicity. For details of the AUT–polyacrylamide gel electrophoresis of histones see [31].

The AUT gel is stained with Coomassie blue and destained. A reference picture of the stained gel is taken and then the gel is soaked in an autoradiography enhancer, EN^{3}HANCE (NEN), for 30 min followed by soaking in deionized distilled H_2O for 60 min. The treated gel, which becomes white, is transferred on a Whatman filter paper. The gel is covered with a piece of plastic wrap and dried at 80 °C in a Gel Dryer system for 60 min. The gel is exposed to X-ray film (Kodak X-OMAT AR) for several days (3 to 7 days on the average, but in some cases 1 month). The intensities of the acetylated H4, H3, and H2B isoforms in the fluorographic films are scanned and analyzed using the one-dimensional gel analysis program (Pharmacia–Amersham).

The intensities of the monoacetylated histone isoforms for H4, H2B, and H3.2 are plotted as function of chase time. The proportion of the radiolabeled monoacetylated histone present in total radiolabeled histone at zero time is arbitrarily set at 100. Fig. 6 shows a pulse–chase experiment to determine the rates of histone acetylation in human breast cancer cells. Fig. 6A shows the AUT gel pattern and accompanying fluorogram containing histone from different chase times. Fig. 6B shows the plots of H4, H2B, and H3.2. The plot shows two rates of acetylation for the histones. The first steep slope corresponds to the rapidly acetylated histone, while the second sustained gradual slope corresponds to the slow rate of histone acetylation.

2.7.3. Calculation of histone acetylation rates

The rate of acetylation ($t_{1/2}$) is calculated as the time for the level of the radiolabeled monoacetylated isoform to decrease to one-half of its initial value. The following formula is applied to determine rates of acetylation:

$$\ln N_0/N = kt$$

$$t_{1/2} = 0.693/k$$

(N_0 is the original radioactivity, N is the changed radioactivity, ln is natural log function, t is period of time). Two rates of acetylation were observed for H4, a fast rate with a $t_{1/2}$ of 8 min and a slow rate with a $t_{1/2}$ of 200–350 min. H3.2 also had two rates of acetylation: a fast rate with a $t_{1/2}$ of 8 min and a slow rate with a $t_{1/2}$ of

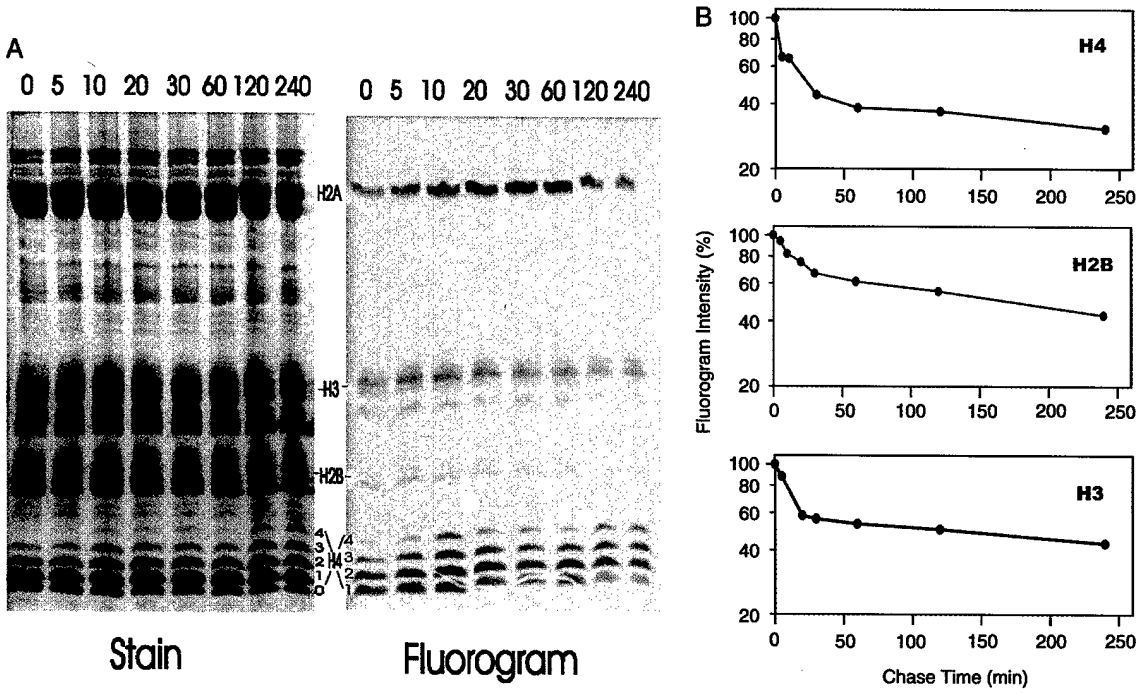

Fig. 6. Histone acetylation rates. Human breast cancer MCF-7 (T5) cells were pulse-labeled with [^{3}H]acetate for 15 min and chased in 10 mM sodium butyrate for 0, 5, 10, 20, 30, 60, 120, and 240 min. Twenty micrograms of histone was loaded on AUT–15% polyacrylamide gel and electrophoresed. (A) The gel was stained with Coomassie blue and fluorographed. (B) The intensities of the bands on the X-ray film were determined and the rate of histone acetylation was calculated and plotted. Aadapted, with permission, from Sun et al. [12].

400 min. The two acetylated rates for H2B were $t_{1/2} = 10$ and 350 min (Fig. 6). These rates of acetylation are comparable to those observed in rat hepatoma cells, human fibroblasts, and avian erythrocytes [12].

2.8. Measurement of histone deacetylation rates

To determine the rate of histone deacetylation, cells are incubated with radiolabeled acetate for 120 min in the presence of butyrate, resulting in radiolabeling of the highest acetylated histone isoforms. The rate of deacetylation is followed after the removal of radiolabel and butyrate.

2.8.1. Pulse–chase labeling cells

Mammalian cells are incubated with cycloheximide (10 μg/ml) for 30 min before labeling. Cycloheximide is also present during the radiolabeling period. The cells are incubated at 37 °C for 120 min in medium containing 10 mM butyrate, cycloheximide, and [^{3}H]acetate (0.1 mCi/ml, specific activity >10 Ci/mmol). After labeling, the cells are washed three times with PBS and then incubated in the medium without sodium butyrate. Following various times of incubation, the cells are washed and harvested.

2.8.2. Calculation of histone deacetylation rates

The isolated histones are electrophoretically resolved on AUT–15% polyacrylamide gels and fluorographed as described in Section 2.7. The X-ray film is scanned and intensities of the radiolabeled acetylated histone isoforms are plotted. Fig. 7 shows the rate of histone deacetylation in human breast cancer cells. The results demonstrate the rapid deacetylation of the hyperacetylated histones (e.g., tetra-acetylated H4).

The radiolabeled histone isoforms detected on the X-ray film are scanned, and the intensities of the hyperacetylated isoform (such as tetra-acetylated H4) are plotted against time of incubation. The amount of labeled tetra-acetylated H4 present at zero time was arbitrarily set at 100. The rate of deacetylation ($t_{1/2}$) is calculated as the time for the level of the radiolabeled tetra-acetylated isoform to decrease to one-half of the initial value using the formula given above (Section 2.6.3).

The rate of deacetylation is rapid, with the intensity of hyperacetylated isoform (such as tetra-acetylated H4) decreasing significantly after 20 min following the removal of sodium butyrate. Calculation of the rate ($t_{1/2}$) of histone deacetylation is similar to that described in Section 2.6.

3. Concluding remarks

Both HAT and HDAC assays are useful in deciding whether a transcription factor recruits a coactivator/HAT complex and/or a corepressor/HDAC complex. Further as HATs, HDACs, and transcription factors are

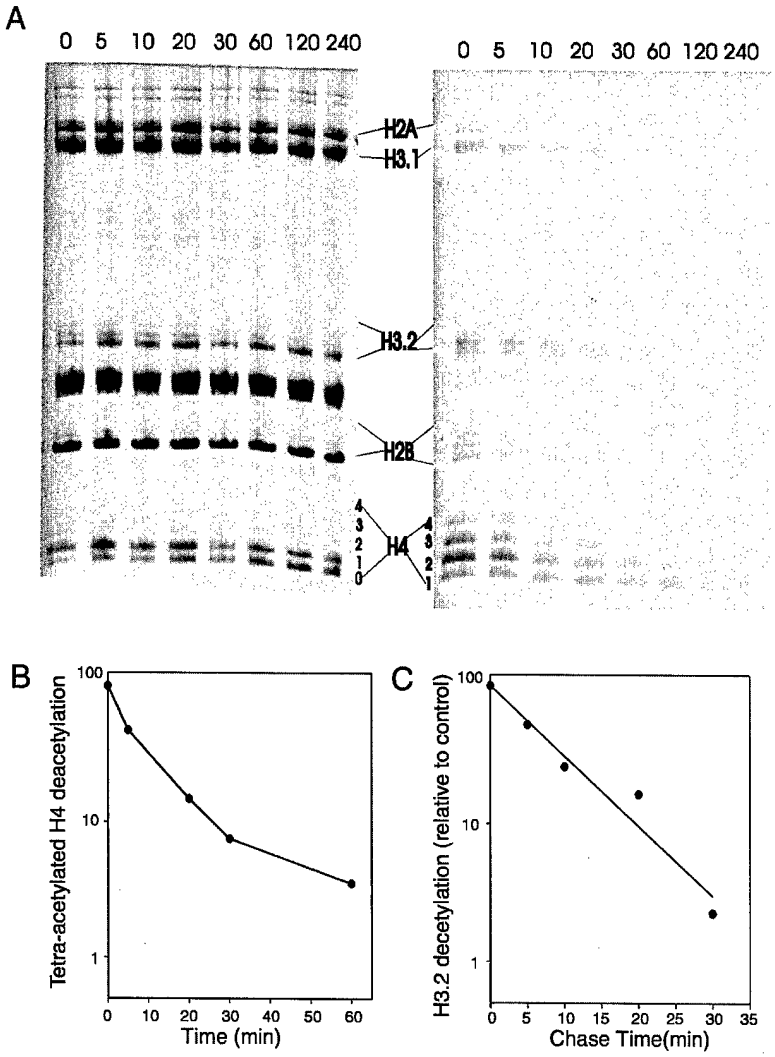

Fig. 7. Histone deacetylation rate. Human breast cancer MCF-7 (T5) cells were pulse-labeled with [^{3}H]acetate for 120 min in the presence of 10 mM sodium butyrate. The cells were chased in the absence of butyrate for 0, 5, 10, 20, 30, 60, 120, and 240 min. Twenty micrograms of histone was loaded on an AUT–15% polyacrylamide gel, and electrophoresed. (A) The gel was stained with Coomassie blue and fluorographed. (B) The intensities of the radiolabeled bands on the X-ray film were determined, and the rate of histone deacetylation was calculated and plotted. Adapted, with permission, from Sun et al. [12].

modified by acetylation, phosphorylation, glycosylation, and/or SUMO-1 conjugation, these assays will be useful in deciding the function of the modification on enzymatic activity [30]. The methods described for measuring HAT and HDAC activities are presented using histone substrates. However, histones may be replaced with HMG or specific transcription factors (e.g., estrogen receptor, GATA-1, Sp3, p53), which are also substrates for these enzymes.

Acknowledgments

This research was supported by grants from U.S. Army Medical and Materiel Command Breast Cancer Research Program (DAMD17-00-1-0319), the Canadian Institutes of Health Research (CIHR) (MT-9186, RGP-15183), the National Cancer Institute of Canada with funds from the Canadian Cancer Society, and Cancer-Care Manitoba Foundation, Inc, and studentships to Lin Li from the Guardian Angels Foundation and to Virginia Spencer from the U.S. Army Medical and Materiel Command Breast Cancer Research Program (DAMD17-01-1-0309).

Appendix A. Reagents

A.1. Blood collection buffer

75 mM NaCl, 25 mM Tris–HCl, pH 7.5, 25 mM EDTA

A.2. TNM buffer

10 mM Tris–HCl, pH 8.0, 100 mM NaCl, 2 mM $MgCl_2$, 0.3 M sucrose

A.3. Reticulocyte standard buffer (RSB)

10 mM Tris–HCl, pH 7.5, 10 mM NaCl, 3 mM $MgCl_2$, 5 mM sodium butyrate

A.4. W&S buffer

1 M hexylene glycol, 10 mM Pipes, pH 7.0, 2 mM $MgCl_2$, 1% thiodiglycol, 30 mM sodium butyrate,1 mM $CaCl_2$

A.5. Low-salt buffer

0.63 M NaCl, 1 mM DTT, 0.1 M potassium phosphate buffer, pH 6.7

A.6. High-salt buffer

2 M NaCl, 1 mM DTT, 0.1 M potassium phosphate buffer, pH 6.7

A.7. IP buffer

50 mM Tris–HCl, pH 8.0, 150 mM NaCl, 0.5% NonidetP-40, 1 mM EDTA, 1 mM PMSF, protease inhibitors (1 μg/ml leupeptin, 0.1 μg/ml aprotinin, 20 μg/ml bestatin), phosphatase inhibitors (10 mM NaF, 1 mM Na_3VO_4, 25 mM β-glycerophosphate)

A.8. Penman digestion buffer

10 mM Pipes (pH 6.8 with KOH), 5 mM NaCl, 0.3 M sucrose, 3 mM $MgCl_2$, 1 mM EGTA, 0.5% Triton X-100, 1 mM PMSF

A.9. CKS buffer

100 mM KCl, 3 mM $MgCl_2$, 10 mM Pipes, pH 6.8, 1 mM EGTA, 0.3 M sucrose, 0.5% thiodiglycol, 1 mM PMSF

A.10. Buffer D

20 mM Hepes, pH 7.9, 20% glycerol, 0.1 M KCl, 0.2 mM EDTA, 0.5 mM PMSF, 0.5 mM DTT

A.11. HAT assay buffer

50 mM Tris–HCl, pH 7.5, 50 mM sodium butyrate, 15 mM 2-mercaptoethanol

References

[1] J.R. Davie, M. Moniwa, Crit Rev. Eukaryot. Gene Expr. 10 (2000) 303–325.
[2] V.A. Spencer, J.R. Davie, Gene 240 (1999) 1–12.
[3] B.G. Pogo, V.G. Allfrey, A.E. Mirsky, Proc. Natl. Acad. Sci. USA 55 (1966) 805–812.
[4] J.C. Hansen, Chemtracts: Biochem. Mol. Biol. 10 (1997) 56–69.
[5] C. Tse, J.C. Hansen, Biochemistry 36 (1997) 11381–11388.
[6] S.C. Moore, J. Ausio, Biochem. Biophys. Res. Commun. 230 (1997) 136–139.
[7] M. Garcia-Ramirez, C. Rocchini, J. Ausio, J. Biol. Chem. 270 (1995) 17923–17928.
[8] V.A. Spencer, J.R. Davie, J. Biol. Chem. 276 (2001) 34810–34815.
[9] J.R. Davie, Mol. Biol. Rep. 24 (1997) 197–207.
[10] J. Covault, R. Chalkley, J. Biol. Chem. 255 (1980) 9110–9116.
[11] D.-E. Zhang, D.A. Nelson, Biochem. J. 250 (1988) 241–245.
[12] J.-M. Sun, H.Y. Chen, J.R. Davie, J. Biol. Chem. 276 (2001) 49435–49442.
[13] D.E. Sterner, S.L. Berger, Microbiol. Mol. Biol. Rev. 64 (2000) 435–459.
[14] T.N. Collingwood, F.D. Urnov, A.P. Wolffe, J. Mol. Endocrinol. 23 (1999) 255–275.
[15] M. Grunstein, Nature 389 (1997) 349–352.
[16] H. Walia, H.Y. Chen, J.-M. Sun, L.T. Holth, J.R. Davie, J. Biol. Chem. 273 (1998) 14516–24522.
[17] C. Tse, T. Sera, A.P. Wolffe, J.C. Hansen, Mol. Cell. Biol. 18 (1998) 4629–4638.
[18] A. Doetzlhofer, H. Rotheneder, G. Lagger, M. Koranda, V. Kurtev, G. Brosch, E. Wintersberger, C. Seiser, Mol. Cell. Biol. 19 (1999) 5504–5511.
[19] B. Nare, J.J. Allocco, R. Kuningas, S. Galuska, R.W. Myers, M.A. Bednarek, D.M. Schmatz, Anal. Biochem. 267 (1999) 390–396.
[20] Y. Kim, K.G. Tanner, J.M. Denu, Anal. Biochem. 280 (2000) 308–314.
[21] M.J. Hendzel, G.P. Delcuve, J.R. Davie, J. Biol. Chem. 266 (1991) 21936–21942.
[22] J.-M. Sun, H.Y. Chen, M. Moniwa, S. Samuel, J.R. Davie, Biochemistry 38 (1999) 5939–5947.
[23] D.-E. Zhang, D.A. Nelson, Biochem. J. 250 (1988) 233–240.
[24] A.F. Williams, J. Cell Sci. 10 (1972) 27–46.
[25] W. Li, H.Y. Chen, J.R. Davie, Biochem. J. 314 (1996) 631–637.
[26] G.P. Delcuve, J.R. Davie, Biochem. J. 263 (1989) 179–186.
[27] M. Bergel, J.E. Herrera, B.J. Thatcher, M. Prymakowska-Bosak, A. Vassilev, Y. Nakatani, B. Martin, M. Bustin, J. Biol. Chem. 275 (2000) 11514–11520.
[28] H. Braun, R. Koop, A. Ertmer, S. Nacht, G. Suske, Nucleic Acids Res. 29 (2001) 4994–5000.
[29] C.D. Laherty, W.-M. Yang, J.-M. Sun, J.R. Davie, E. Seto, R.N. Eisenman, Cell 89 (1997) 349–356.
[30] J.M. Sun, H.Y. Chen, M. Moniwa, D.W. Litchfield, E. Seto, J.R. Davie, J. Biol. Chem. 277 (2002) 35783–35786.
[31] G.P. Delcuve, J.R. Davie, Anal. Biochem. 200 (1992) 339–341.

Accelerated Publication

THE JOURNAL OF BIOLOGICAL CHEMISTRY
Vol. 277, No. 39, Issue of September 27, pp. 35783–35786, 2002

The Transcriptional Repressor Sp3 Is Associated with CK2-phosphorylated Histone Deacetylase 2*

Received for publication, June 25, 2002,
and in revised form, August 7, 2002
Published, JBC Papers in Press, August 9, 2002,
DOI 10.1074/jbc.C200378200

Jian-Min Sun, Hou Yu Chen, Mariko Moniwa, David W. Litchfield‡, Edward Seto§, and James R. Davie¶

From the Manitoba Institute of Cell Biology, Winnipeg, Manitoba R3E 0V9, Canada, ‡Department of Biochemistry, University of Western Ontario, London, Ontario N6A 5C1, Canada, and §H. Lee Moffitt Cancer Center and Research Institute, University of South Florida, Tampa, Florida 33612

Sp1 and Sp3 are ubiquitously expressed mammalian transcription factors that function as activators or repressors. Although both transcription factors share a common domain involved in forming multimers, we demonstrate that Sp1 and Sp3 form separate complexes in estrogen-dependent human breast cancer cells. Sp1 and Sp3 complexes associate with histone deacetylases (HDACs) 1 and 2. Although most HDAC2 is not phosphorylated in the breast cancer cells, HDAC2 bound to Sp1 and Sp3 and cross-linked to chromatin *in situ* is highly enriched in a phosphorylated form that has a reduced mobility in SDS-polyacrylamide gels. We show that protein kinase CK2 is associated with and phosphorylates HDAC2. Alkaline phosphatase treatment of HDAC2 and Sp1 and Sp3 complexes reduced the associated HDAC activity. Protein kinase CK2 is up-regulated in several cancers including breast cancer, and Sp1 and Sp3 have key roles in estrogen-induced proliferation and gene expression in estrogen-dependent breast cancer cells. CK2 phosphorylation of HDAC2 recruited by Sp1 or Sp3 could regulate HDAC activity and alter the balance of histone deacetylase and histone acetyltransferase activities and dynamic chromatin remodeling of estrogen-regulated genes.

Remodeling of chromatin structure mediated by ATP-driven chromatin-remodeling complexes and histone-modifying enzymes has a crucial role in gene expression. Acetylation of the core histones favors decondensation of the chromatin fiber by preventing interfiber interactions, whereas the unacetylated histone state contributes to chromatin condensation (1, 2). Dynamic histone acetylation catalyzed by histone deacetylases (HDAC)[1] and histone acetyltransferases allows the chromatin fiber to rapidly oscillate from the condensed and decondensed states (3, 4). In mammalian cells three classes of HDACs are identified. Class I HDACs, such as HDAC1 and HDAC2, are homologous to yeast RPD3, whereas class II HDACs are similar to yeast HDA1. Class III HDACs are related to yeast SIR2 (5, 6). HDAC1 and -2 are components of large multisubunit complexes called Sin3 or NuRD, which are recruited by transcriptional factors such as Mad, YY1, and Rb (5, 7–9).

Mammalian cells ubiquitously express Sp1 and Sp3. Sp3 has three isoforms, a long (L-Sp3) and two short forms (M1-Sp3, M2-Sp3) that are the products of differential translational initiation (10). Sp3 may act as a repressor or an activator, with the short forms acting only as repressors (10). The protein structure of L-Sp3 is very similar to that of Sp1, except that Sp3 has a repression domain located N-terminal to the zinc finger DNA-binding domain (11). It has been reported that the relative levels of Sp3 forms change with differentiation, with the differentiated Caco-2 cells expressing more long than short forms (12). Further, alterations in the relative levels of Sp1 to Sp3 have been recorded, with Sp3 levels being greater than Sp1 in primary keratinocytes (13).

In this study we investigated the association of histone deacetylase with Sp3 in human breast cancer cells. We found that Sp3 and Sp1 were associated with HDAC1 and a modified form of HDAC2. HDAC2 is shown to be associated with protein kinase CK2 and phosphorylated by this enzyme. The low abundance phosphorylated form of HDAC2 is preferentially associated with chromatin.

EXPERIMENTAL PROCEDURES

Cells and Plasmid—Human breast cancer T5 cells, estrogen receptor-positive and hormone-dependent, were grown in Dulbecco's modified Eagle's medium and 5% fetal bovine serum as previously described (4). T5 cells were grown under estrogen-depleted conditions, and in some cases estradiol was added for 20 min as reported (4). Plasmid pGST-HDAC2 has been described previously (14).

Cisplatin and Formaldehyde DNA Cross-linking—T5 cells were incubated with 1 mM cisplatin at 37 °C for 2 h or with 1% formaldehyde at room temperature for 10 min as described previously (3, 15). The methods for isolating the proteins cross-linked to DNA *in situ* are described in detail (16, 17). Briefly, following cross-linking, cells were washed twice with TNM buffer (100 mM NaCl, 300 mM sucrose, 10 mM Tris-HCl, pH 8.0, 2 mM $MgCl_2$, 1% thiodiglycol) containing 1 mM PMSF, phosphatase inhibitors (25 mM β-glycerophosphate, 10 mM sodium fluoride, 1 mM sodium orthovanadate) and protease inhibitor mixture (Roche Molecular Biochemicals). The cells were resuspended in cross-linking lysis buffer (5 M urea, 2 M guanidine hydrochloride, 2 M NaCl, and 0.2 M potassium phosphate buffer, pH 7.5) containing 1 mM PMSF, and the lysate was incubated with prehydrated hydroxyapatite (Bio-Rad). DNA-protein cross-links were reversed, and proteins were isolated.

Immunoprecipitation—T5 cells were lysed in immunoprecipitation buffer (50 mM Tris-HCl, pH 8.0, 150 mM NaCl, 0.5% Nonidet P-40, 1 mM EDTA) containing 1 mM PMSF, phosphatase inhibitors, and protease inhibitors mixture. The cells were sonicated twice for 15 s. The cell lysate was collected by centrifugation at 10,000 × *g* for 10 min at 4 °C and incubated with anti-Sp1 or anti-Sp3 antibodies for 16 h at 4 °C. The

* This research was supported in part by Canadian Institute of Health Research (CIHR) Grant MT-9186 and United States Army Medical and Material Command Breast Cancer Research Program Grant DAMD17-00-1-0319. The costs of publication of this article were defrayed in part by the payment of page charges. This article must therefore be hereby marked "*advertisement*" in accordance with 18 U.S.C. Section 1734 solely to indicate this fact.

¶ Recipient of a CIHR Senior Scientist award. To whom correspondence should be addressed: Manitoba Institute of Cell Biology, 675 McDermot Ave., Winnipeg, Manitoba R3E 0V9, Canada. Tel.: 204-787-2391; Fax: 204-787-2190; E-mail: davie@cc.umanitoba.ca.

[1] The abbreviations used are: HDAC, histone deacetylase; CK2, protein kinase CK2; L-Sp3, long form of Sp3; M1- and M2-Sp3, short forms of Sp3; PMSF, phenylmethylsulfonyl fluoride; GST, glutathione *S*-transferase; IP, immunoprecipitation; ID, immunodepletion.

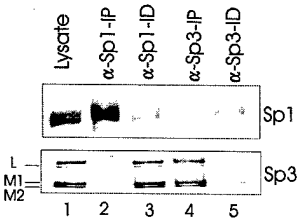

FIG. 1. **Sp1 is not associated with Sp3.** Two A_{260} of T5 cell lysate were incubated with 4 μg of anti-Sp1 antibodies, and the immunoprecipitation (*IP*, *lane 2*) and immunodepletion (*ID*, *lane 3*) fractions were collected. The immunodepleted fraction was next incubated with anti-Sp3 antibodies, yielding IP (*lane 4*) and ID (*lane 5*) fractions. Ten μl of cell lysate (*lane 1*), IP, and ID fractions were loaded onto a SDS-10% polyacrylamide gel, transferred to nitrocellulose membranes, and immunochemically stained with anti-Sp1 and anti-Sp3 antibodies. The long (L) and short (M1 and M2) forms of Sp3 are identified.

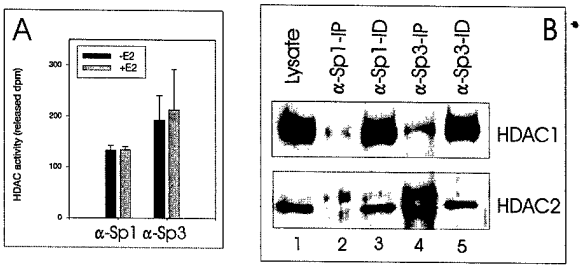

FIG. 2. **Sp1 and Sp3 are associated with HDAC1 and HDAC2.** Two A_{260} of T5 cell lysate treated with (*+E2*) or without (*−E2*) 10 nM estradiol was immunoprecipitated using 4 μg of anti-Sp1 and anti-Sp3 antibodies. HDAC activities of immunoprecipitated fractions were analyzed using ^{3}H-labeled histones (*A*). Each value represents the mean ± S.E. of three different preparations. In *B*, 10 μl of cell lysate, IP, and ID fractions prepared as described in Fig. 1 were loaded onto a SDS-10% polyacrylamide gel, transferred to nitrocellulose membranes, and immunochemically stained with anti-HDAC1 and HDAC2 antibodies.

beads were washed four times with 5 volumes of immunoprecipitation buffer and frozen at −80 °C.

Sequential Immunoprecipitations—Sequential immunoprecipitations were done as described above. Briefly, cell lysates were incubated with anti-Sp1 antibodies. The immunoprecipitated and immunodepleted (supernatant) fractions were collected. Secondary immunoprecipitations were done with anti-Sp3 antibodies, and the immunoprecipitated and immunodepleted fractions were collected.

Immunoblot Analysis—Immunoblot analysis was carried out as described previously (4). Polyclonal antibodies against human HDAC1 (Affinity Bioreagents Inc. (ABR)), HDAC2 (ABR), HDAC3 (ABR), Sp1 (Santa Cruz Biotechnology Inc.), and Sp3 (Santa Cruz) were used. Polyclonal antibodies against CK2α and -α' were described previously (18). Quantification of proteins on immunoblots was done as described previously (19).

HDAC Activity Assay—HDAC activity assays were performed as reported previously (20).

Protein Phosphatase Digestion—Immunoprecipitated fractions and DNA cross-linked protein fractions were incubated with or without calf intestinal alkaline phosphatase (Amersham Biosciences) at 37 °C for 1 h. The protein was separated on SDS-12% polyacrylamide gels and transferred onto nitrocellulose membrane for immunochemical staining.

Protein Kinase CK2 Assay—Purified GST-HDAC2 was incubated in a buffer consisting of 50 mM Tris-HCl, pH 7.5, 10 mM $MgCl_2$, 1 mM dithiothreitol, 25 mM β-glycerophosphate, 10 mM sodium fluoride, 1 mM sodium orthovanadate, 1 mM PMSF, and 100 μM ATP solution containing [γ-^{32}P]ATP at a final concentration of 1 μCi/μl. The reaction tube was preincubated at 30 °C for 10 min before the addition of purified CK2 (from bovine testis as described previously (18, 21)). The reaction was incubated for 10 min before termination upon the addition of SDS sample buffer. The sample was boiled for 5 min and loaded into a SDS-15% polyacrylamide gel. After electrophoresis, the gel was dried and autoradiographed.

RESULTS AND DISCUSSION

Sp1 and Sp3 contain a similar D domain that is required for the proteins to form multimers (22–24). *In vitro* evidence suggests that Sp1 and Sp3 may form heteromultimers (24). Sequential immunoprecipitations and immunoblotting experiments tested whether Sp1 associated with Sp3 *in situ* in T5 human breast cancer cells. A T5 cell lysate was incubated with anti-Sp1 antibodies, and the immunoprecipitate was collected. The immunodepleted supernatant was next incubated with anti-Sp3 antibodies, and the immunoprecipitate was harvested. Fig. 1 shows the analyses of the fractions immunochemically stained with anti-Sp3 or anti-Sp1 antibodies. Anti-Sp1 antibodies efficiently immunoprecipitated Sp1 but not Sp3 (*lane 2*), whereas antibodies against Sp3 immunoprecipitated Sp3 but not Sp1 (*lane 4*). The results demonstrated that Sp1 does not associate with Sp3 in T5 cells. Further, the immunoblot results show that T5 breast cancer cells express the L-, M1-, and M2-Sp3 forms, with the latter lower molecular mass forms of Sp3 predominating. Quantification of Sp1 and Sp3 levels on immunoblots indicated that Sp1 was 3-fold more abundant than Sp3.

It has been reported that Sp1 recruits HDAC1 to repress transcription (25). It is conceivable that Sp3 also recruits HDAC to repress transcription. Fig. 2*A* shows that Sp1 and Sp3 were associated with HDAC activity. Culturing breast cancer cells in the absence or presence of estradiol did not affect the HDAC activity associated with these transcription factors. The sequential immunoprecipitation strategy with anti-Sp1 followed by anti-Sp3 antibodies was applied to decide which of the HDACs was bound to Sp1 or Sp3. Fig. 2*B* shows that Sp1 and Sp3 were associated with HDAC1 and HDAC2. Both immunoprecipitates were highly enriched in a slower migrating form of HDAC2. Neither Sp1 nor Sp3 was associated with HDAC3 (data not shown).

The preferential association of the slower migrating form of HDAC2 with the transcription factors Sp1 and Sp3 suggested that this form of HDAC2 may be selectively in contact with chromatin. T5 cells were incubated with the cross-linker cisplatin, and the proteins cross-linked to nuclear DNA *in situ* were isolated. Unlike formaldehyde, cisplatin does not form protein-protein cross-links. Fig. 3*A* shows that the slower migrating form of HDAC2 was enriched in the proteins cross-linked to DNA. Similar results were obtained with the cross-linker formaldehyde. HDAC3 was not cross-linked to nuclear DNA with cisplatin.

As HDAC1 is phosphorylated (26, 27), we determined whether the slower migrating form of HDAC2 was phosphorylated by incubating the proteins cross-linked to DNA with alkaline phosphatase. Fig. 3*B* demonstrates that incubation of the protein sample with alkaline phosphatase resulted in the disappearance of the slower migrating form of HDAC2 and the appearance of a band co-migrating with the major HDAC2 band present in the cell lysate. Identical results were obtained when the Sp1 or Sp3 immunoprecipitates were incubated with alkaline phosphatase (data not shown). The phosphorylated form of HDAC1 has a reduced mobility on SDS gels (27). However, we did not observe an enrichment of the slower migrating HDAC1-phosphorylated form in the Sp1 or Sp3 immunoprecipitates or in the protein fraction cross-linked to DNA with cisplatin. Treatment of these fractions with alkaline phosphatase did not alter the mobility of HDAC1, ruling out the possibility that the entire HDAC1 population was phosphorylated.

Recently, HDAC1 was shown to be phosphorylated by CK2 (26, 27). The CK2 phosphorylation sites located in the C-terminal region of HDAC1 are conserved in HDAC2 (27). Fig. 4*A* illustrates that incubation of HDAC2 in the cell lysate with CK2 and ATP generates the slower migrating HDAC2 form. Inhibition of CK2 with apigenin prevented the appearance of this band. Further, GST-HDAC2 and casein but not GST were radiolabeled with CK2 and [^{32}P]ATP (Fig. 4*B*). To decide if CK2

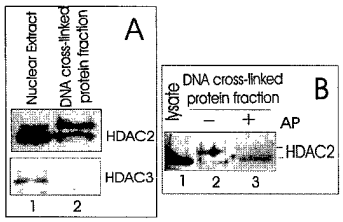

FIG. 3. **Phosphorylated HDAC2 is preferentially associated with chromatin.** T5 cells were incubated with 1 mM cisplatin, and proteins cross-linked to DNA were isolated. Ten μg of protein was separated on a SDS-12% polyacrylamide gel, transferred onto nitrocellulose membranes, and immunochemically stained with anti-HDAC2 and anti-HDAC3 antibodies (*A*). Protein cross-linked to DNA was incubated with or without alkaline phosphatase, separated on a SDS-12% polyacrylamide gel, and immunochemically stained with anti-HDAC2 antibodies (*B*).

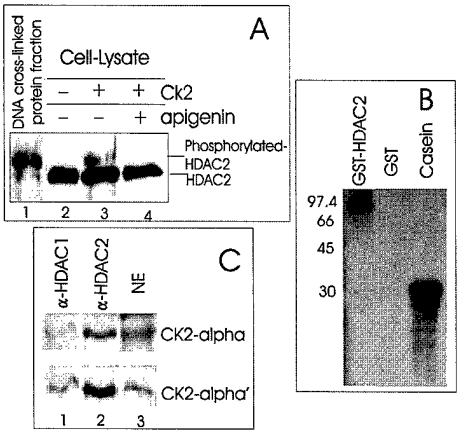

FIG. 4. **Protein kinase CK2 phosphorylates HDAC2.** An equal amount of cell lysate protein (20 μg) was incubated with or without purified CK2 and with or without 80 μM apigenin in the presence ATP. The control and treated samples and 10 μg of protein cross-linked to DNA with cisplatin were loaded onto a SDS-12% polyacrylamide gel, transferred onto nitrocellulose membranes, and immunochemically stained with anti-HDAC2 antibody (*A*). Purified GST-HDAC2 fusion protein, GST, and casein were incubated with purified CK2 in the presence of [γ-^{32}P]ATP. The samples were loaded onto a SDS-15% polyacrylamide gel. The dried gel was autoradiographed (*B*). *C*, an equal amount of T5 cell lysate (2 A_{260}) was immunoprecipitated with 4 μg of anti-HDAC1 and anti-HDAC2 antibodies. After washing with immunoprecipitation buffer, the beads were boiled in SDS loading buffer. The immunoprecipitated samples and nuclear extracted protein (10 μg) were loaded onto a SDS-10% polyacrylamide gel, transferred to a nitrocellulose membrane, and immunochemically stained with anti-CK2α and anti-CK2α' antibodies.

was associated with HDAC2, HDAC2 and HDAC1 immunoprecipitates were analyzed by immunoblotting with anti-CK2α or anti-CK2α' antibodies (Fig. 4*C*). HDAC2 and to a lesser extent HDAC1 were bound to CK2. Immunoblotting experiments of Sp1 and Sp3 immunoprecipitates revealed the presence of CK2 (data not shown).

In immunoprecipitation and immunoblotting experiments we determined that most HDAC2 was in complex with HDAC1 in T5 breast cancer cells. HDAC1, which was more abundant than HDAC2, was in complex with HDAC2 and with other complexes not containing HDAC2. Incubation of HDAC1 and HDAC2 immunoprecipitates with alkaline phosphatase reduced the HDAC activity of the complexes (Fig. 5). The associated HDAC activities with Sp1 and Sp3 immunoprecipitates were also reduced when incubated with alkaline phosphatase.

In summary, we demonstrate that Sp3 and Sp1 are associated with HDAC1 and CK2-phosphorylated HDAC2. Although most HDAC2 is in an unmodified state, phosphorylated HDAC2 is preferentially associated with Sp1, Sp3, and chromatin in human breast cancer cells. CK2 is up-regulated in

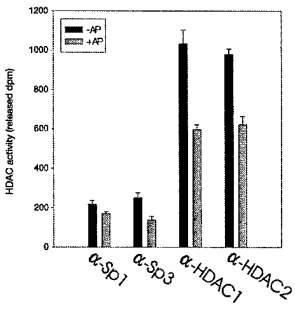

FIG. 5. **Phosphatase digestion reduces HDAC activity associated with Sp1 and Sp3.** An equal amount of cell lysate (2 A_{260}) was immunoprecipitated with anti-Sp1, anti-Sp3, anti-HDAC1, and anti-HDAC2 antibodies. These immunoprecipitated fractions were incubated with (*+AP*) or without (*−AP*) alkaline phosphatase, and HDAC activities were measured. Each value represents the mean ± S.E. of three different preparations.

several cancers including breast cancer, and there is evidence that CK2 may promote breast cancer by deregulating key transcription processes (28–30). Many estrogen-induced genes (*e.g.* cathepsin D, c-*fos*, adenine deaminase, and c-*myc*) in human breast cancer cells have a half-site estrogen response element positioned next to a Sp1 binding site (31–33). Sp3 would compete with Sp1 to bind the regulatory regions of these genes. Both Sp1 and Sp3 may recruit HDAC1 and phosphorylated HDAC2 to these sites, whereas the estrogen receptor recruits histone acetyltransferases CBP (cAMP-response element-binding protein (CREB)-binding protein) and p300, resulting in dynamic acetylation of histones and transcription factors located at the promoters of these genes (4, 34, 35). CK2 phosphorylation of HDAC2 recruited by Sp1 or Sp3 would regulate HDAC activity and alter the balance of histone deacetylase and histone acetyltransferase activities and dynamic chromatin remodeling of these estrogen-regulated promoters.

REFERENCES

1. Wang, X., He, C., Moore, S. C., and Ausio, J. (2001) *J. Biol. Chem.* **276,** 12764–12768
2. Tse, C., Sera, T., Wolffe, A. P., and Hansen, J. C. (1998) *Mol. Cell. Biol.* **18,** 4629–4638
3. Spencer, V. A., and Davie, J. R. (2001) *J. Biol. Chem.* **276,** 34810–34815
4. Sun, J.-M., Chen, H. Y., and Davie, J. R. (2001) *J. Biol. Chem.* **276,** 49435–49442
5. Davie, J. R., and Moniwa, M. (2000) *Crit Rev. Eukaryotic Gene Expression* **10,** 303–325
6. Fischle, W., Kiermer, V., Dequiedt, F., and Verdin, E. (2001) *Biochem. Cell Biol.* **79,** 337–348
7. Ferreira, R., Naguibneva, I., Pritchard, L. L., Ait-Si-Ali, S., and Harel-Bellan, A. (2001) *Oncogene* **20,** 3128–3133
8. Lai, A., Kennedy, B. K., Barbie, D. A., Bertos, N. R., Yang, X. J., Theberge, M. C., Tsai, S. C., Seto, E., Zhang, Y., Kuzmichev, A., Lane, W. S., Reinberg, D., Harlow, E., and Branton, P. E. (2001) *Mol. Cell. Biol.* **21,** 2918–2932
9. Yao, Y. L., Yang, W. M., and Seto, E. (2001) *Mol. Cell. Biol.* **21,** 5979–5991
10. Kennett, S. B., Udvadia, A. J., and Horowitz, J. M. (1997) *Nucleic Acids Res.* **25,** 3110–3117
11. Suske, G. (1999) *Gene (Amst.)* **238,** 291–300
12. Gartel, A. L., Goufman, E., Najmabadi, F., and Tyner, A. L. (2000) *Oncogene* **19,** 5182–5188
13. Apt, D., Watts, R. M., Suske, G., and Bernard, H. U. (1996) *Virology* **224,** 281–291
14. Yang, W. M., Yao, Y. L., Sun, J. M., Davie, J. R., and Seto, E. (1997) *J. Biol. Chem.* **272,** 28001–28007
15. Samuel, S. K., Spencer, V. A., Bajno, L., Sun, J.-M., Holth, L. T., Oesterreich, S., and Davie, J. R. (1998) *Cancer Res.* **58,** 3004–3008
16. Spencer, V. A., and Davie, J. R. (2002) in *The Protein Protocols Handbook* (Walker, J. M., ed) pp. 747–752, Humana Press, Totowa, NJ
17. Spencer, V. A., and Davie, J. R. (2002) in *The Protein Protocols Handbook* (Walker, J. M., ed) pp. 753–760, Humana Press, Totowa, NJ
18. Gietz, R. D., Graham, K. C., and Litchfield, D. W. (1995) *J. Biol. Chem.* **270,** 13017–13021
19. Zhao, H., Hart, L. L., Keller, U., Holth, L. T., and Davie, J. R. (2002) *J. Cell. Biochem.* **86,** 365–375
20. Hendzel, M. J., Delcuve, G. P., and Davie, J. R. (1991) *J. Biol. Chem.* **266,** 21936–21942
21. Sun, J.-M., Chen, H. Y., Litchfield, D. W., and Davie, J. R. (1996) *J. Cell. Biochem.* **62,** 454–466
22. Mastrangelo, I. A., Courey, A. J., Wall, J. S., Jackson, S. P., and Hough, P. V. (1991) *Proc. Natl. Acad. Sci. U. S. A.* **88,** 5670–5674

23. Pascal, E., and Tjian, R. (1991) *Genes Dev.* **5,** 1646–1656
24. Kennett, S. B., Moorefield, K. S., and Horowitz, J. M. (2002) *J. Biol. Chem.* **277,** 9780–9789
25. Doetzlhofer, A., Rotheneder, H., Lagger, G., Koranda, M., Kurtev, V., Brosch, G., Wintersberger, E., and Seiser, C. (1999) *Mol. Cell. Biol.* **19,** 5504–5511
26. Cai, R., Kwon, P., Yan-Neale, Y., Sambuccetti, L., Fischer, D., and Cohen, D. (2001) *Biochem. Biophys. Res. Commun.* **283,** 445–453
27. Pflum, M. K., Tong, J. K., Lane, W. S., and Schreiber, S. L. (2001) *J. Biol. Chem.* **276,** 47733–47741
28. Landesman-Bollag, E., Romieu-Mourez, R., Song, D. H., Sonenshein, G. E., Cardiff, R. D., and Seldin, D. C. (2001) *Oncogene* **20,** 3247–3257
29. Landesman-Bollag, E., Song, D. H., Romieu-Mourez, R., Sussman, D. J., Cardiff, R. D., Sonenshein, G. E., and Seldin, D. C. (2001) *Mol. Cell Biochem.* **227,** 153–165
30. Tawfic, S., Yu, S., Wang, H., Faust, R., Davis, A., and Ahmed, K. (2001) *Histol. Histopathol.* **16,** 573–582
31. Safe, S. (2001) *Vitam. Horm.* **62,** 231–252
32. Dubik, D., and Shiu, R. P. (1992) *Oncogene* **7,** 1587–1594
33. Abdelrahim, M., Samudio, I., Smith, R., III, Burghardt, R., and Safe, S. (2002) *J. Biol. Chem.* **277,** 28815–28822
34. Chen, H., Lin, R. J., Xie, W., Wilpitz, D., and Evans, R. M. (1999) *Cell* **98,** 675–686
35. Shang, Y., Hu, X., DiRenzo, J., Lazar, M. A., and Brown, M. (2000) *Cell* **103,** 843–852

ACADEMIC PRESS

Available online at www.sciencedirect.com

SCIENCE DIRECT®

Methods 31 (2003) 67–75

METHODS

www.elsevier.com/locate/ymeth

Chromatin immunoprecipitation: a tool for studying histone acetylation and transcription factor binding

Virginia A. Spencer, Jian-Min Sun, Lin Li, and James R. Davie*

Manitoba Institute of Cell Biology, University of Manitoba, Winnipeg, Manitoba, Canada R3E 0V9

Accepted 19 February 2003

Abstract

The function of a protein in gene expression can often be explained, in part, by the location of that protein along a specific gene sequence. In recent years, the chromatin immunoprecipitation (ChIP) assay has been developed to study the association of proteins located within 2 Å of DNA such as transcription factors and modified histones. Numerous important findings have been published using the ChIP assay and many questions about transcription have been answered. In this article, we present the ChIP assay currently used in our lab and discuss the various ways to optimize this assay for one's own use.

Keywords: Chromatin immunoprecipitation; Histone; Transcription factor; Formaldehyde; Cisplatin

1. Introduction

The chromatin immunoprecipitation (ChIP) assay has become a very popular technique for fine-mapping the location of modified histones, transcription factors, and nonhistone chromosomal proteins. Moreover, it is an in situ technique that offers a more physiological representation of nuclear events involved in the processing of DNA. In this assay, cells are incubated briefly with the crosslinker formaldehyde to prevent the separation of DNA-associated proteins from their target DNA sequence in subsequent steps (Fig. 1). The cells are then sonicated to fragment the DNA, and the lysate is centrifuged to remove insoluble cellular debris. The cleared lysate is incubated with a primary antibody, and the antibody–antigen complexes are then captured with protein A– or protein G–Sepharose depending on the nature of the antibody. The Sepharose is washed several times with buffers containing different salt and detergent concentrations, and the antibody–antigen complexes are eluted from the protein A/G with a high detergent elution buffer. The protein complement of the immune complexes is then digested away and the DNA isolated by ethanol precipitation.

Initially, the ChIP assay was used to study the association of hyperacetylated histones with specific DNA sequences to further understand the role of histone acetylation in transcription [1]. However, more recent studies have used the ChIP protocol to characterize DNA sequences associated with specific transcription factors [2,3].

To date, numerous articles have presented different versions of the ChIP protocol. However, minute yet significant details that may improve the success of this protocol are often excluded from these articles. The purpose of this article is to present a ChIP protocol used to study DNA sequences associated with both acetylated histones and transcription factors and to discuss the various ways to optimize this protocol.

2. Methods

2.1. Chromatin immunoprecipitation

The following protocol has been devised from previously published protocols [1,4].

2.1.1. Formaldehyde crosslinking

MCF-7 (T5) cells grown on a 150 × 20-mm tissue culture dish to approximately 80–90% confluence are

* Corresponding author. Fax: +204-787-2190.
E-mail address: Davie@cc.umanitoba.ca (J.R. Davie).

1046-2023/$ - see front matter © 2003 Published by Elsevier Science (USA).
doi:10.1016/S1046-2023(03)00089-6

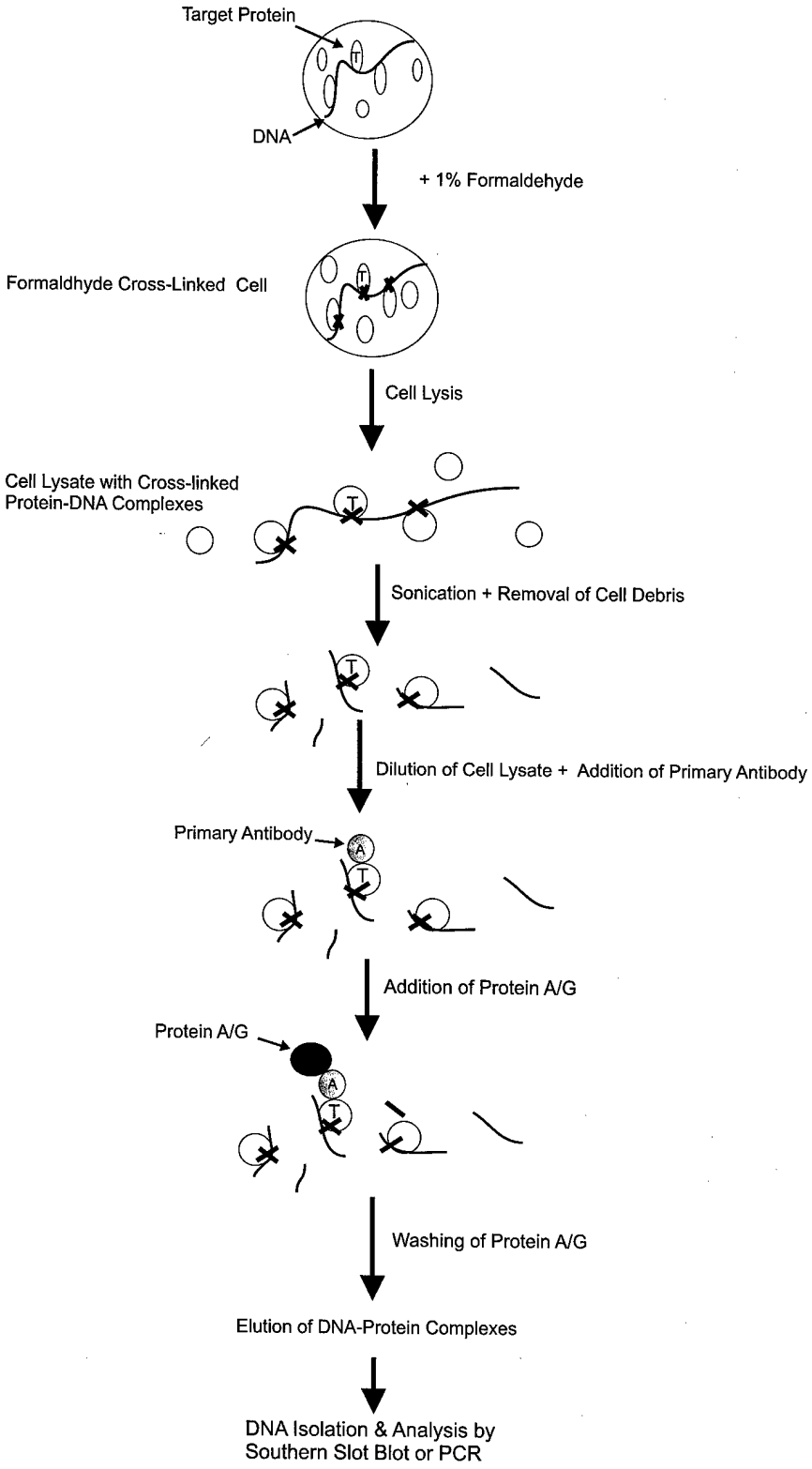

Fig. 1. Schematic representation of the ChIP protocol. In the ChIP protocol, cells are treated with 1% formaldehyde to crosslink proteins to DNA. The cells are then lysed and sonicated to fragment the DNA. The sonicated lysate is centrifuged to remove cell debris, and diluted to 2 A_{260} units/ml with dilution or 1× RIPA buffer. Primary antibody is added to the sample, and the sample is incubated for 2 h to overnight. Protein A/G–Sepharose is then added to the sample to capture the immune complexes and the sample is incubated for 2 h. Proteins and DNA nonspecifically associated with the protein A/G are removed by washing the resin. Immune complexes are eluted from the protein A/G resin and the DNA associated with the target antigen is isolated and analyzed by Southern slot-blot analysis or PCR.

incubated with 10 ml of 1% formaldehyde in 1× PBS for 8–10 min at room temperature (see Sections 3.3 and 3.4). The cells are washed two times with 1× ice-cold PBS, harvested with a rubber policeman, and then either stored at −80 °C or resuspended in 750 μl of lysis buffer A containing protease inhibitors (1 mM PMSF, 1 μg/ml aprotinin, 10 μg/ml leupeptin, 50 μM iodoacetamide). Depending on the nature of the target protein to be investigated, phosphatase and kinase inhibitors as well as deacetylase inhibitors may be included in the lysis buffer.

2.1.2. Preparation of the cell lysate for immunoprecipitation

The cell lysate is placed on ice and sonicated for 14-30-s pulses at 40% output with a Braun-Sonic 1510 Sonicator. These sonication conditions may vary with different types of sonicators. As well, the degree of sample sonication may vary depending on the length and location of the target DNA sequence (see Section 3.6). Therefore, to determine the ideal conditions for sonication, one should perform a preliminary experiment where a cell lysate is sonicated for various time lengths and the size of the DNA fragments determined by agarose gel electrophoresis.

To determine the size of DNA fragments, 10–20 μl of sonicated cell lysate is made up to 100 μl with double-distilled water. The sample is then incubated at 68 °C for 6 h to overnight and supplemented with 50 μg/μl proteinase K for another 1–2 h at 55 °C. After protein removal, an equal volume of phenol:chloroform:isoamyl alcohol (24:23:1) is added to the sample and the sample is mixed, then centrifuged at 10,000 rpm for 3 min in a microcentrifuge. The top aqueous phase is transferred to a new microcentrifuge tube and supplemented with 1/10th the volume of sodium acetate and 2–3 vol of absolute ethanol. The DNA is then precipitated by incubating the sample at −80 °C for at least 1 h. Following precipitation, the DNA is washed once with ice-cold 70% ethanol, resuspended in 20 μl double-distilled water, supplemented with loading buffer, and analyzed on an ethidium bromide-stained agarose gel.

After sonication, the cell lysate is centrifuged at 10,000 rpm for 10 min at 4 °C in a microcentrifuge. This step removes the insoluble cellular debris. Following this, the amount of A_{260} units/ml is determined by spectrophotometry and the cell lysate is diluted to 2 A_{260} units/ml with 1× RIPA containing 1 mM PMSF, 1 μg/ml aprotinin, 10 μg/ml leupeptin, and 50 μM iodoacetamide. As mentioned previously, inhibitors of kinases, phosphatases, and/or histone deacetylases can be added to the diluted sample depending on the nature of the target protein. Alternative buffers can be used such as dilution buffer or buffers with lower salt and detergent concentration. However, decreasing the salt and detergent concentrations may increase the amount of non-specific protein–DNA complexes that associate with protein A/G. The cell lysate is diluted before antibody addition to reduce the amount of complexes brought down nonspecifically by the protein A/G–Sepharose in the subsequent step.

Two hundred microliters of the diluted lysate is set aside to represent input DNA sequences in the ChIP DNA analyses. This sample is diluted to 350 μl with double-distilled water and incubated at 68 °C for 6 h to overnight to reverse the formaldehyde DNA–protein complexes. RNase A is then added to the diluted input to a final concentration of 40 μg/μl, and the sample incubated at 37 °C for 1 h. Following RNA digestion, the proteins are removed and the ChIP DNA is isolated as described in Section 2.1.4.

2.1.3. Immunoprecipitation of the target protein

Primary antibody is added to the diluted lysate and the sample incubated 30 min to overnight at 4 °C (see Section 3.1). Shorter time intervals such as 30 min are recommended for incubation with the primary antibody to limit the amount of nonspecific proteins associated with the antibody. The amount of DNA associated nonspecifically with protein A/G should be controlled for by including a no antibody control and a preimmune serum control. In the latter case, one should ideally use a volume of preimmune serum (preferentially isolated from the animal prior to immunization) that is equivalent to that of the test primary antibody. However, this approach is usually not feasible and instead an isotype-matched antibody recognizing a nonnuclear, and non-DNA-binding protein can be used.

After the initial primary antibody incubation, 5 μg of sonicated *Escherichia coli* or salmon sperm competitor DNA and 10 μg of BSA are added to the sample to reduce the nonspecific association of protein or DNA sequences with the protein A/G–Sepharose. Fifty microliters of 50:50 (v/v) protein A/G:Sepharose (Amersham Pharmacia, NJ) is then added to the sample to capture the immune complexes and the sample incubated at 4 °C for 2 h (see Section 3.5). To further reduce the levels of DNA and proteins nonspecifically associated with the protein A/G–Sepharose, the resin can be pretreated with 0.1 mg/ml of sonicated salmon sperm or *E. coli* DNA and 1 mg/ml BSA for a minimum of 1 h.

DNA and proteins nonspecifically associated with the protein A/G–Sepharose are removed by washing the resin three times with 1× RIPA, three times with 1× RIPA supplemented with NaCl to a final concentration of 1 M, two times with 250 mM LiCl buffer, and two times with TE (pH 8) buffer. Each wash is performed over 4 min. Alternatively, the protein A/G–Sepharose can be washed for 5–10 min each with low-salt buffer, high-salt buffer and 250 mM LiCl buffer, and then twice with TE (pH 8) buffer. The number and type of washes

depend on the amount of nonspecific protein–DNA complexes associated with the protein A/G–Sepharose.

Once the protein A/G–Sepharose has been washed, the immunoprecipitated DNA–protein complexes are collected at room temperature by incubating the Sepharose in 200 μl of 1.5% SDS (w/v) elution buffer for 15 min, centrifuging the beads in a microcentrifuge at 3000 rpm for 1 min, and then transferring the eluted complexes to a microcentrifuge tube. The beads are then resuspended in 150 μl of 0.5% SDS (w/v) elution buffer for 15 min and centrifuged, and the additional eluted complexes are pooled together with the complexes in 1.5% SDS elution buffer. Alternatively, protein–DNA complexes can be removed by incubating the protein A/G in an elution buffer containing 1% SDS (w/v) and 0.1 M $NaHCO_3$.

2.1.4. Isolation of DNA associated with the immunoprecipitated protein

The eluted protein–DNA complexes are incubated at 68 °C for 6 h to overnight to reverse the formaldehyde crosslinks, and then at 55 °C for 2 h in the presence of 200 mM NaCl, 10 mM EDTA (pH 8), 40 mM Tris–HCl (pH 6.5), and 50 μg/ml proteinase K to digest the protein. The sample is then extracted with a 25:24:1 mixture of phenol:chloroform:isoamyl alcohol and precipitated in the presence of carrier DNA with 2–3 vol of absolute ethanol. Between 5 and 10 μg glycogen is typically used as carrier. Other carriers such as tRNA can also be used, however, tRNA is 70 to 90 nucleotides long and, when stained with ethidium bromide, appears as a smear below 100 bp on an agarose gel. To remove any residual salt, the ChIP DNA is washed once with ice-cold 70% ethanol, air-dried, and resuspended in 20 μl double-distilled water or TE buffer (pH 8). If one wishes to avoid this method of DNA purification, a DNA isolation kit can be used but the efficiency of this kit in the isolation of very small amounts of DNA should be tested first.

A ChIP DNA sample will contain anywhere from 50 to several hundred nanograms of DNA depending on the antibody's ability to efficiently immunoprecipitate its target protein. However, the exact amount of immunoprecipitated DNA in a sample is difficult to determine since competitor DNA is also present. Because of this, ChIP DNA samples are usually analyzed by volume.

2.1.5. Analysis of DNA associated with the immunoprecipitated protein

The DNA isolated from a ChIP assay can be analyzed by either Southern slot blot analysis or PCR. If analyzed by Southern slot-blotting, the DNA can be applied to a nylon membrane and hybridized to radiolabeled or digoxygenin (DIG)-labeled DNA probes [5]. Alternatively, the ChIP DNA can be radiolabeled or DIG-labeled and used as a probe to hybridize to specific genomic DNA sequences blotted on a nylon membrane [6].

In the past few years, the method of choice for ChIP DNA analysis has been PCR. For studying the association of acetylated H3, acetylated H4, ERα, and HDAC1 with a specific DNA region, we typically use 2 μl of input DNA in one PCR and 4 μl of ChIP DNA in another identical PCR, with both reactions containing primers to the target DNA region. However, different antibodies display different efficiencies in their ability to immunoprecipitate their target antigen. Therefore, the volume of ChIP DNA in each PCR is ultimately dependent on the quality of the antibody. The PCR is carried out until the reaction is in the linear stage of amplification. This typically takes between 27 and 31 cycles depending on the primer set. The rate of amplification can be determined by conducting the PCR amplification procedure in an iCycler (Bio-Rad, CA). Alternatively, a classic PCR approach can be used whereby identical PCRs are carried out for different cycle numbers and the level of PCR product in each reaction is measured by agarose gel electrophoresis combined with scanning densitometry. The level of PCR product in each PCR can then be plotted against the cycle number to determine the number of cycles required to reach a linear stage of amplification.

To determine if a specific DNA sequence becomes associated with a transcription factor or a modified histone after a treatment, we measure the levels of PCR product from ChIP and input DNA in control and treated cells by agarose gel electrophoresis using ethidium bromide to stain DNA and scanning densitometry for quantification. Then we determine the level of DNA sequence enrichment in ChIP DNA for both control and treated cells by dividing the net density of PCR product from ChIP DNA by the net density of product from the respective input DNA. The fold enrichment of DNA sequence in the treated sample is then determined by dividing the level of sequence enrichment for the treated sample by that for the control sample.

Although the ChIP protocol is useful for studying the binding of proteins to DNA, it is usually more of a qualitative than a quantitative approach. One can determine if a specific protein is associated with a specific DNA sequence; however, whether this association is true for every cell in the cell lysate is difficult to determine.

3. Optimization of the ChIP protocol

In the ChIP assay, an antibody is used to capture a specific DNA-associated protein. The success of this protocol is entirely dependent on the quality of the antibody used. An antibody of good quality should be

specific and efficient in the immunoprecipitation of a specific protein.

3.1. Determining the efficiency of an antibody to immunoprecipitate its target antigen

A procedure we find useful for determining the efficiency of immunoprecipitation of an antibody involves lysing cells with lysis buffer A. For this test, we recommend that the cells not be crosslinked with formaldehyde prior to lysis since formaldehyde crosslinking may interfere with subsequent steps in this protocol. The cell lysate is diluted to $2A_{260}$ units/ml with dilution buffer or 1× RIPA buffer containing protease inhibitors (1 mM PMSF, 1 μg/ml aprotinin, 10 μg/ml leupeptin, and 50 μM iodoacetamide). One milliliter of the diluted lysate is aliquoted into each of several microcentrifuge tubes, and different amounts of test antibody are added to each tube so that different dilutions (i.e., 1/100, 1/250, 1/400, 1/1000) of the antibody are tested. The tubes are then incubated for 30 min to overnight at 4 °C. The length of time for incubation with the primary antibody will vary with each type of antibody and the propensity for the antibody to associate with nontarget proteins.

Following primary antibody incubation, 50 μl of a 50:50 (v/v) protein A/G slurry is added to each tube for every milliliter of cell lysate (refer to Section 3.5 for a discussion of the type of protein Sepharose to add). The tubes are incubated for an additional 2 h and then centrifuged for 3 min at 3000 rpm in a microcentrifuge. Low-speed centrifugation is used to protect the protein A/G resin from damage. The supernatant is then transferred to a fresh microcentrifuge tube, and the protein A/G–Sepharose is saved for determining the antibody specificity (see Section 3.2). An equal volume of supernatant (i.e., 20 μl) is then withdrawn from each tube, and placed into a fresh microcentrifuge tube containing SDS loading buffer (i.e., 5 μl of 5×). The samples are boiled for 3 min., electrophoresed onto a SDS gel, and transferred to nitrocellulose membrane. If the protein in question migrates at a molecular weight close to that of the primary antibody's heavy and light chains, β-mercaptoethanol should be excluded from the loading buffer as this will prevent the dissociation of the primary antibody and prevent the antibody from entering the gel during electrophoresis. The nitrocellulose membrane is then immunoblotted with the test antibody to detect for the presence or absence of the target protein from the supernatant. If the antibody is efficient at removing its target antigen from the supernatant, the level of antigen should decrease as the amount of antibody present is increased (Fig. 2A). If formaldehyde-crosslinked cells are used for this preliminary protocol, the charge of the target protein may become altered, causing the target protein to migrate to a slightly different position on a SDS gel. In addition, the formaldehyde may crosslink the target protein to another protein and this may also alter its migration.

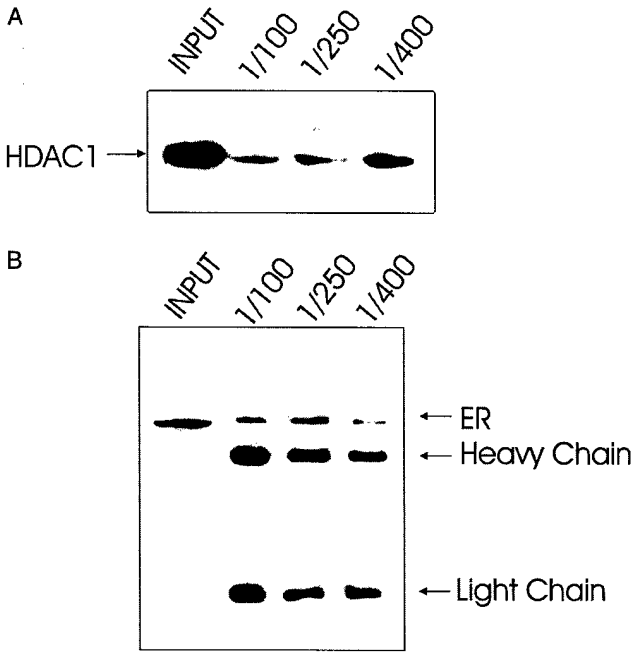

Fig. 2. Determining the immunoprecipitation efficiency of an antibody. (A) Cell lysate diluted to 2 A_{260} units/ml was divided into four aliquots. One aliquot was used as input and anti-HDAC 1 antibody (ABR, CO) was added to the remaining three to final dilutions of 1/100, 1/250, and 1/400, respectively. After a 2-h incubation, 50 μl of a 50:50 (v/v) protein A slurry was added to each sample for 2 h. Twenty microliters of supernatant was removed from each sample, supplemented with SDS loading buffer, electrophoresed onto a 10% SDS–polyacrylamide gel, and transferred to nitrocellulose. The resulting membrane was subjected to Western blot analysis using the same anti-HDAC 1 antibody. (B). Diluted cell lysate was divided into four aliquots. One aliquot was used as input and anti-ERα antibody (Novacastra, UK) was added to the remaining three to final dilutions of 1/100, 1/250, and 1/400, respectively. After a 2-h incubation, 50 μl of a 50:50 (v/v) protein A slurry was added to each sample for 2 h. Ten microliters of TE buffer (pH 8) and SDS–PAGE loading buffer were added to the protein A. The sample was boiled for 5 min, electrophoresed onto a 10% SDS–polyacrylamide gel, and transferred to nitrocellulose. The resulting membrane was subjected to Western blot analysis using the same anti-ERα antibody. HDAC1 and ER signify the locations of histone deacetylase 1 and estrogen receptor α, respectively.

3.2. Determining the specificity of an antibody for its target antigen

Specificity is extremely important to determine since many commercially available antibodies can nonspecifically immunoprecipitate proteins. In fact some commercial antibodies immunoprecipitate nontarget protein substrates more efficiently than their target proteins. To determine the specificity and functionality of an antibody, the protein A/G–Sepharose saved in Section 3.1 from each ChIP sample is washed with various high-salt and/or high-detergent buffers as described in Section

2.1.3 to remove nonspecifically bound material. Following the washes, the associated proteins are isolated by resuspending the Sepharose in TE buffer (pH 8) containing SDS loading buffer and boiling the sample for 3–5 min. The extracted proteins are then loaded onto a SDS gel and transferred to nitrocellulose membrane, and the membrane is immunoblotted with the test antibody. A functional antibody will show an increase in antigen associated with protein A/G as the amount of antibody is increased (Fig. 2B). The absence of antigen from the Sepharose may indicate that the antibody is nonfunctional for immunoprecipitation assays or that the immunoprecipitation buffer and/or wash buffers are too stringent to allow binding of the antibody to its target antigen.

3.3. Optimization of formaldehyde crosslinking

Formaldehyde crosslinks protein to DNA, RNA, and protein [7–9]. This reagent is capable of causing cancer and heritable genetic lesions. In addition, formaldehyde is toxic by inhalation and readily absorbed through the skin. When working with this reagent, one should wear a respirator, chemical-resistant gloves, safety goggles, and other protective clothing such as a lab coat. This reagent should be handled only in a chemical fume hood to avoid inhalation of the vapors. Formaldehyde is combustible and should therefore be kept away from heat and open flame and stored in a cool dry place.

The ability to fine-map a protein to a specific DNA sequence is dependent on the extent to which DNA, RNA, and protein become crosslinked to protein. In the ChIP assay, cells are treated with 1% formaldehyde for a brief time (i.e., 8–10 min depending on cell type) so that only nuclear components located within 2 Å of DNA become crosslinked to DNA [10]. This means that proteins located within 2 Å of DNA will become crosslinked to DNA whether they are bound to or situated next to DNA. Furthermore, a brief exposure to 1% formaldehyde (i.e., 1 min) can crosslink histones to one another [8]. Thus, a target protein may appear to be directly associated with a specific DNA region, when, in fact, its association is indirect. Several transcriptional co-activators have been shown to be indirectly associated with specific DNA sequences in response to transcriptional initiation by the ChIP assay [2].

When determining the optimal conditions for formaldehyde crosslinking, it is important to consider that as the time of formaldehyde crosslinking increases, soluble cellular components become more insoluble as they are crosslinked to one another and to the insoluble cellular material. Therefore, extensively crosslinking a cell may decrease the solubility of any target DNA–protein complex by causing this complex to become trapped in the insoluble nuclear material.

To determine the optimal conditions for formaldehyde crosslinking, the extent to which the DNA within a cell is fragmented and the amount of DNA released from the insoluble cell material should be determined. But first the ability of formaldehyde to crosslink the target protein to DNA must be confirmed. To determine if a specific protein is associated with DNA in situ the following protocol can be used. Crosslinked cells are suspended in lysis buffer B containing 5 M urea, 2 M NaCl, 2 M guanidine hydrochloride, and 200 mM potassium phosphate (pH 7.5). Preequilibrated hydroxyapatite is then added to the lysate to bind the DNA, and all unbound proteins are removed by washing the hydroxyapatite several times with lysis buffer B. Finally, the protein–DNA crosslinks are reversed by incubating the hydroxyapatite resin at 65 °C for 6 h, and the released proteins analyzed by SDS–PAGE. Proteins of low abundance should be analyzed by Western blotting. For a more detailed description of this protocol refer to [11].

The extent of sonication is determined simply by isolating the DNA from formaldehyde-treated cells and analyzing the size of the DNA fragments on a gel (see Section 2.1.2). The amount of DNA released from the cellular material of a crosslinked cell is determined by reading the A_{260} of the cell lysate, centrifuging the cell lysate, and reading the A_{260} of the supernatant. The A_{260} of the supernatant is then divided by the A_{260} of the cell lysate and this resulting value is multiplied by 100 to determine the percentage of DNA released from the cellular material. For a more detailed description refer to [11].

3.4. Alternative crosslinking agents

The current view of the loading and clearance of transcription factors onto promoters is based on our interpretation of ChIP assays using formaldehyde. As was previously mentioned, formaldehyde crosslinks protein to DNA, RNA, or protein [7–9]. Thus, when formaldehyde is used, the indirect association of a specific protein with a particular DNA sequence may be mistaken for a direct association. To avoid this, an alternative crosslinker should be used that crosslinks only proteins directly associated with DNA.

Cisplatin crosslinks proteins to DNA but not protein to protein. The crosslinking distance of cisplatin (4 Å) is double that of formaldehyde (2 Å). Furthermore, cisplatin crosslinks predominantly nuclear matrix proteins to DNA [12], while it does not crosslink histones to DNA to a significant extent [13,14]. The nuclear matrix is the site of many nuclear processes. Therefore, cisplatin would be a useful reagent for studying the involvement of specific DNA-associated nuclear matrix proteins in these nuclear processes [15].

Cisplatin is a dusty and highly toxic substance that has the potential to cause cancer and heritable genetic

damage. This agent should be stored in a cool dry place and in a tightly closed bottle. Cisplatin should be used only in a chemical fume hood in combination with a respirator to avoid dust inhalation. Direct contact with this agent should also be avoided by wearing chemical-resistant gloves, safety goggles, and other protective clothing such as a lab coat.

If one were to use cisplatin to crosslink DNA to its associated proteins, the cells would be incubated with cisplatin using our established protocol [16]. Our standard crosslinking condition is 1 mM cisplatin for 2 h at 37 °C. Apoptosis is not observed under these conditions [17]. However, the time and concentration of cisplatin treatment can vary from 30 to 120 min and 0.3 to 1 mM, depending on the extent of cisplatin-induced interstrand DNA crosslinks and the ability of cisplatin to efficiently crosslink a specific protein to DNA [17]. Note that intrastrand DNA crosslinks are far more prevalent than interstrand crosslinks [18]. Intrastrand crosslinks can be readily reversed, but breaking interstrand crosslinks is difficult. Protein–DNA crosslinks are reversed with thiourea [16], and platinated adducts (intrastrand crosslinks) can be removed by treatment with NaCN [18,19]. However, in some cases, intrastrand crosslinks may not be problematic and treatment with NaCN may not be needed [20]. The treatment of platinated DNA with the cyanide ion does not cleave DNA [18].

To determine if cisplatin is capable of crosslinking a specific protein to DNA, cells are incubated with cisplatin in the absence of NaCl and lysed in 5 M urea, 2 M NaCl, 2 M guanidine hydrochloride, and 200 mM potassium phosphate (pH 7.5). The cell lysate is then incubated with hydroxyapatite resin as previously described in Section 3.3. The resin is washed several times and the crosslinks are reversed by incubating the protein–DNA complexes in a reverse lysis buffer containing 1 M thiourea, 5 M urea, 2 M guanidine hydrochloride, and 200 mM potassium phosphate (pH 7.5). Following this, the released proteins are isolated and analyzed by either SDS–PAGE or Western blotting. Once cisplatin has been shown to crosslink a protein of interest to DNA and the optimal concentration for this reagent has been determined, parameters such as sonication efficiency and DNA solubility after sonication can be determined as previously described (see Section 3.3).

3.5. Determining the type and amount of protein–Sepharose to use

Whether one chooses protein A or G to isolate antibody–antigen complexes depends on the nature of the primary antibody. The antibodies produced in rabbits have an equal binding affinity for protein A and G while goat antibodies, which bind both protein A and protein G, display a preference for protein G. When an antibody is capable of binding to both proteins A and G, one can add a 50:50 (v/v) resin slurry containing both protein A– and protein G–Sepharose in an equal molar ratio to improve the yield of immunoprecipitated antibody–antigen complexes. However, in most cases, a 50:50 (v/v) slurry containing only one type of resin is added. The quality of Protein A– and protein G–Sepharoses also varies between companies. Thus, different company brands should always be tested before starting the ChIP protocol.

Once the quality of the antibody and the crosslinking conditions have been determined, the amount of protein A/G necessary for capturing the primary antibody must be determined. This is accomplished by aliquoting the buffer (1× RIPA or dilution buffer) used to dilute the cell lysate to 2 A_{260} units/ml into several microcentrifuge tubes and adding the predetermined optimal amount of primary antibody to this buffer (see Section 3.1). Different amounts of 50:50 protein A/G slurry (i.e., 20, 40, 50, and 60 μl) are added to each tube and the sample is incubated for 2 h. The samples are then centrifuged at 3000 rpm in a microcentrifuge tube for 3 min and the supernatant is transferred to a fresh tube. An aliquot of the supernatant from each tube is collected, transferred to its respective tube, supplemented with SDS loading buffer, and boiled for 3 min. The sample is then electrophoresed on to a SDS gel and transferred to nitrocellulose membrane. The primary antibody has already been added to the samples and, therefore, is immobilized on the membrane. Because of this, the membrane is immunoblotted only with secondary antibody to ultimately visualize the progressive decrease in unbound primary antibody with increasing amounts of protein A/G–Sepharose.

3.6. Sonication efficiency

The extent to which one can fine-map the location of a specific protein along a gene depends on the extent of DNA fragmentation. For example, when studying the association of a specific protein with a 200-bp region of DNA, and the genomic DNA is sonicated to an average size of 500 bp, one should consider that a total of 300 bp of DNA sequence adjacent to the target DNA region will be immunoprecipitated alongside the target DNA sequence in the ChIP assay. Thus, the amplification of this 200-bp region from ChIP DNA would suggest that the target immunoprecipitated protein is associated either within this 200-bp region or within a region up to 300 bp away from this target sequence. For further explanation about this concept, refer to [21].

Besides the extent of crosslinking, the volume of a sample and the depth to which the sonication probe is

placed in the sample affect the efficiency of sonication. During sonication, the sample volume should not exceed 1 ml and the sonicator probe should be placed approximately 1 cm deep into the sample. Smaller sample volumes of 400–500 μl are more ideal to use. However, as the sample volume decreases it becomes more difficult to place the sonicator probe 1 cm deep into the sample. To increase the depth of a sample, the sonicated cell lysate is transferred to a microcentrifuge tube. In the ChIP assay, the cell lysate contains SDS. Therefore, positioning the sonicator probe too close to the sample surface tends to cause foaming, which decreases the efficency of sonication. Cooling the sample between sonication pulses and placing the sample in an ice water bath during sonication decrease the incidence of foaming. As well, the chance of sample foaming is greatly reduced when the output energy emitted from the sonicator probe is decreased.

4. Conclusion

The ChIP protocol is a very useful procedure for studying transcription factor binding and alterations in chromatin structure. Although it appears to be simple, the ChIP protocol can sometimes be a complicated procedure. The quality of the primary antibody, the degree of sample sonication, the amount of protein A/G–Sepharose, and the types of salt and/or detergent washes can all make a difference in accurately determining the distribution of a protein along a specific DNA sequence. However, provided that the appropriate controls are used, the ChIP protocol can serve as a valuable tool for studying nuclear events involved in the processing of DNA.

Acknowledgments

The authors thank Alison Clayton and Louis Mahadevan for valuable advice in troubleshooting the ChIP protocol. This research was supported by grants from the U.S. Army Medical and Materiel Command Breast Cancer Research Program (DAMD17-00-1-0319), the Canadian Institutes of Health Research (CIHR) (MT-9186, RGP-15183), the National Cancer Institute of Canada with funds from the Canadian Cancer Society, and CancerCare Manitoba Foundation, Inc., and studentships to Lin Li from the Guardian Angels Breast Cancer studentship fund and to Virginia Spencer from the U.S. Army Medical and Materiel Command Breast Cancer Research Program (DAMD 17-01-1-0309).

Appendix A: Recipes

1× RIPA buffer	
0.1% SDS	1 ml 10%
0.1% sodium deoxycholate	0.1 g
1% Triton X-100	1 ml 100%
1 mM EDTA	400 μl 250 mM
0.5 mM EGTA	200 μl 250 mM
140 mM NaCl	3.5 ml 4 M
10 mM Tris–HCl, pH 8	1 ml 1 M to 100 ml with double-distilled H_2O
1× RIPA + 1 M NaCl	
RIPA buffer	50 ml 2×
NaCl	5.844 g to 100 ml with double-distilled H_2O
Lysis buffer A	
1% SDS	10 ml 10%
10 mM EDTA	4 ml 250 mM
50 mM Tris–HCl, pH 8	5 ml 1 M to 100 ml with double-distilled H_2O
Lysis buffer B	
5 M urea	150 g
2 M guanidine hydrochloride	95.5 g
2 M NaCl	58.5 g
200 mM KH_2PO_4	16 ml 1 M
200 mM K_2HPO_4	84 ml 1 M to 500 ml with double-distilled H_2O
Reverse lysis buffer	
1 M thiourea	3.8 g
2 M guanidine hydrochloride	9.55 g
2 M NaCl	5.85 g
200 mM KH_2PO_4	1.6 ml 1 M
200 mM K_2HPO_4	8.4 ml 1 M to 100 ml with double-distilled H_2O
Dilution buffer	
0.01% SDS	100 μl 10%
1.1% Triton X-100	1.1 ml 100%
1.2 mM EDTA	480 μl 250 M
16.7 mM Tris–HCl, pH 8	1.67 ml 1 M
167 mM NaCl	4.18 ml 4 M to 100 ml with double-distilled H_2O
Low salt buffer	
0.1% SDS	1 ml 10%

Appendix A (*continued*)

1% Triton X-100	1 ml 100%
2 mM EDTA	800 μl 250 mM
20 mM Tris–HCl, pH 8	2 ml 1 M
150 mM NaCl	3.75 ml 4 M to 100 ml with double-distilled H_2O
High salt buffer	
0.1% SDS	1 ml 10%
1% Triton X-100	1 ml 100%
2 mM EDTA	800 μl 250 mM
20 mM Tris–HCl, pH 8	2 ml 1 M
500 mM NaCl	12.5 ml 4 M to 100 ml with double-distilled H_2O
LiCl buffer	
0.25 M LiCl	6.25 ml 4 M
1% Nonidet P-40	1 ml 100%
1% SDC	1 g
1 mM EDTA	400 μl 250 mM
10 mM Tris–HCl, pH 8	1 ml 1 M to 100 ml with double-distilled H_2O
TE buffer, pH 8	
20 mM Tris–HCl, pH 8	2 ml 1 M
1 mM EDTA, pH 8	400 μl 250 mM to 100 ml with double-distilled H_2O
1.5% SDS elution buffer	
1.5 g SDS in 100 ml double-distilled H_2O	
0.5% SDS elution buffer	
0.5 g SDS in 100 ml double-distilled H_2O	
1% SDS elution buffer with $NaHCo_3$	
1 g SDS	
0.84 g 0.1 M $NaHCo_3$ to 100 ml with double-distilled H_2O	

References

[1] H. Chen, R.J. Lin, W. Xie, D. Wilpitz, R.M. Evans, Cell 98 (1999) 675–686.
[2] Y. Shang, X. Hu, J. DiRenzo, M.A. Lazar, M. Brown, Cell 103 (2000) 843–852.
[3] D. Sharma, J.D. Fondell, Proc. Natl. Acad. Sci. USA 99 (2002) 7934–7939.
[4] A.L. Clayton, S. Rose, M.J. Barratt, L.C. Mahadevan, EMBO J. 19 (2000) 3714–3726.
[5] V.A. Spencer, J.R. Davie, J. Biol. Chem. 276 (2001) 34810–34815.
[6] D.N. Chadee, M.J. Hendzel, C.P. Tylipski, C.D. Allis, D.P. Bazett-Jones, J.A. Wright, J.R. Davie, J. Biol. Chem. 274 (1999) 24914–24920.
[7] K. Moller, J. Rinke, A. Ross, G. Buddle, R. Brimacombe, Eur. J. Biochem. 76 (1977) 175–187.
[8] V. Jackson, Cell 15 (1978) 945–954.
[9] M.J. Solomon, A. Varshavsky, Proc. Natl. Acad. Sci. USA 82 (1985) 6470–6474.
[10] V. Orlando, Trends Biochem. Sci. 25 (2000) 99–104.
[11] V.A. Spencer, J.R. Davie, in: J.M. Walker (Ed.), The Protein Protocols Handbook, Humana Press, Totowa, 2002, pp. 753–757.
[12] V.A. Spencer, S.K. Samuel, J.R. Davie, Cancer Res. 61 (2001) 1362–1366.
[13] S.J. Lippard, J.D. Hoeschele, Proc. Natl. Acad. Sci. USA 76 (1979) 6091–6095.
[14] J. Filipski, K.W. Kohn, W.M. Bonner, FEBS Lett. 152 (1983) 105–108.
[15] J.R. Davie, Int. Rev. Cytol. A 162 (1995) 191–250.
[16] V.A. Spencer, J.R. Davie, in: J.M. Walker (Ed.), The Protein Protocols Handbook, Humana Press, Totowa, 2002, pp. 747–757.
[17] S.K. Samuel, V.A. Spencer, L. Bajno, J.M. Sun, L.T. Holth, S. Oesterreich, J.R. Davie, Cancer Res. 58 (1998) 3004–3008.
[18] S.F. Bellon, J.H. Coleman, S.J. Lippard, Biochemistry 30 (1991) 8026–8035.
[19] F.A. Blommaert, C.P. Saris, Nucleic Acids Res. 23 (1995) 1300–1306.
[20] H. Koga, W. Deppert, Oncogene 19 (2000) 4178–4183.
[21] D. Kadosh, K. Struhl, Mol. Cell. Biol. 18 (1998) 5121–5127.

Inhibition of Histone Deacetylase Activity by Butyrate[1,2]

James R. Davie[3]

Manitoba Institute of Cell Biology, Winnipeg, Manitoba, Canada

ABSTRACT This article reviews the effects of the short-chain fatty acid butyrate on histone deacetylase (HDAC) activity. Sodium butyrate has multiple effects on cultured mammalian cells that include inhibition of proliferation, induction of differentiation and induction or repression of gene expression. The observation that butyrate treatment of cells results in histone hyperacetylation initiated a flurry of activity that led to the discovery that butyrate inhibits HDAC activity. Butyrate has been an essential agent for determining the role of histone acetylation in chromatin structure and function. Interestingly, inhibition of HDAC activity affects the expression of only 2% of mammalian genes. Promoters of butyrate-responsive genes have butyrate response elements, and the action of butyrate is often mediated through Sp1/Sp3 binding sites (e.g., $p21^{Waf1/Cip1}$). We demonstrated that Sp1 and Sp3 recruit HDAC1 and HDAC2, with the latter being phosphorylated by protein kinase CK2. A model is proposed in which inhibition of Sp1/Sp3–associated HDAC activity leads to histone hyperacetylation and transcriptional activation of the $p21^{Waf1/Cip1}$ gene; $p21^{Waf1/Cip1}$ inhibits cyclin-dependent kinase 2 activity and thereby arrests cell cycling. Pending the cell background, the nonproliferating cells may enter differentiation or apoptotic pathways. The potential of butyrate and HDAC inhibitors in the prevention and treatment of cancer is presented. J. Nutr. 133: 2485S–2493S, 2003.

KEY WORDS: • *sodium butyrate* • *histone deacetylase* • *$p21^{Waf1/Cip1}$* • *histone acetylation* • *gene expression* • *Sp1* • *Sp3*

Butyrate is a short-chain fatty acid that is produced by anaerobic bacterial fermentation of dietary fibers. It was suggested (1,2) that butyrate may inhibit the development of colon cancer. This article reviews the action of butyrate in altering gene expression and arresting cell proliferation by inhibition of the chromatin-remodeling activity of histone deacetylases (HDAC).[4]

MATERIALS AND METHODS

Cell culture

Human breast cancer cell lines MCF-7 (T5) [estrogen-receptor (ER) positive and estrogen dependent] and MDA MB 231 (ER negative and estrogen independent) were cultured as described previously (3).

Pulse-chase labeling cells for analyses of histone acetylation rates

Human breast cancer cells and avian immature erythrocytes were pulse-labeled with [^{3}H]acetate and subsequently incubated in the absence of radiolabel and with sodium butyrate (10 mmol/L) as described previously (3,4). Rates of histone acetylation were determined as previously described (5,6).

Immunoprecipitation

The following is an efficient method to solubilize nuclear proteins. MCF-7 (T5) human breast cancer cells were lysed in immunoprecipitation buffer (50 mmol Tris-HCl/L, pH 8.0, 150 mmol NaCl/L, 0.5% Nonidet P-40 and 1 mmol EDTA/L) that contained 1 mmol phenylmethylsulfonyl fluorid/L, phosphatase inhibitors and protease-inhibitor cocktail. The cells were sonicated twice for 15 s. The cell lysate was collected by centrifugation at 10,000 × *g* for 10 min and incubated with anti-HDAC1, anti-HDAC2, anti-Sp1 or anti-Sp3 antibodies for 16 h at 4°C (7).

Sequential immunoprecipitations

Sequential immunoprecipitations were done as previously described (7). Briefly, cell lysates were incubated with anti-Sp1 antibodies. The immunoprecipitated and immunodepleted (supernatant) fractions were collected. Secondary immunoprecipitations were performed with the Sp1-immunodepleted (supernatant) fraction and anti-Sp3 antibodies, and the immunoprecipitated and immunodepleted fractions were collected.

---

[1] Published in a supplement to *The Journal of Nutrition*. Presented at the "Nutritional Genomics and Proteomics in Cancer Prevention Conference" held September 5–6, 2002, in Bethesda, MD. This meeting was sponsored by the Center for Cancer Research, National Cancer Institute; Division of Cancer Prevention, National Cancer Institute; National Center for Complementary and Alternative Medicine, National Institutes of Health; Office of Dietary Supplements, National Institutes of Health; Office of Rare Diseases, National Institutes of Health; and the American Society for Nutritional Sciences. Guest editors for the supplement were Young S. Kim and John A. Milner, Nutritional Science Research Group, Division of Cancer Prevention, National Cancer Institute, Bethesda, MD.

[2] This research was supported by the U.S. Army Medical and Materiel Command Breast Cancer Research Program (grant DAMD17-00-1-0319), the Canadian Institutes of Health Research (grants MT-9186 and RGP-15183), National Cancer Institute of Canada with funds from the Canadian Cancer Society, and CancerCare Manitoba Foundation, Inc.

[3] To whom correspondence should be addressed. E-mail: davie@cc.umanitoba.ca.

[4] Abbreviations used: AUT, acetic acid–urea–Triton X-100; Cdk, cyclin-dependent kinase; ER, estrogen receptor; HAT, histone acetyltransferase; HDAC, histone deacetylase; NuRD, nucleosome-remodeling histone deacetylase complex; Rb, retinoblastoma protein; TSA, trichostatin A.

RESULTS

Effects of butyrate on cell proliferation and HDAC

In the mid-1970s several research groups reported that sodium butyrate halts DNA synthesis, arrests cell proliferation, alters cell morphology and increases or decreases gene expression (8). Treatment of erythroleukemic cells with butyrate was shown to be very effective in inducing differentiation in these cells (9). A turning point in understanding the mechanism of butyrate action was the observation by Ingram and colleagues (10) that butyrate increased the level of acetylated histones in cultured HeLa and Friend erythroleukemic cells. Several chromatin investigators interested in histone acetylation recognized that to increase histone acetylation, either the activity of histone acetyltransferases (HAT) was increased, or conversely, the activity of HDAC was inhibited. The latter, inhibition of HDAC activity, was found to be the mode of butyrate action (11–14).

Histone acetylation: a dynamic process that regulates chromatin structure

HDAC catalyzes the removal of acetate from modified lysine residues located in the N-terminal tail region of the core histones H2A, H2B, H3 and H4 (Fig. 1A). These core histones form a histone octamer around which is wrapped 146 bp of DNA. The four core histones have a similar structure that consists of a basic N-terminal domain, a central histone-fold domain (which mediates histone-histone and histone-DNA interactions) and a C-terminal tail (15). The crystal structure of the nucleosome shows that the N-terminal tails emanate from the nucleosome in all directions (Fig. 1B) (16). Reversible acetylation occurs on specific lysines that are located in the N-terminal tail domains of the core histones (Fig. 1A). With the exception of H2A, the core histones are acetylated at four or five sites; thus a nucleosome has potentially 28 or more sites of acetylation. In addition to acetylation, the core histones are modified by methylation, phosphorylation and ubiquitination (17).

Although we have known since the 1960s that histone acetylation has a role in chromatin structure and function, we still know little about what this modification does to remodel chromatin structure (18). However, one function of histone acetylation is to alter the compaction of chromatin. Acetylation of the histone tails disrupts higher-order chromatin folding (19) and promotes the solubility of chromatin at physiological ionic strength (20). Nucleosomes do not have to be maximally acetylated to prevent chromatin compaction. Hansen and colleagues (21) demonstrated that acetylation to 46% of maximal site occupancy is sufficient to prevent higher-order folding and stimulation of transcription by RNA polymerase III. It was proposed (22,23) that acetylation of core histone tails interferes with interactions with proteins and/or DNA and thereby destabilizes higher-order chromatin organization. These combined effects of histone acetylation on the destabilization of chromatin structure facilitate transcription (21,24) (Fig. 1C).

Enzymes catalyze dynamic histone acetylation

The steady state of acetylated histones in a eukaryotic cell and at a specific gene locus is governed by the net activities of histone acetyltransferases (HATs) and HDAC (Fig. 2). HATs often have transcriptional coactivator activity and when recruited to a gene promoter by a transcription factor will increase the level of acetylated histones and enhance transcriptional activity of the promoter (17,25). The most potent HAT in

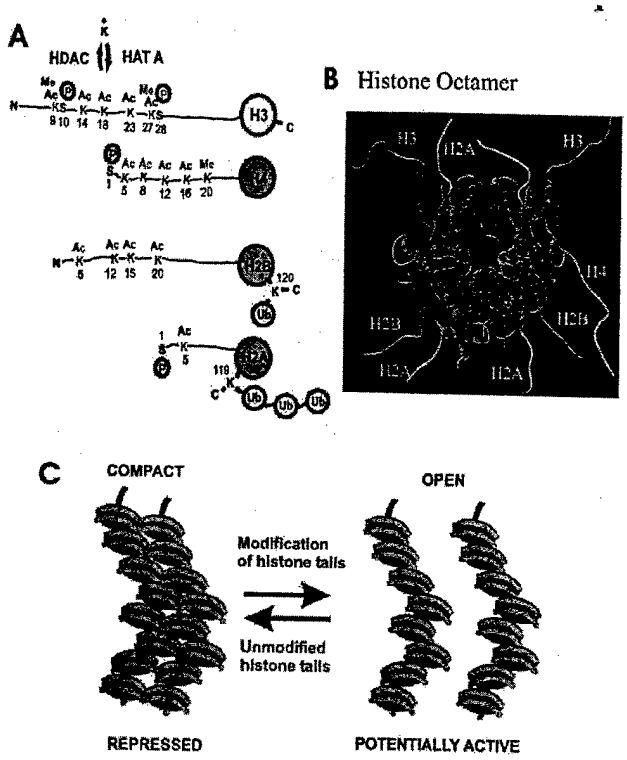

FIGURE 1 (*A*) Sites of postsynthetic modifications on the core histones. Structures of the core histones H2A, H2B, H3 and H4 and the sites of modification are indicated. Modifications shown are acetylation (Ac), phosphorylation (P), ubiquitination (Ub) and methylation (Me). Enzymes that catalyze reversible acetylation and phosphorylation are also shown. (*B*) Crystal structure of the nucleosome [adapted with permission from Dr. Timothy Richmond (15)]. (*C*) Chromatin fibers bearing unmodified tails interact; however, these interactions are disfavored when the tails are modified. HAT, histone acetyltransferase; HDAC, histone deacetylase.

mammalian cells are the following (17,26): cAMP response-element binding protein (CREB) binding protein (CBP), p300, p300/CREB binding protein-associated factor (PCAF) and HIV Tat interactive 60-kDa protein (Tip60). Steroid receptor coactivators 1 and 3 (SRC-1 and -3, respectively) are HATs recruited by steroid receptors (17).

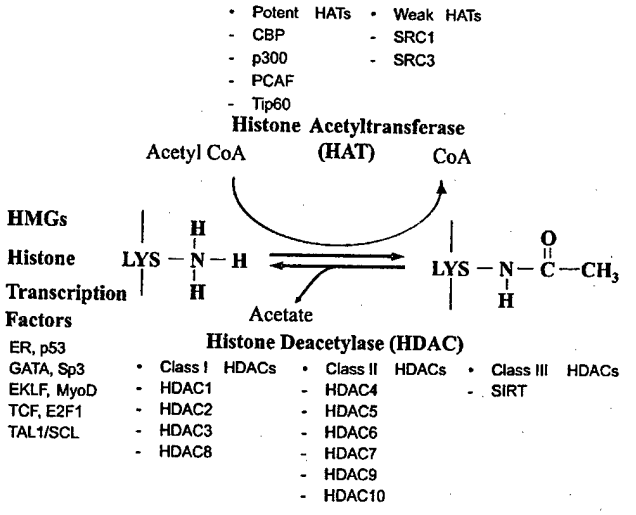

FIGURE 2 Dynamic histone acetylation is catalyzed by HAT and HDAC.

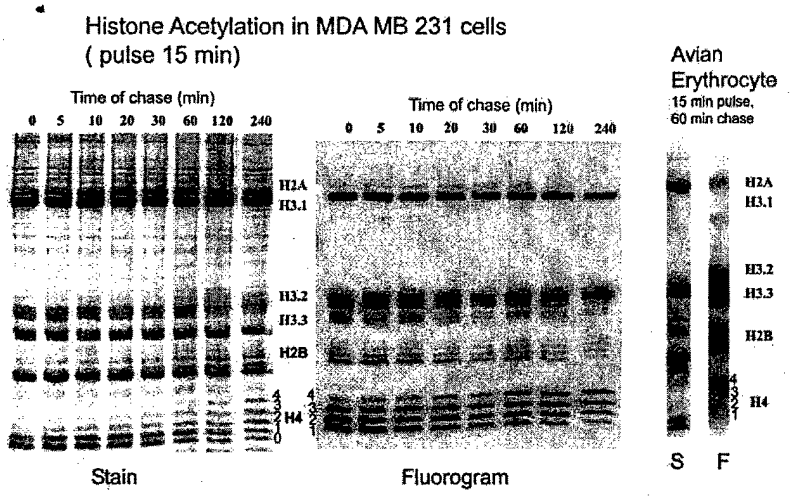

FIGURE 3 Effects of sodium butyrate on dynamic histone acetylation in MDA MB 231 human breast cancer cells and avian immature erythrocytes. MDA MB 231 cells were pulse-labeled with [^{3}H]acetate for 15 min and then chased for 0–240 min in the presence of 10 mmol sodium butyrate/L. Histones were resolved by acetic–acid urea–Triton X-100 polyacrylamide gel eletrophoresis (AUT-PAGE; 60 μg of protein/lane). The Coomassie blue–stained gel (S, *left panel*) and accompanying fluorogram (F, *right panel*) are shown. The two lanes at far right contained histones from avian immature erythrocytes that were pulse-labeled with [^{3}H]acetate for 15 min and chased for 60 min in the presence of 10 mmol sodium butyrate/L. The acetylated species of H4 are denoted numerically as 0, 1, 2, 3 and 4, which represent the un-, mono-, di-, tri- and tetra-acetylated species, respectively (3). (J. Biol. Chem. 276: 49435–49442, with permission.)

Three classes of HDAC are known. Class I HDAC consist of the mammalian HDAC1, -2 (mammalian homolog of yeast RPD3), -3 and -8. Class II HDAC include mammalian HDAC4, -5, -6, -7, -9 and -10 (27–32). Class III HDAC are members of the sirtuin family of HDAC, among which yeast Sir2 is the founding member (30).

Butyrate inhibits most HDAC except class III HDAC and class II HDAC6 and -10. During inhibition of HDAC activity, HAT activity continues, which results in histone hyperacetylation. Histones, however, are not the only substrates of these enzymes. High-mobility group proteins are acetylated. This modification has a wide range of effects on the function of the high-mobility group proteins in remodeling chromatin structure and regulating gene expression (33–35). Multiple transcription factors are acetylated (36) (Fig. 2). Acetylation of a transcription factor may alter its properties (37). For example, CBP acetylates p53 and GATA-1 and potentiates the activities of these transcription factors (36,38).

Dynamic histone acetylation: rates of acetylation and deacetylation

Histone acetylation is a dynamic process that occurs at different rates. In mammalian cells, one population of core histones is characterized by rapid hyperacetylation and rapid deacetylation ($t_{1/2}$ = 3–7 min). This highly dynamic acetylation-deacetylation process is limited to 10–15% of the core histones (3). A second population is acetylated and deacetylated at a slower rate ($t_{1/2}$ = 30 min) (39). Approximately 60–70% of the histones of cultured mammalian cells participate in reversible acetylation. The remainder of the histones is "frozen" in low- or nonacetylated states (25).

Incubation of human breast cancer cells (MDA MB 231) with sodium butyrate for 2 h has a major impact on the steady-state levels of acetylated histones (see acetylated H4 levels in Fig. 3). Histones were electrophoretically resolved on an acetic acid–urea–Triton X-100 (AUT) 15% polyacrylamide gel, which resolves histones according to size, charge and hydrophobicity. Thus, this gel system is ideal for separating modified histones and histone variants. For example, H3 has three variants (H3.1, H3.2 and H3.3) that are resolved with this gel system (40).

To study the fast rate of histone acetylation, cells were pulse-labeled with [^{3}H]acetate for 15 min, the label was removed and the cells were incubated with sodium butyrate to drive the dynamically acetylated histones into highly acetylated isoforms (Fig. 3, fluorogram). The fluorogram clearly shows the movement of the label in H4, H2B and H3 moving into the highly acetylated isoforms.

In contrast with mammalian cells in culture, only 2% of the histones in terminally differentiated avian immature erythrocytes participate in dynamic acetylation. Also, only the fast rate of histone acetylation is observed in these cells (6). Thus, a shift in the steady state of acetylated histone is not observed on the

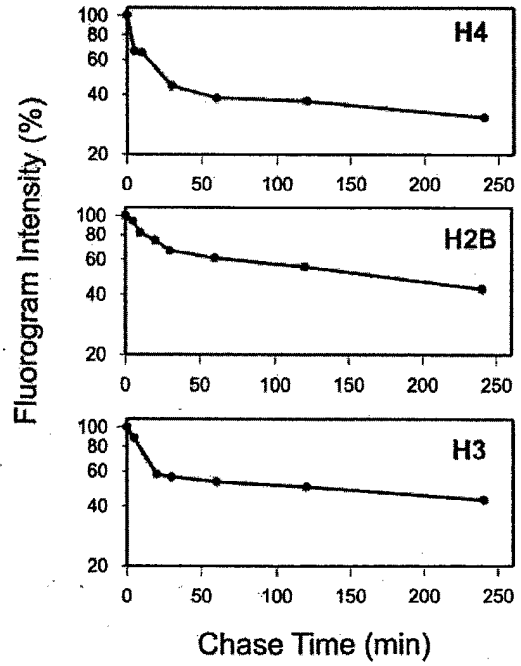

FIGURE 4 Analysis of the rates of histone acetylation in MCF-7 (T5) human breast cancer cells that were cultured under estrogen-replete conditions. MCF-7 (T5) cells were pulse-labeled with [^{3}H]acetate for 15 min and then chased for 0–240 min in the presence of 10 mmol sodium butyrate/L. Histones were resolved by AUT-PAGE (60 μg of protein/lane). Proportions of total radiolabeled H4, H2B and H3 associated with the monoacetylated form were determined by scanning the fluorograms. Proportion of labeled monoacetylated isoforms (H4-Ac1, H3.2-Ac1 and H2B-Ac1) present in total labeled H4, H3 and H2B at zero time was arbitrarily set at 100. The rapid rate of acetylation was determined using the data obtained from the 0–20 min butyrate-chase period, whereas the slower rate of acetylation was determined using data from the 60–240 min butyrate-chase period (3). (J. Biol. Chem. 276: 49435–49442, with permission.)

stained AUT gel pattern when avian cells are incubated with sodium butyrate for 1 h. Pulse-labeling of the cells with [^{3}H]acetate for 15 min followed by a chase for 60 min in the presence of butyrate rapidly drives the histones participating in dynamic acetylation into the highest acetylated isoforms. The dynamically acetylated histones are limited to transcriptionally active and competent regions of the avian erythrocyte genome (41). In mammalian cells, the bulk of the dynamically acetylated histones may serve a surveillance function (42).

By measurement of the rate of loss of label in the monoacetylated histone isoform (e.g., H4, H2B and H3.2 in Fig. 3), the rate of histone acetylation is determined. **Figure 4** shows that H4, H3.2 and H2B have two rates of acetylation in human breast cancer cells [MCF-7 (T5)]. For H4, the fast rate of acetylation has a $t_{1/2}$ time of 8 min, but the slower rate of acetylation has a $t_{1/2}$ time of 200–350 min (3,39).

Butyrate: the mode of action

Recently, the crystal structure of an HDAC-like protein from the hyperthermophilic bacterium *Aquifex aeolicus* with the HDAC inhibitor trichostatin A (TSA; **Fig. 5**) was reported (43). The structure shows the position of the essential zinc atom that is involved in catalysis of class I and II HDAC. HDAC-like protein shares 35.2% similarity over a 390-residue region with mammalian HDAC1; this region constitutes the deacetylase core. The aliphatic chain of TSA occupies a hydrophobic cleft on the surface of the enzyme (Fig. 5). Possibly two butyrate molecules also could occupy the hydrophobic pocket and inhibit the enzyme. However, butyrate was found to be a noncompetitive inhibitor of HDAC, which argues that butyrate does not associate with the substrate-binding site (44). The binding site and mechanism by which butyrate inhibits HDAC activity remain unknown.

HDAC complexes and transcription

Mammalian HDAC1 and -2 exist in large multiprotein complexes, Sin3 complex and nucleosome-remodeling histone deacetylase complex (NuRD; **Fig. 6**). The Sin3 complex, which has an estimated size of 1–2 MDa, contains mammalian (m)Sin3, Sin3-associated proteins of 18 and 30 kDa and retinoblastoma-associated proteins (RbAp)46 and -48 (25,30,45, 46). The Sin3 complex is directed to its target chromatin location by sequence-specific DNA binding proteins that interact directly with mSin3 and other components of Sin3 complex. Some examples of DNA binding proteins that recruit the Sin3 complex include the Mad family proteins, unliganded hormone receptors, methyl cytosine guanine dinucleotide (CpG) binding protein, p53, repressor element (RE)-1 silencing transcription factor and the Ikaros family proteins (25,30,46,47).

The complex called NuRD is ~2 MDa in size and consists of metastasis-associated protein 2 (which is highly related to metastasis-associated protein 1), Mi2, RbAp46 and -48 and methyl CpG binding domain-containing protein 3 (MBD3). NuRD has both ATP-dependent chromatin remodeling and HDAC activities (25,30).

When ER are bound to hydroxytamoxifen, ER recruit nuclear receptor corepressor/silencing mediator for retinoic and thyroid hormone receptors and HDAC to the promoter of an estrogen-responsive promoter and thereby repress promoter activity. However, when estradiol is bound to the ER, ER recruit coactivator/HAT and chromatin-remodeling complexes to the promoter to enable transcription (48,49). It is important to note that the steady-state level of acetylation at a regulatory element (e.g., promoter) or along the coding region of a gene is dictated by the balance of HAT and HDAC recruited to those sites. Because the occurrence of histone acetylation at transcriptionally active genes is a dynamic and rapid process, alterations in recruitment of factors for HAT or HDAC quickly change the balance of these two activities toward increasing or decreasing the steady-state level of acetylated histones. For example, a ligand-binding steroid receptor or a phosphorylated transcription factor (e.g., nuclear factor-κB) can be quickly changed to recruiting HDAC to HAT and vice versa (50,51).

Effects of estradiol on global histone acetylation dynamics in human breast cancer cells

This investigation is an example of studies that use sodium butyrate to determine histone acetylation and deacetylation rates. In this study, we investigated the effects of estradiol on

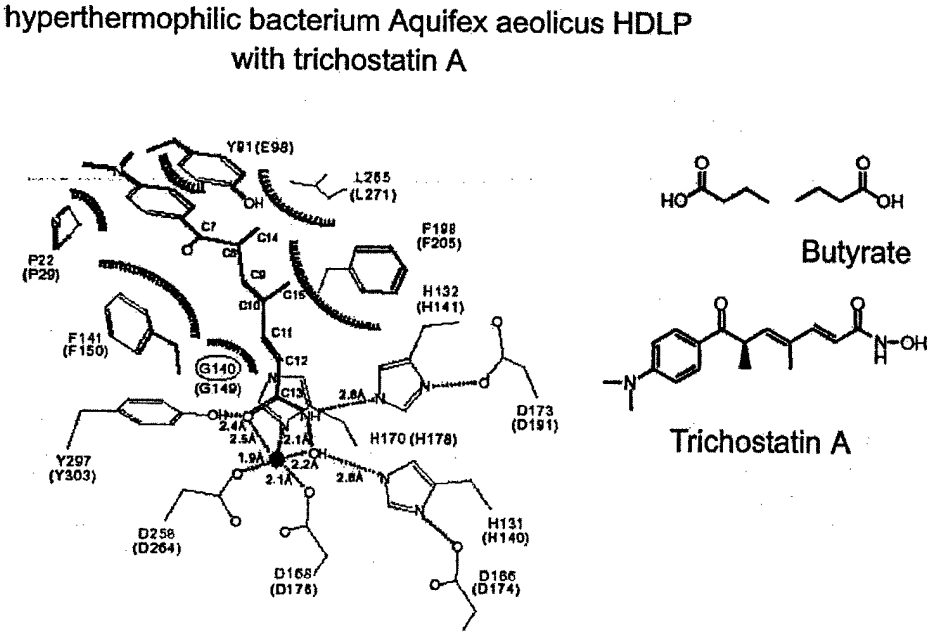

FIGURE 5 Schematic representation of histone deacetylase-like protein (HDLP, gray) interactions with trichostatin A (TSA, black) in the crystal structure of an HDAC homolog from the hyperthermophilic bacterium *Aquifex aeolicus*. HDLP residues are labeled in gray and their counterparts in HDAC1 are indicated in black [adapted with permission from Dr. Nikola P. Pavletich (43)]. Structures of TSA and butyrate are shown. (Nature 401: 188–193, with permission.)

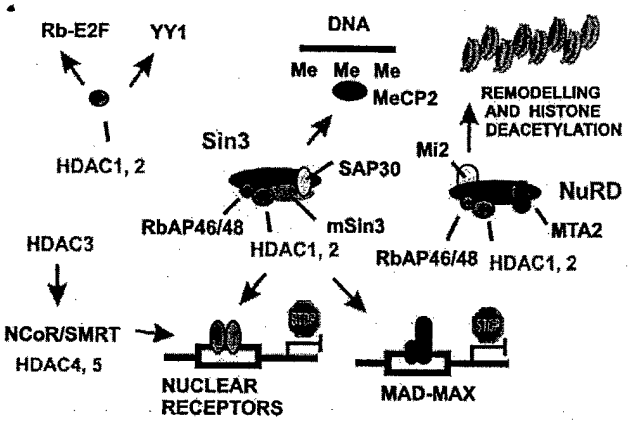

FIGURE 6 HDAC multiprotein complexes are recruited to specific genomic sites by regulatory proteins. HDAC1 and HDAC2 together with retinoblastoma-associated proteins (RbAp)46 and -48 are components of two large multiprotein complexes [Sin3 and nucleosome-remodeling histone deacetylase complex (NuRD)] that contain mSin3A/B or chromodomain helicase DNA binding protein 3/-4, respectively (25).

global dynamic histone acetylation in hormone-responsive human breast cancer cells (3). Histone acetylation–labeling experiments and immunoblot analyses of dynamically acetylated histones show that estradiol rapidly increases histone acetylation in ER-positive hormone-dependent MCF-7 (T5) human breast cancer cells. The effects of estradiol on the rates of histone acetylation and deacetylation in MCF-7 (T5) cells were determined. Estradiol increased the level of acetylated histones by reducing the rate of histone deacetylation, whereas the rates of histone acetylation were not altered.

Butyrate response element and gene expression

Studies reveal that among the fatty acids, butyrate is the most effective in inhibiting HDAC activity and arresting cell proliferation (52). Butyrate also is the most effective fatty acid in stimulating or repressing the expression of specific genes (**Table 1**). Considering the actions of butyrate to inhibit HDAC activity and promote histone hyperacetylation (see Fig. 3), it is surprising to learn that expression of only 2% of the mammalian genes is affected when HDAC activity is inhibited (53,54).

Within the promoter of butyrate-responsive genes is found a butyrate response element (55–59). It appears that these butyrate elements may be separated into different groups depending on the DNA sequence of the butyrate response element (**Table 2**). One group of genes that are either induced or repressed by butyrate has a common DNA sequence in the butyrate response elements, which suggests that a common transcription factor binds to this site. Another group, which includes the cyclin-dependent kinase 2 (Cdk2) inhibitor $p21^{Waf1/Cip1}$, shares an Sp1/Sp3 binding site in the butyrate response elements.

TABLE 2

Butyrate response elements (55–59)[1]

Gene	Butyrate response	Butyrate response element
Group 1		
Cyclin D1	Repression	AGCCACCTCCA
Intestinal trefoil factor	Repression	.....AG .....
Calbindin-D28k	Induction	..... A.G .....
Metallothionein IIA	Induction	.....C...T.....
Group 2		
Galectin 1	Induction	Sp1/Sp3 binding site
$G\alpha_i2$	Induction	Sp1/Sp3 binding site
IGF-binding protein 3	Induction	Sp1/Sp3 binding site
Cdk2 inhibitor $p21^{Waf1/Cip1}$	Induction	Sp1/Sp3 binding site

[1] IGF, insulin-like growth factor; Cdk2, cyclin-dependent kinase 2.

Sp1, Sp3 and recruitment of HDAC

Sp1 and Sp3 are ubiquitously expressed mammalian transcription factors that function as activators or repressors. Sp1 and Sp3 bind with equivalent affinity to GC boxes via their three zinc fingers located in the C-terminal region of the protein (60). Activation domains A and B (Gln- and Ser/Thr-rich regions, respectively) are located in the N-terminal part of the protein, whereas the D domain, which is found in the C-terminal region, is involved in multimerization (61,62). Synergistic transcriptional activation is mediated through the capacity of the Sp1 D domain to form multimers (61,62). Scanning transmission electron microscopy provides evidence (61) that Sp1 first forms a tetramer and then assembles multiple stacked tetramers at the DNA binding site. The interesting feature of this structure is that an Sp1 multimer presents several interacting surfaces to proteins that associate with Sp1 [e.g., p300/CBP, HDAC1, transcriptional activator factor II subunits of transcription factor IID, cofactor required for Sp1 activation, E2F transcription factor 1, and ER (63–66)]. The net activity of these factors to promote or hinder transcription depends on the abundance, affinity and residence time of these factors on the Sp1 multimer.

Sp3 has three isoforms, a long (L-Sp3) and two short (M1- and M2-Sp3) forms that are the products of differential translational initiation (67,68). The protein structure of L-Sp3 is very similar to that of Sp1 except that Sp3 has a repression domain located at the N-terminal to the zinc-finger DNA binding domain (60). The factors that regulate the translational initiation of Sp3 mRNA are currently unknown.

TABLE 1

Effects of fatty acids on mammalian cells in culture (52)

No. of carbons in fatty acid	Effect on fibroblast growth *% control*	Induction of alkaline phosphatase (HeLa) *% control*	Inhibition of estradiol-induced synthesis of transferring mRNA	Inhibition of histone deacetylase (calf thymus)
C2, acetate	82	170	18	10
C3, propionate	45	160	77	60
C4, butyrate	0	630	95	80
C5, valeroic	71	420	—	65
C6, caproate	—	120	—	30

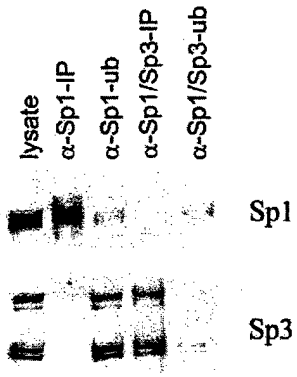

FIGURE 7 Sp1 is not associated with Sp3. MCF-7 (T5) cell lysate was incubated with anti-Sp1 antibodies, and the immunoprecipitation (IP, lane 2) and immunodepletion (ub, lane 3) fractions were collected. The immunodepleted fraction was then incubated with anti-Sp3 antibodies, which yielded IP (lane 4) and ub (lane 5) fractions. Proteins of the cell lysate (lane 1), IP and ub fractions were loaded onto a sodium dodecyl sulfate (SDS) 10% polyacrylamide gel, transferred to nitrocellulose membranes and immunochemically stained with anti-Sp1 and -Sp3 antibodies. Long (L) and short (M1 and M2) forms of Sp3 are identified (7). (J. Biol. Chem. 277: 35783–35786, with permission.)

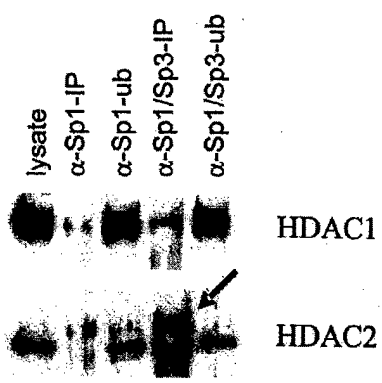

FIGURE 8 Sp1 and Sp3 are associated with HDAC1 and HDAC2. MCF-7 (T5) cell lysate, IP and ID fractions were prepared as described for Fig. 7 and were loaded onto an SDS 10% polyacrylamide gel, transferred to nitrocellulose membranes and immunochemically stained with anti-HDAC1 and -HDAC2 antibodies. Arrow indicates the HDAC2 species with reduced mobility (7). (J. Biol. Chem. 277: 35783–35786, with permission.)

Although Sp1 and Sp3 share a common D domain that is involved in forming multimers, we reported that Sp1 and Sp3 form separate complexes in estrogen-dependent human breast cancer cells (7). In performing these studies, we wanted to ensure efficient solubilization of nuclear proteins, because Sp1 and Sp3 are tightly bound to the nucleus of MCF-7 (T5) breast cancer cells (see Materials and Methods). Sequential immunoprecipitations were done first with anti-Sp1 antibodies and then with anti-Sp3 antibodies (see Materials and Methods). **Figure 7** shows that Sp1 and Sp3 form separate complexes.

Next, we determined whether Sp1 and Sp3 were associated with HDAC activity. A previous report showed that Sp1 was associated with HDAC1 (64). Both Sp1 and Sp3 were associated with HDAC activity in human breast cancer cells (7). In immunoblot analyses of the Sp1 and Sp3 immunoprecipitated complexes, we observed that HDAC1 and -2, but not HDAC3, were associated with Sp1 and Sp3 (**Fig. 8**). However, it was very interesting to find a major enrichment of a slower migrating HDAC2 species associating with Sp1 and Sp3. Additional investigation revealed that this slower migrating species was protein kinase CK2–phosphorylated HDAC2 (7,69). Alkaline phosphatase treatment of HDAC2, Sp1 and Sp3 complexes reduced the associated HDAC activity.

The protein kinase CK2 is a tetramer that consists of two α- (or α'-) and two β-subunits (70). In immunoprecipitation experiments, we found that CK2 was associated with HDAC2 and to a lesser extent with HDAC1 (**Fig. 9**). Although we found that HDAC2 is associated with MBD3 (a component of the NuRD HDAC complex) and Sin3A (a component of the Sin3 complex; see Fig. 6), it remains to be determined whether CK2 or HDAC2 is associated with either of these complexes. CK2 is upregulated in several cancers including breast cancer, and there is evidence that CK2 may promote breast cancer by deregulating key transcription processes (71–74).

A model for butyrate induction of p21$^{Waf1/Cip1}$ gene expression and inhibition of cell cycle

The p21$^{Waf1/Cip1}$ promoter has six Sp1 binding sites (the butyrate response element). Evidence has been presented that Sp3 and not Sp1 is associated with this promoter (75). Also, the

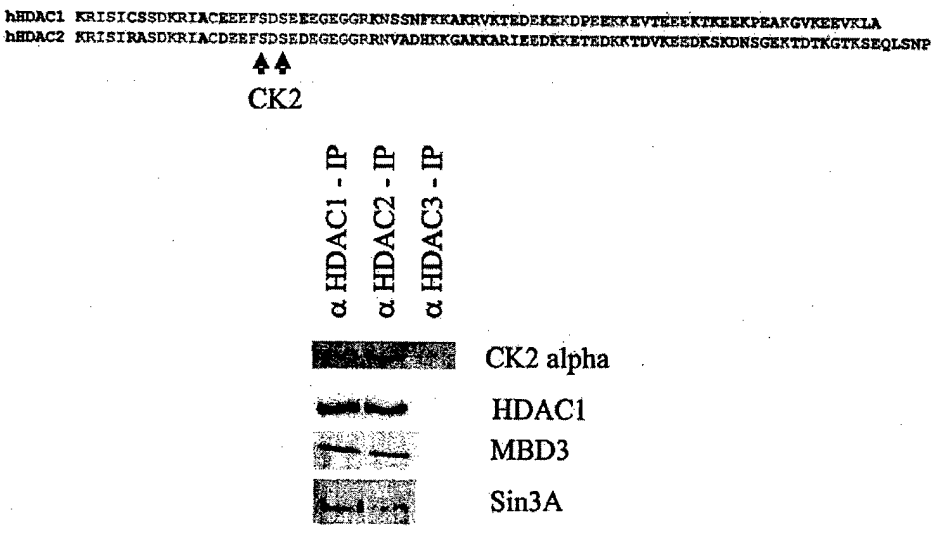

FIGURE 9 HDAC2 is associated with and phosphorylated by protein kinase CK2. The C-terminal amino acid sequences of mammalian HDAC1 and HDAC2 and the sites of protein kinase CK2 phosphorylation are shown. Equal amounts of MCF-7 (T5) cell lysate were immunoprecipitated with anti-HDAC1, -HDAC2 or -HDAC3 antibodies. Immunoprecipitated samples and nuclear extracted protein (10 μg) were loaded onto an SDS 10% polyacrylamide gel, transferred to a nitrocellulose membrane and immunochemically stained with anti-CK2α, -HDAC1, -MBD3 and -Sin3 antibodies (7). (J. Biol. Chem. 277: 35783–35786, with permission.)

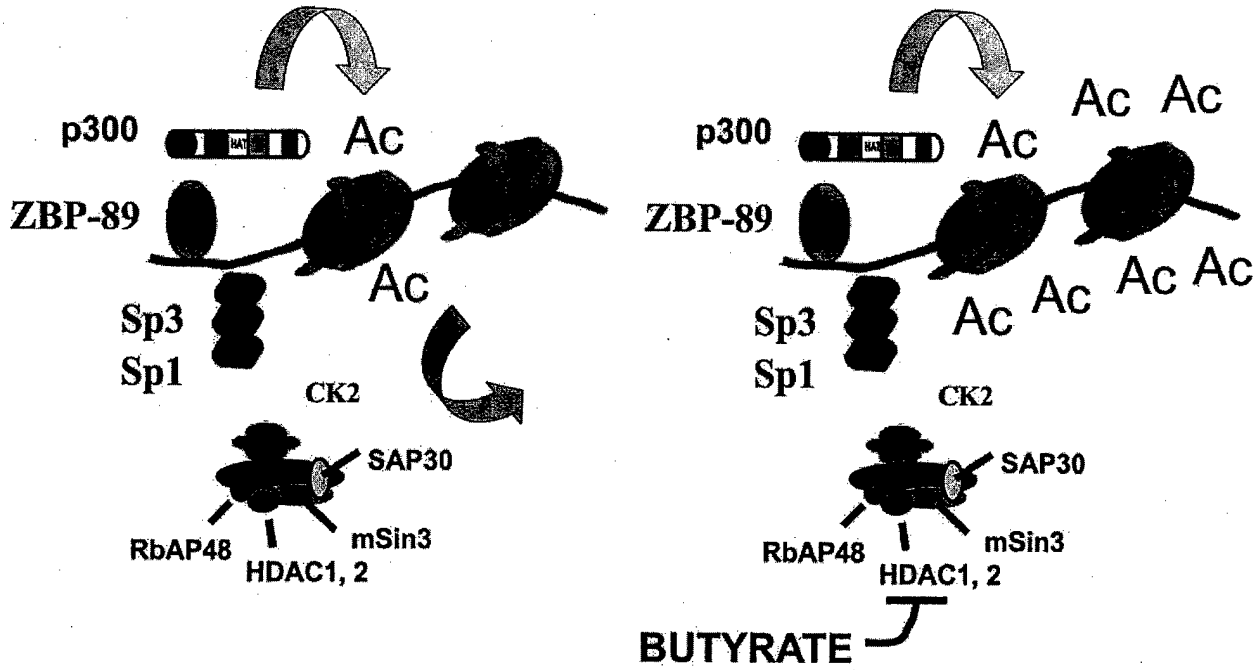

FIGURE 10 Model for the butyrate induction of the Cdk2 inhibitor $p21^{Waf1/Cip1}$. In the absence of butyrate, zinc-finger DNA binding protein 89 and Sp3/Sp1 recruit the p300 and HDAC1,2/CK2 complex, respectively. The steady-state level of histone acetylation is low and not supportive of transcription (*left panel*). When butyrate is present, HDAC activity is inhibited, which allows the histones to become hyperacetylated. The modified chromatin then supports transcription (*right panel*).

Sp1-like protein zinc-finger DNA binding protein 89 (ZBP-89) is associated with one or more of the Sp1 sites. ZBP-89 recruits p300, which is a coactivator/HAT (76). Thus, ZBP-89 would recruit HAT activity to the promoter, whereas Sp3 would recruit HDAC activity to the $p21^{Waf1/Cip1}$ promoter and result in dynamic histone acetylation (**Fig. 10**). The steady-state level of acetylated histones associated with the $p21^{Waf1/Cip1}$ promoter is low, which favors a condensed chromatin structure and inactive promoter (77). Inhibition of HDAC activity with sodium butyrate allows the HAT activity of p300 to increase the histone acetylation levels at the promoter and nearby regions (77). Hyperacetylation of the histones would support chromatin opening and induction of $p21^{Waf1/Cip1}$ gene expression.

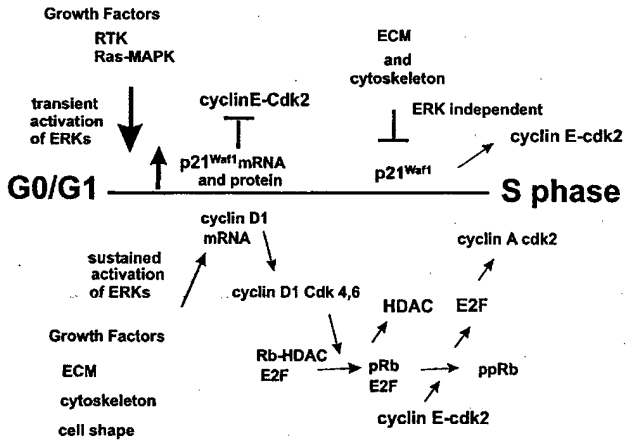

FIGURE 11 Induction of $p21^{Waf1/Cip1}$ gene expression by transient activation of extracellular signal-related kinase activity. Elevated levels of $p21^{Waf1/Cip1}$ inhibit cyclin E–Cdk2 activity and promote the assembly of stable cyclin D1–Cdk4/6 kinase complexes. The $p21^{Waf1/Cip1}$ gene is repressed and $p21^{Waf1/Cip1}$ protein levels decline, which allows activation of cyclin E–Cdk2. Both cyclin D1–Cdk4,6 and cyclin E–Cdk2 are involved in the phosphorylation of Rb and the release of E2F, which activates the promoters of genes involved in progression through the S phase of the cell cycle. Butyrate would induce expression of $p21^{Waf1/Cip1}$ and inhibit cyclin E–Cdk2 activity and thereby arrest cell cycle progression. ECM, extracellular matrix; RTK, receptor tyrosine kinase.

In the transition from the G1 to the S phase of the cell cycle, $p21^{Waf1/Cip1}$ has a key role (**Fig. 11**). Initially, there is an increase in $p21^{Waf1/Cip1}$ expression after the transient activation of the extracellular signal-related kinase and the Ras mitogen-activated protein kinase pathway (78). The $p21^{Waf1/Cip1}$ inhibits the activity of cyclin E–Cdk2 kinase and promotes the assembly of stable cyclin D1–Cdk4/6 kinase complexes (79). Subsequently, $p21^{Waf1/Cip1}$ gene expression is repressed, which results in the lowering of $p21^{Waf1/Cip1}$ protein levels and the activation of cyclin E–Cdk2. Cyclin E–Cdk2 activity is required for the final-stage phosphorylation of Rb and the release of the transcription factor E2F, which induces the expression of genes that are involved in taking cells through the S phase (DNA synthesis phase) of the cell cycle (25,79–81). Butyrate induces expression of $p21^{Waf1/Cip1}$ and thereby inhibits cyclin E–Cdk2 activity and halts the subsequent events that are required for cells to enter S phase. The cell cycle–arrested cells may differentiate or undergo cell death by apoptosis.

Butyrate and HDAC inhibitors in prevention and treatment of cancer

By inhibiting the HDAC activity recruited to the $p21^{Waf1/Cip1}$ promoter by Sp1 or Sp3, butyrate induces the expression of $p21^{Waf1/Cip1}$ and thereby stops cell proliferation. This is a p53-independent process (82). Several studies (1,2) suggest that the production of butyrate in the colon may be protective against colon carcinogenesis. Current studies and clinical trials (83–88) strongly suggest that HDAC inhibitors such as TSA and sub-

eroylanilide hydroxamic acid, which also induce $p21^{Waf1/Cip1}$ expression, are effective in arresting cancer cell proliferation and lead to cells undergoing differentiation (as in acute promelocytic anemia) or apoptosis. These new strategies for prevention and treatment of cancer have been termed "gene-regulating chemoprevention," "gene-regulating chemotherapy" and "transcription therapy" (88,89). No matter which term wins the day, these are exciting times for the dietary micronutrient butyrate and HDAC inhibitors in the challenge of preventing and treating cancer.

LITERATURE CITED

1. Hinnebusch, B. F., Meng, S., Wu, J. T., Archer, S. Y. & Hodin, R. A. (2002) The effects of short-chain fatty acids on human colon cancer cell phenotype are associated with histone hyperacetylation. J. Nutr. 132: 1012–1017.
2. Emenaker, N. J., Calaf, G. M., Cox, D., Basson, M. D. & Qureshi, N. (2001) Short-chain fatty acids inhibit invasive human colon cancer by modulating uPA, TIMP-1, TIMP-2, mutant p53, Bcl-2, Bax, p21 and PCNA protein expression in an in vitro cell culture model. J. Nutr. 131 (suppl. 11): 3041S–3046S.
3. Sun, J.-M., Chen, H. Y. & Davie, J. R. (2001) Effect of estradiol on histone acetylation dynamics in human breast cancer cells. J. Biol. Chem. 276: 49435–49442.
4. Hendzel, M. J., Delcuve, G. P. & Davie, J. R. (1991) Histone deacetylase is a component of the internal nuclear matrix. J. Biol. Chem. 266: 21936–21942.
5. Covault, J. & Chalkley, R. (1980) The identification of distinct populations of acetylated histone. J. Biol. Chem. 255: 9110–9116.
6. Zhang, D.-E. & Nelson, D. A. (1988) Histone acetylation in chicken erythrocytes: rates of acetylation and evidence that histones in both active and potentially active chromatin are rapidly modified. Biochem. J. 250: 233–240.
7. Sun, J. M., Chen, H. Y., Moniwa, M., Litchfield, D. W., Seto, E. & Davie, J. R. (2002) The transcriptional repressor Sp3 is associated with CK2 phosphorylated histone deacetylase 2. J. Biol. Chem. 277: 35783–35786.
8. Prasad, K. N. & Sinha, P. K. (1976) Effect of sodium butyrate on mammalian cells in culture: a review. In Vitro 12: 125–132.
9. Leder, A. & Leder, P. (1975) Butyric acid, a potent inducer of erythroid differentiation in cultured erythroleukemic cells. Cell 5: 319–322.
10. Riggs, M. G., Whittaker, R. G., Neumann, J. R. & Ingram, V. M. (1977) n-Butyrate causes histone modification in HeLa and Friend erythroleukaemia cells. Nature 268: 462–464.
11. Candido, E. P. M., Reeves, R. & Davie, J. R. (1978) Sodium butyrate inhibits histone deacetylation in cultured cells. Cell 14: 105–113.
12. Sealy, L. & Chalkley, R. (1978) The effect of sodium butyrate on histone modification. Cell 14: 115–121.
13. Boffa, L. C., Vidali, G., Mann, R. S. & Allfrey, V. G. (1978) Suppression of histone deacetylation in vivo and in vitro by sodium butyrate. J. Biol. Chem. 253: 3364–3366.
14. Vidali, G., Boffa, L. C., Bradbury, E. M. & Allfrey, V. G. (1978) Suppression of histone deacetylation by butyrate leads to accumulation of multiacetylated forms of histones H3 and H4 and increased DNase I-sensitivity of the associated DNA sequences. Proc. Natl. Acad. Sci. U.S.A. 75: 2239–2243.
15. Luger, K., Mader, A. W., Richmond, R. K., Sargent, D. F. & Richmond, T. J. (1997) Crystal structure of the nucleosome core particle at 2.8 A resolution. Nature 389: 251–260.
16. Luger, K. & Richmond, T. J. (1998) The histone tails of the nucleosome. Curr. Opin. Genet. Dev. 8: 140–146.
17. Spencer, V. A. & Davie, J. R. (1999) Role of covalent modifications of histones in regulating gene expression. Gene 240: 1–12.
18. Pogo, B. G., Allfrey, V. G. & Mirsky, A. E. (1966) RNA synthesis and histone acetylation during the course of gene activation in lymphocytes. Proc. Natl. Acad. Sci. U.S.A. 55: 805–812.
19. Garcia-Ramirez, M., Rocchini, C. & Ausio, J. (1995) Modulation of chromatin folding by histone acetylation. J. Biol. Chem. 270: 17923–17928.
20. Wang, X., He, C., Moore, S. C. & Ausio, J. (2001) Effects of histone acetylation on the solubility and folding of the chromatin fiber. J. Biol. Chem. 276: 12764–12768.
21. Tse, C., Sera, T., Wolffe, A. P. & Hansen, J. C. (1998) Disruption of higher order folding by core histone acetylation dramatically enhances transcription of nucleosomal arrays by RNA polymerase III. Mol. Cell. Biol. 18: 4629–4638.
22. Hansen, J. C., Tse, C. & Wolffe, A. P. (1998) Structure and function of the core histone N-termini: more than meets the eye. Biochemistry 37: 17637–17641.
23. Wang, X., Moore, S. C., Laszczak, M. & Ausio, J. (2000) Acetylation increases the alpha-helical content of the histone tails of the nucleosome. J. Biol. Chem. 275: 35013–35020.
24. Nightingale, K. P., Wellinger, R. E., Sogo, J. M. & Becker, P. B. (1998) Histone acetylation facilitates RNA polymerase II transcription of the drosophila *hsp26* gene in chromatin. EMBO J. 17: 2865–2876.
25. Davie, J. R. & Moniwa, M. (2000) Control of chromatin remodeling. Crit. Rev. Eukaryot. Gene Expr. 10: 303–325.
26. Sterner, D. E. & Berger, S. L. (2000) Acetylation of histones and transcription-related factors. Microbiol. Mol. Biol. Rev. 64: 435–459.
27. Fischle, W., Emiliani, S., Hendzel, M. J., Nagase, T., Nomura, N., Voelter, W. & Verdin, E. (1999) A new family of human histone deacetylases related to *Saccharomyces cerevisiae* HDA1p. J. Biol. Chem. 274: 11713–11720.
28. Grozinger, C. M., Hassig, C. A. & Schreiber, S. L. (1999) Three proteins define a class of human histone deacetylases related to yeast Hda1p. Proc. Natl. Acad. Sci. U.S.A. 96: 4868–4873.
29. Fischle, W., Kiermer, V., Dequiedt, F. & Verdin, E. (2001) The emerging role of class II histone deacetylases. Biochem. Cell Biol. 79: 337–348.
30. Grozinger, C. M. & Schreiber, S. L. (2002) Deacetylase enzymes: biological functions and the use of small-molecule inhibitors. Chem. Biol. 9: 3–16.
31. Guardiola, A. R. & Yao, T. P. (2002) Molecular cloning and characterization of a novel histone deacetylase HDAC10. J. Biol. Chem. 277: 3350–3356.
32. Kao, H. Y., Lee, C. H., Komarov, A., Han, C. C. & Evans, R. M. (2002) Isolation and characterization of mammalian HDAC10, a novel histone deacetylase. J. Biol. Chem. 277: 187–193.
33. Herrera, J. E., Sakaguchi, K., Bergel, M., Trieschmann, L., Nakatani, Y. & Bustin, M. (1999) Specific acetylation of chromosomal protein HMG-17 by PCAF alters its interaction with nucleosomes. Mol. Cell. Biol. 19: 3466–3473.
34. Munshi, N., Merika, M., Yie, J., Senger, K., Chen, G. & Thanos, D. (1998) Acetylation of HMG I(Y) by CBP turns off IFN beta expression by disrupting the enhanceosome. Mol. Cell 2: 457–467.
35. Sterner, R., Vidali, G. & Allfrey, V. G. (1979) Studies of acetylation and deacetylation in high mobility group proteins: identification of the sites of acetylation in HMG 1. J. Biol. Chem. 254: 11577–11583.
36. Braun, H., Koop, R., Ertmer, A., Nacht, S. & Suske, G. (2001) Transcription factor Sp3 is regulated by acetylation. Nucleic Acids Res. 29: 4994–5000.
37. Cheung, W. L., Briggs, S. D. & Allis, C. D. (2000) Acetylation and chromosomal functions. Curr. Opin. Cell Biol. 12: 326–333.
38. Berger, S. L. (1999) Gene activation by histone and factor acetyltransferases. Curr. Opin. Cell Biol. 11: 336–341.
39. Davie, J. R. (1997) Nuclear matrix, dynamic histone acetylation and transcriptionally active chromatin. Mol. Biol. Rep. 24: 197–207.
40. Wu, R. S., Panusz, H. T., Hatch, C. L. & Bonner, W. M. (1986) Histones and their modifications. CRC Crit. Rev. Biochem. 20: 201–263.
41. Spencer, V. A. & Davie, J. R. (2001) Dynamically acetylated histone association with transcriptionally active and competent genes in the avian adult β-globin gene domain. J. Biol. Chem. 276: 34810–34815.
42. Perry, M. & Chalkley, R. (1982) Histone acetylation increases the solubility of chromatin and occurs sequentially over most of the chromatin. A novel model for the biological role of histone acetylation. J. Biol. Chem. 257: 7336–7347.
43. Finnin, M. S., Donigian, J. R., Cohen, A., Richon, V. M., Rifkind, R. A., Marks, P. A., Breslow, R. & Pavletich, N. P. (1999) Structures of a histone deacetylase homologue bound to the TSA and SAHA inhibitors. Nature 401: 188–193.
44. Cousens, L. S., Gallwitz, D. & Alberts, B. M. (1979) Different accessibilities in chromatin to histone acetylase. J. Biol. Chem. 254: 1716–1723.
45. Ayer, D. E. (1999) Histone deacetylases: transcriptional repression with SINers and NuRDs. Trends Cell Biol. 9: 193–198.
46. Knoepfler, P. S. & Eisenman, R. N. (1999) Sin meets NuRD and other tails of repression. Cell 99: 447–450.
47. Gray, S. G. & Teh, B. T. (2001) Histone acetylation/deacetylation and cancer: an "open" and "shut" case? Curr. Mol. Med. 1: 401–429.
48. Shang, Y., Hu, X., DiRenzo, J., Lazar, M. A. & Brown, M. (2000) Cofactor dynamics and sufficiency in estrogen receptor-regulated transcription. Cell 103: 843–852.
49. Hart, L. L. & Davie, J. R. (2002) The estrogen receptor: more than the average transcription factor. Biochem. Cell Biol. 80: 335–341.
50. Ghosh, S. (1999) Regulation of inducible gene expression by the transcription factor NF-kappaB. Immunol. Res. 19: 183–189.
51. Zhong, H., May, M. J., Jimi, E. & Ghosh, S. (2002) The phosphorylation status of nuclear NF-kappaB determines its association with CBP/p300 or HDAC-1. Mol. Cell 9: 625–636.
52. Kruh, J. (1982) Effects of sodium butyrate, a new pharmacological agent, on cells in culture. Mol. Cell. Biochem. 42: 65–82.
53. Van Lint, C., Emiliani, S. & Verdin, E. (1996) The expression of a small fraction of cellular genes is changed in response to histone hyperacetylation. Gene Expr. 5: 245–253.
54. Mariadason, J. M., Corner, G. A. & Augenlicht, L. H. (2000) Genetic reprogramming in pathways of colonic cell maturation induced by short chain fatty acids: comparison with trichostatin A, sulindac, and curcumin and implications for chemoprevention of colon cancer. Cancer Res. 60: 4561–4572.
55. Yang, J., Kawai, Y., Hanson, R. W. & Arinze, I. J. (2001) Sodium butyrate induces transcription from the G alpha(i2) gene promoter through multiple Sp1 sites in the promoter and by activating the MEK-ERK signal transduction pathway. J. Biol. Chem. 276: 25742–25752.
56. Siavoshian, S., Segain, J. P., Kornprobst, M., Bonnet, C., Cherbut, C., Galmiche, J. P. & Blottiere, H. M. (2000) Butyrate and trichostatin A effects on the proliferation/differentiation of human intestinal epithelial cells: induction of cyclin D3 and p21 expression. Gut 46: 507–514.
57. Tran, C. P., Familari, M., Parker, L. M., Whitehead, R. H. & Giraud, A. S. (1998) Short-chain fatty acids inhibit intestinal trefoil factor gene expression in colon cancer cells. Am. J. Physiol. Gastrointest. Liver Physiol. 275: G85–G94.
58. Lu, Y. & Lotan, R. (1999) Transcriptional regulation by butyrate of mouse galectin-1 gene in embryonal carcinoma cells. Biochim. Biophys. Acta 1444: 85–91.

59. Walker, G. E., Wilson, E. M., Powell, D. & Oh, Y. (2001) Butyrate, a histone deacetylase inhibitor, activates the human IGF binding protein-3 promoter in breast cancer cells: molecular mechanism involves an Sp1/Sp3 multiprotein complex. Endocrinology 142: 3817–3827.

60. Suske, G. (1999) The Sp-family of transcription factors. Gene 238: 291–300.

61. Mastrangelo, I. A., Courey, A. J., Wall, J. S., Jackson, S. P. & Hough, P. V. (1991) DNA looping and Sp1 multimer links: a mechanism for transcriptional synergism and enhancement. Proc. Natl. Acad. Sci. U.S.A. 88: 5670–5674.

62. Pascal, E. & Tjian, R. (1991) Different activation domains of Sp1 govern formation of multimers and mediate transcriptional synergism. Genes Dev. 5: 1646–1656.

63. Ryu, S., Zhou, S., Ladurner, A. G. & Tjian, R. (1999) The transcriptional cofactor complex CRSP is required for activity of the enhancer-binding protein Sp1. Nature 397: 446–450.

64. Doetzlhofer, A., Rotheneder, H., Lagger, G., Koranda, M., Kurtev, V., Brosch, G., Wintersberger, E. & Seiser, C. (1999) Histone deacetylase 1 can repress transcription by binding to Sp1. Mol. Cell. Biol. 19: 5504–5511.

65. Xiao, H., Hasegawa, T. & Isobe, K. (2000) p300 collaborates with Sp1 and Sp3 in $p21^{waf1/cip1}$ promoter activation induced by histone deacetylase inhibitor. J. Biol. Chem. 275: 1371–1376.

66. Porter, W., Saville, B., Hoivik, D. & Safe, S. (1997) Functional synergy between the transcription factor Sp1 and the estrogen receptor. Mol. Endocrinol. 11: 1569–1580.

67. Kennett, S. B., Udvadia, A. J. & Horowitz, J. M. (1997) Sp3 encodes multiple proteins that differ in their capacity to stimulate or repress transcription. Nucleic Acids Res. 25: 3110–3117.

68. Philipsen, S. & Suske, G. (1999) A tale of three fingers: the family of mammalian Sp/XKLF transcription factors. Nucleic Acids Res. 27: 2991–3000.

69. Tsai, S. C. & Seto, E. (2002) Regulation of histone deacetylase 2 by protein kinase CK2. J. Biol. Chem. 277: 31826–31833.

70. Niefind, K., Guerra, B., Ermakowa, I. & Issinger, O. G. (2001) Crystal structure of human protein kinase CK2: insights into basic properties of the CK2 holoenzyme. EMBO J. 20: 5320–5331.

71. Landesman-Bollag, E., Song, D. H., Romieu-Mourez, R., Sussman, D. J., Cardiff, R. D., Sonenshein, G. E. & Seldin, D. C. (2001) Protein kinase CK2: signaling and tumorigenesis in the mammary gland. Mol. Cell. Biochem. 227: 153–165.

72. Landesman-Bollag, E., Romieu-Mourez, R., Song, D. H., Sonenshein, G. E., Cardiff, R. D. & Seldin, D. C. (2001) Protein kinase CK2 in mammary gland tumorigenesis. Oncogene 20: 3247–3257.

73. Tawfic, S., Yu, S., Wang, H., Faust, R., Davis, A. & Ahmed, K. (2001) Protein kinase CK2 signal in neoplasia. Histol. Histopathol. 16: 573–582.

74. Pflum, M. K., Tong, J. K., Lane, W. S. & Schreiber, S. L. (2001) Histone deacetylase 1 phosphorylation promotes enzymatic activity and complex formation. J. Biol. Chem. 276: 47733–47741.

75. Sowa, Y., Orita, T., Minamikawa-Hiranabe, S., Mizuno, T., Nomura, H. & Sakai, T. (1999) Sp3, but not Sp1, mediates the transcriptional activation of the p21/WAF1/Cip1 gene promoter by histone deacetylase inhibitor. Cancer Res. 59: 4266–4270.

76. Bai, L. & Merchant, J. L. (2000) Transcription factor ZBP-89 cooperates with histone acetyltransferase p300 during butyrate activation of p21waf1 transcription in human cells. J. Biol. Chem. 275: 30725–30733.

77. Richon, V. M., Sandhoff, T. W., Rifkind, R. A. & Marks, P. A. (2000) Histone deacetylase inhibitor selectively induces p21WAF1 expression and gene-associated histone acetylation. Proc. Natl. Acad. Sci. U.S.A. 97: 10014–10019.

78. Bottazzi, M. E., Zhu, X., Bohmer, R. M. & Assoian, R. K. (1999) Regulation of $p21^{cip1}$ expression by growth factors and the extracellular matrix reveals a role for transient ERK activity in G1 phase. J. Cell Biol. 146: 1255–1264.

79. Cheng, M., Olivier, P., Diehl, J. A., Fero, M., Roussel, M. F., Roberts, J. M. & Sherr, C. J. (1999) The $p21^{Cip1}$ and $p27^{Kip1}$ CDK "inhibitors" are essential activators of cyclin D-dependent kinases in murine fibroblasts. EMBO J. 18: 1571–1583.

80. Assoian, R. K. (1997) Anchorage-dependent cell cycle progression. J. Cell Biol. 136: 1–4.

81. Roovers, K. & Assoian, R. K. (2000) Integrating the MAP kinase signal into the G1 phase cell cycle machinery. Bioessays 22: 818–826.

82. Nakano, K., Mizuno, T., Sowa, Y., Orita, T., Yoshino, T., Okuyama, Y., Fujita, T., Ohtani-Fujita, N., Matsukawa, Y., Tokino, T., Yamagishi, H., Oka, T., Nomura, H. & Sakai, T. (1997) Butyrate activates the WAF1/Cip1 gene promoter through Sp1 sites in a p53-negative human colon cancer cell line. J. Biol. Chem. 272: 22199–22206.

83. Butler, L. M., Webb, Y., Agus, D. B., Higgins, B., Tolentino, T. R., Kutko, M. C., LaQuaglia, M. P., Drobnjak, M., Cordon-Cardo, C., Scher, H. I., Breslow, R., Richon, V. M., Rifkind, R. A. & Marks, P. A. (2001) Inhibition of transformed cell growth and induction of cellular differentiation by pyroxamide, an inhibitor of histone deacetylase. Clin. Cancer Res. 7: 962–970.

84. Marks, P. A., Rifkind, R. A., Richon, V. M. & Breslow, R. (2001) Inhibitors of histone deacetylase are potentially effective anticancer agents. Clin. Cancer Res. 7: 759–760.

85. Richon, V. M., Zhou, X., Rifkind, R. A. & Marks, P. A. (2001) Histone deacetylase inhibitors: development of suberoylanilide hydroxamic acid (SAHA) for the treatment of cancers. Blood Cells Mol. Dis. 27: 260–264.

86. Marks, P. A., Richon, V. M. & Rifkind, R. A. (2000) Histone deacetylase inhibitors: inducers of differentiation or apoptosis of transformed cells. J. Natl. Cancer Inst. 92: 1210–1216.

87. Warrell, R. P., Jr., He, L. Z., Richon, V., Calleja, E. & Pandolfi, P. P. (1998) Therapeutic targeting of transcription in acute promyelocytic leukemia by use of an inhibitor of histone deacetylase. J. Natl. Cancer Inst. 90: 1621–1625.

88. He, L. Z., Tolentino, T., Grayson, P., Zhong, S., Warrell, R. P., Jr., Rifkind, R. A., Marks, P. A., Richon, V. M. & Pandolfi, P. P. (2001) Histone deacetylase inhibitors induce remission in transgenic models of therapy-resistant acute promyelocytic leukemia. J. Clin. Invest. 108: 1321–1330.

89. Sowa, Y. & Sakai, T. (2000) Butyrate as a model for "gene-regulating chemoprevention and chemotherapy." Biofactors 12: 283–287.

Journal of Cellular Biochemistry 84:439–446 (2002)

FAST TRACK

Isolation of Transcriptionally Active Chromatin From Human Breast Cancer Cells Using Sulfolink Coupling Gel Chromatography

Jian-Min Sun, Hou Yu Chen, and James R. Davie*

Manitoba Institute of Cell Biology, McDermot Avenue, Winnipeg, Manitoba, Canada

Abstract The process of transcription unfolds the nucleosome. The unfolded nucleosome structure will be maintained as long as the histones are in a highly acetylated state. Typically the cysteine residue at position 110 of histone H3 is buried in the interior of the nucleosome. However, the transcribed unfolded nucleosome has its H3 cysteine exposed, offering a tag to isolate and study transcribed nucleosomes. In this study, we applied Sulfolink Coupling Gel chromatography to isolate unfolded nucleosomes from estrogen dependent human cancer T5 cells. Inhibition of histone deacetylase activity did not enhance the yield of unfolded nucleosomes from these cells. We show that the estrogen receptor and c-*myc* transcribed DNA sequences are associated with unfolded nucleosomes. In chromatin immunoprecipitation (ChIPs) assays, we found that the coding regions of the estrogen receptor and c-*myc* genes are bound to highly acetylated H3 and H4 in cultured T5 Cells. We conclude that in cultured T5 breast cancer cells H3 and H4 are in highly acetylated states maintaining the unfolded structure of the transcribed nucleosome and facilitating subsequent rounds of elongation. J. Cell. Biochem. 84: 439–446, 2002.

Key words: transcriptionally active chromatin; histone acetylation; unfolded nucleosomes; chromatin fractionation; transcription

In mammalian cells, histone H3 is the only cysteine containing histone. The H3 cysteine residue at position 110 is typically buried in the interior of the nucleosome and is not available to thiol reactive reagents. However, nucleosomes associated with transcribing DNA are exceptions. These nucleosomes are unfolded, exposing the H3 cysteine to thiol reactive reagents [Bazett-Jones et al., 1996]. To unfold the nucleosome, the transcription process is absolutely necessary [Chen and Allfrey, 1987].

To maintain the unfolded structure, the nucleosomal histones need to be in a highly acetylated state. In studies with chicken immature erythrocyte chromatin, we found that both transcription elongation and highly acetylated histones were required to detect the thiol reactive nucleosome [Walia et al., 1998]. The unfolded, thiol reactive nucleosome structure was maintained for as long as the histones remained highly acetylated. Once the histones were deacetylated, the nucleosomes folded to a thiol unreactive state [Walia et al., 1998].

The balance of histone acetyltransferases and deacetylases located at a transcriptionally active chromatin site governs the dynamics and steady state levels of acetylated histone isoforms at that site. Our results suggest that in avian immature erythrocytes, there is a relatively higher level of histone deacetylases to histone acetyltransferases associated with the transcribing chromatin with the steady state of highly acetylated histone isoforms being low.

Several groups have exploited the unique thiol reactive property of transcriptionally

Abbreviations used: MAR, matrix attachment region; ChIPs, chromatin immunoprecipitation; AUT-PAGE, acetic acid- urea- Triton X-100-polyacrylamide gel; PMSF, phenylmethylsulfonyl fluoride.

Grant sponsor: U.S. Army Medical and Material Command Breast Cancer Research Program ; Grant number: #DAM17–97–1–7175; Grant sponsor: Canadian Institutes of Health Research (CIHR); Grant number: MT-9186.

*Correspondence to: James Davie, Manitoba Institute of Cell Biology, 675 McDermot Avenue, Winnipeg, MB, R3E 0V9, Canada. E-mail: davie@cc.umanitoba.ca

Received 15 June 2001; Accepted 20 June 2001

DOI 10.1002/jcb.1302

active nucleosomes to isolate and characterise transcribing chromatin by organomercury affinity column chromatography, a method developed by Dr. Allfrey and colleagues [Allegra et al., 1987; Guo et al., 1998; Walia et al., 1998; Cui et al., 1999]. Characterisation of the mercury bound nucleosomes demonstrated that the unfolded nucleosomes were associated with highly acetylated histones.

With the commercial discontinuation of the organomercurial agarose gel product, we developed an alternate method to isolate thiol-reactive transcriptionally active nucleosomes from human breast cancer cells. Using this method we investigated whether inhibition of histone deacetylases influenced the yield of thiol reactive unfolded nucleosomes. Further, we applied chromatin immunoprecipitation (ChIPs) assays with antibodies to highly acetylated H3 and H4 to decide the status of the highly acetylated histones associated with the coding regions of genes expressed in estradiol dependent breast cancer cells.

MATERIALS AND METHODS

Fractionation of Breast Cancer Chromatin

Human breast cancer cell line T5 (ERα positive and estrogen dependent) and MDA MB 231 (ERα negative and estrogen independent) were grown in DMEM (GIBCO, Grand Island, NY) medium supplemented with 5% fetal bovine serum, penicillin (100 U/ml), streptomycin (100 mg/ml), and 5% glucose [Coutts et al., 1996]. Treatment of cells with 10 mM sodium butyrate was for 2 h. Chromatin fractionation was done as described previously [Ridsdale et al., 1988; Delcuve and Davie, 1989]. In brief, nuclei from human breast cancer T5 cells were isolated in TNM buffer (10 mM Tris-HCl, pH 8, 100 mM NaCl, 2 mM $MgCl_2$, 0.3 M sucrose, 1 mM PMSF) and resuspended to 20 A_{260}/ml. Micrococcal nuclease (Worthington, New Jersey) and $CaCl_2$ were added to a final concentration of 15 U/ml and 1 mm, respectively. After incubation at 37°C for 10 min, digested nuclei were collected by centrifugation at 12,000*g* for 10 min. The pellets were resuspended in 10 mM EDTA (pH 7.5) and left on ice for at least 30 min to release chromatin fragments into solution. The soluble chromatin fraction (SE) was separated by centrifugation at 12,000*g* for 10 min. The percentage of SE released from nuclei of untreated cells was 33±7 (n= 3), while the ratio of SE released from nuclei from butyrate treated cells was 35±5 (n=3).

Sulfolink Coupling Gel Column Chromatography

Sulfolink Coupling Gel was obtained from Pierce (Rockford, Illinois). Sulfolink Coupling Gel consists of immobilised iodoacetyl on a cross-linked agarose support. All procedures were carried out in the dark. The Sulfolink agarose beads were washed with five volumes of coupling buffer (50 mM Tris-HCl, pH 8.5, 5 mM EDTA). The chromatin fraction SE was diluted 10-fold in coupling buffer and then loaded onto a Sulfolink column (20 A_{260} of chromatin/1 ml of Sulfolink gel). The column was incubated at room temperature with rotation for 15 min, then without rotation for another 15 min. The unbound fraction was collected. The column was washed with five volumes of coupling buffer. Five volumes of 0.8 M NaCl in coupling buffer was passed through the column. Five volumes of 1.2 M NaCl in coupling buffer and 2 M NaCl in coupling buffer were subsequently passed through the column to elute chromatin bound to the column.

To check the specificity of Sulfolink column, a cysteine block experiment was done. The Sulfolink beads were washed with five volumes of coupling buffer. The beads were incubated with 50 mM cysteine in coupling buffer, and untreated beads were incubated with equal volume of coupling buffer at room temperature for 15 min with rotation, then for 15 min without rotation. After centrifugation to remove the buffer, the beads were washed with five volumes of coupling buffer. Chromatin fraction SE was added to the treated and untreated Sulfolink beads and incubated as described above. The aliquots of unbound fractions were collected, and the OD_{260} (optical density at 260 nm) measured. The ratios of OD_{260} for unbound from the treated and untreated columns were calculated.

DNA Preparation and Southern Blotting

DNA preparation was done as described previously [Delcuve and Davie, 1989]. DNA was isolated from chromatin fraction by digestion with RNase A and proteinase K followed by extraction with phenol and chloroform. Ten micrograms of DNA was loaded onto a 0.8% agarose gel. After electrophoresis, DNA was

transferred onto Hybond N+ (Amersham Pharmacia Biotech, Bale d'Urfe, Quebec) nylon membrane, and hybridised with ^{32}P labeled probes. The cloned probes were: pHsp70myc, which contains the human c-*myc* exon 2 and exon 3 (obtained from Dr. B. Shiu, University of Manitoba); pHGER5, which consists of the human ERα exon 3 (obtained from Dr. L. Murphy, University of Manitoba); RH10, which contains the human apolipoprotein B 5′ matrix attachment region (MAR) sequence (from Dr. G. Delcuve, Cangene). Inserts from the plasmids were processed as follows: pGHER5/EcoR I and Sal I to yield a 2.8 kb fragment; RH10/Xba I to yield a 2.5 kb fragment; pHsp70myc/BamH I to linearize plasmid. The DNA probes were labeled with ^{32}P α-dCTP using the RadPrime DNA Labelling System (Gibco BRL, Grand Island, NY). Before hybridisation the slot-blot was incubated in aqueous pre-hybridisation (APH) solution (5X SSC, 5X Denhardt solution, 1% (w/v) SDS, 100 μ/ml denatured salmon sperm DNA) for 1 h at 68°C. The probe (about 10 ng/ml of APH solution) was then denatured by boiling for 10 min, and then added to the slot blot along with fresh, pre-warmed APH-solution. The hybridisation took place overnight at 68°C, and was proceeded by 2–5 min washes in 2X SSC/0.1% SDS at room temperature, 2–5 min washes in 0.2X SSC/0.1% SDS at room temperature, 2–15 min washed in pre-warmed (42°C) 0.2X SSC/0.1% SDS for 15 min at 42°C, and finally, one quick rinse in 2X SSC at room temperature.

Protein Preparation, AUT Polyacrylamide Gel, and Western Blotting

Histones were extracted from the chromatin fractions with 0.4 N sulphuric acid and TCA precipitated as described [Delcuve and Davie, 1989]. Electrophoresis of proteins was performed using AUT (acetic acid–urea–Triton X-100)-15% polyacrylamide gels as described [Delcuve and Davie, 1992]. Anti-acetylated H3 antibodies were obtained from Upstate and were used to analyse acetylated histones in Western blotting.

ChIPs Assay

ChIPs assays were performed as described previously [Chadee et al., 1999]. Immunoprecipitation of chromatin fragments with highly acetylated histones was performed using polyclonal antibodies to di-acetylated (acetylated lysines 9 and 14) H3 and penta-acetylated H4 (Upstate Biotechnology, NY). The cells were grown to approximately 80% confluence and then washed twice with PBS. Histones were cross-linked to DNA by incubation of cells in PBS containing 1% formaldehyde for 8 min at 37°C. The cross-linked cells were then washed twice with cold PBS containing proteinase inhibitors (1 mM PMSF, 1 μg/ml leupeptin, 1 μg/ml of aprotinin) and harvested. About 1×10^6 cells were resuspended in 1 ml of Lysis buffer (1% SDS, 10 mM EDTA, 50 mM Tris-HCl, pH 8.1), and incubated on ice for 10 min. The cell lysate was sonicated with four sets of 10-s pulses. Under these conditions, the DNA fragment lengths ranged between 200 and 2,000 base pairs. After a brief spin, the supernatant was diluted to A_{260}/ml with Dilution Buffer (0.01% SDS, 1.1% Triton X-100, 1.2 mM EDTA, 16.7 mM Tris-HCl, pH 8.1, 167 mM NaCl). Eighty microliters of protein A-agarose slurry pre-treated with salmon sperm DNA was added to 1 ml of cell lysate (1 A_{260}) and incubated at 4°C for 30 min with agitation. After a brief spin, the supernatant was transferred to a fresh tube, and 5 μl of anti-acetyl histone H3 serum or anti-acetylated H4 serum was added. A tube not containing antibody was used as the control. After incubation at 4°C for 16–18 h with rotation, 60 μl of protein A agarose slurry was added to each tube, and incubated at 4°C for 1 h with agitation. The beads were pelleted, and washed with the following buffers: once with Low salt buffer (0.1% SDS, 1% Triton X-100, 2 mM EDTA, 20 mM Tris-HCl, pH 8.1, 150 mM NaCl), once with High salt buffer (0.1% SDS, 1% Triton X-100, 2 mM EDTA, 20 mM Tris-HCl, pH 8.1, 500 mM NaCl), once with LiCl buffer (0.25 M LiCl, 1% NP-40, 1% deoxycholate, 1 mM EDTA, 10 mM Tris-HCl, pH 8.1), twice with TE buffer (10 mM Tris-HCl, pH 8.0, 1 mM EDTA). For each wash, 1 ml buffer was added, and the tubes were agitated at 4°C for 5 min, then the beads were pelleted. Histone-DNA complexes were eluted by adding 250 μl of Elution buffer (1% SDS, 0.1 M $NaHCO_3$) to the beads. The tubes were incubated and rotated at room temperature for 15 min. The beads were pelleted, and the supernatant was transferred to a fresh tube. The elution step was repeated once, and the supernatants were combined. DNA cross-links were reversed by adding 25 μl of 4 M NaCl to the 0.5 ml elute, and incubated at 65°C for 4 h. The elutant was treated with proteinase K

(10 μg/ml) in EDTA, Tris-HCl (pH 6.5) at 55°C for 1 h. DNA was extracted with phenol/chloroform, precipitated with ethanol, and resuspended in TE. DNA fragments isolated by ChIPs or from the input were used as a template in PCR reactions. Primers were human ERα-exon I (upstream 5′-TTCGTCCTGGGAGCTGCACTT-3′ and downstream 5′-GCAGAAGGCTCAGAAACCGGC-3′) and human c-*myc* exon I (upstream 5′-GAGCTGTGCTGCTCGCGGCCG CCA-3′ and downstream 5′-CCCTATTCGCTC CGGATCTCCCTT-3′). PCR was carried out as previously described [Sun et al., 1999].

RESULTS

Isolation of Transcribing Chromatin From Human Breast Cancer Cells

To isolate thiol reactive unfolded transcriptional active nucleosomes, we tested the application of the Sulfolink Coupling Gel, which consists of immobilized iodoacetyl groups on a cross-linked agarose support. Human breast cancer T5 cells were incubated for 2 h with sodium butyrate to drive dynamically acetylated histones into a highly acetylated state, with the intention of maximising the yield of unfolded transcribing nucleosomes [Walia et al., 1998]. The low ionic strength soluble chromatin fraction isolated from micrococcal nuclease digested T5 nuclei was applied to the Sulfolink Coupling Gel. The Sulfolink column may retain chromatin fragments indirectly by non-histone chromosomal proteins, which have reactive thiols, or directly by the thiol-reactive H3 of unfolded nucleosomes. To disrupt interactions between thiol-reactive non-histone chromosomal proteins and chromatin fragments, the column was washed with 0.8 M NaCl. At this concentration of NaCl, there will be some dissociation of H2A and H2B dimers from nucleosomal DNA; however, unfolded nucleosomes that have reacted with the iodoacetyl group will remain bound to DNA [Li et al., 1993; Walia et al., 1998]. A 21±4.7% of A_{260}-absorbing material remained bound to the column following the 0.8 M NaCl wash (Fig. 1). To test whether the chromatin fragments were being retained through reactive sulphydryls, the column was pre-treated with cysteine to block the iodoacetyl groups before the application of the T5 chromatin fraction SE. A 3.5±1.5% of the A_{260}-absorbing material was bound to the cysteine-blocked column (Fig. 1). These results

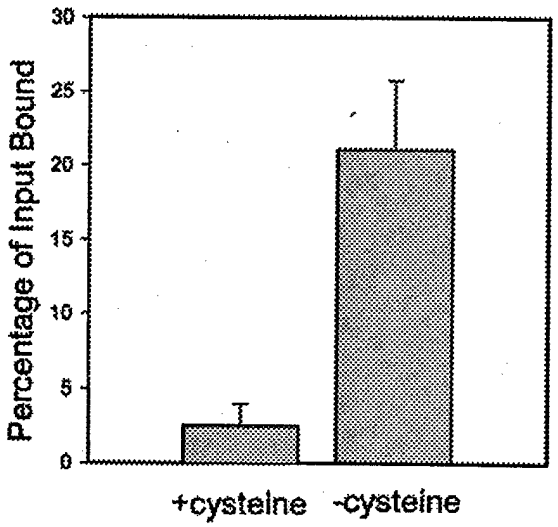

Fig. 1. Isolation of unfolded nucleosomes by Sulfolink coupling gel chromatography. SE chromatin fraction from the T5 cells incubated with 10 mM sodium butyrate was applied to a Sulfolink column that was either untreated or treated with cysteine to block the iodoacetyl groups. The fraction of input chromatin remaining bound to the column following a 0.8 M NaCl wash is indicated. DNA was measured by absorbance at 260 nm. The results are the means±standard error of the mean for eight separate experiments.

provide evidence that chromatin fragments were retained by reactive sulphydryls.

Histones and DNA fragments of the unbound and bound column fractions were analyzed. SE chromatin was applied to the Sulfolink column, which was subsequently washed with a buffer containing 0.8 M NaCl. The histones in the unbound fractions and those remaining bound to the column were isolated by acid extraction and electrophoresed on AUT polyacrylamide gels. The AUT gels were either Coomassie Blue stained or transferred onto a nitrocellulose filter for Western blotting. The Coomassie Blue stained gels show that the Sulfolink bound fractions were enriched in hyperacetylated isoforms of H4 (Fig. 2B,C). Western blot analysis using anti-acetylated H3 antibody shows the bound fraction was enriched in hyperacetylated isoforms of H3 (Fig. 2C). Thus, in agreement with previous studies, H3-thiol reactive nucleosomes are associated with highly acetylated H3 [Walia et al., 1998].

Figure 2A shows the DNA fragment lengths present in the various column fractions. The unbound fraction contained oligonucleosomes (Fig. 2A, lane 2), while the bound fraction consisted of shorter mono- and di-nucleosomes (Fig. 2A, lane 3). This result shows that the column matrix was not trapping long chromatin

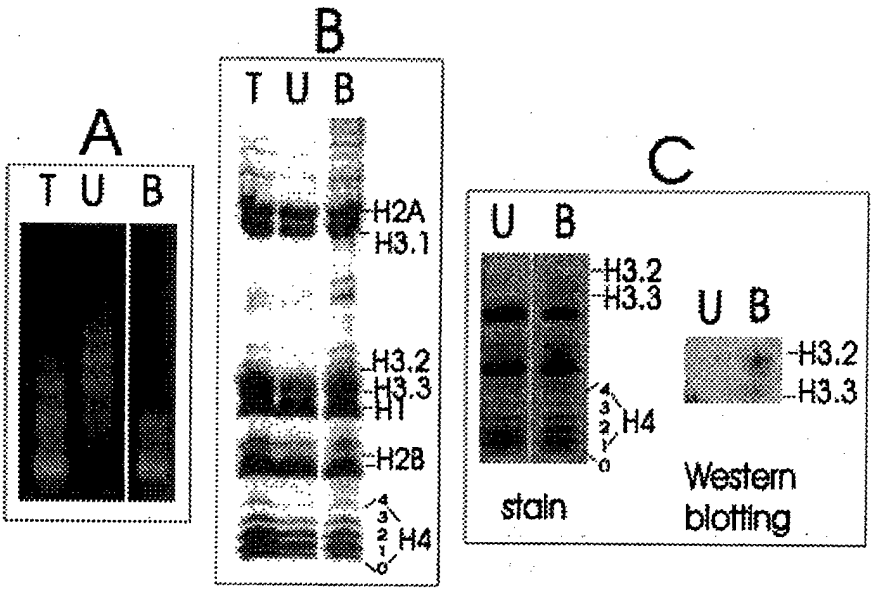

Fig. 2. Characterisation of chromatin fragments isolated by Sulfolink coupling gel chromatography. The SE chromatin fraction from T5 cells incubated with sodium butyrate was applied to a Sulfolink coupling gel chromatography column. The column was washed with a 0.8 M NaCl-containing buffer. The unbound fraction consists of the initial flow through and 0.8 M NaCl eluted fraction. **Panel A:** DNA fragments (8 μg) extracted from the input (T), unbound (U), and bound chromatin (B) were electrophoretically resolved on a 0.8% agarose gel and then visualized by ethidium staining. **Panel B:** Histones were isolated by acid extraction of the input (T), unbound (U), and bound chromatin (B). Each lane had 10 μg of protein. The histones were resolved by AUT 15% PAGE, and the gel was subsequently stained with Coomassie Blue. Panel **C:** An AUT 15% PAGE gel containing histones (10 μg) from the unbound and bound fractions was stained with Coomassie Blue (left panel), or the proteins were transferred to nitrocellulose membranes and immunochemically stained with anti-acetylated H3 antibodies (right panel). Variants of H3, H3.1, H3.2, and H3.3 are shown. The numbers 0, 1, 2, 3, and 4 indicate the position of un-, mono-, di-, tri-, and tetra-acetylated isoforms of H4, respectively.

fragments. As micrococcal nuclease processes transcriptionally active chromatin faster than bulk chromatin, finding that the column retains shorter chromatin fragments is consistent with the retention of transcriptionally active chromatin [Delcuve and Davie, 1989].

Following the wash with 0.8 M NaCl, the bound chromatin fragments were dissociated from the column by washes with 1.2 and 2.0 M NaCl. The 1.2 M NaCl wash was chosen to dissociate DNA from highly acetylated H3, while 2.0 M NaCl release the remaining DNA that is bound to less modified H3 [Li et al., 1993]. The DNA fragments isolated from the Sulfolink column with SE chromatin fragments were resolved by agarose gel electrophoresis and transferred to membranes for Southern blot analysis. We studied the distribution of transcriptionally active genomic DNA sequences, c-*myc* (exon 2 and 3) and estrogen receptor (ERα, exon 3), and one repressed DNA sequence, apolipoprotein 5′ MAR. Figure 3 shows the transcriptionally active DNA sequences (ERα and c-*myc*) were present in the 1.2 and 2 M NaCl fractions. These results demonstrate that unfolded transcriptionally active nucleosomes can be captured on a Sulfolink column.

Association of Highly Acetylated H3 and H4 With Transcriptional Active Genes

To decide whether inhibition of histone deacetylases affected the yield of transcribing nucleosomes retained by the Sulfolink column, SE chromatin from T5 cells not incubated with sodium butyrate was applied to the column, which was subsequently washed with 0.8 M NaCl. A 27±6.3% of A_{260}-absorbing material was retained by the column. Thus, preventing the deacetylation of dynamically acetylated histones did not affect the yield of unfolded nucleosomes.

The isolation of unfolded nucleosomes from T5 cells suggested that the steady state of histone acetylation along the transcribed chromatin in the cultured cells was sufficiently high to maintain the unfolded nucleosome. To test this directly we applied ChIPs assays to find out whether the coding regions of transcriptionally active genes were associated with highly

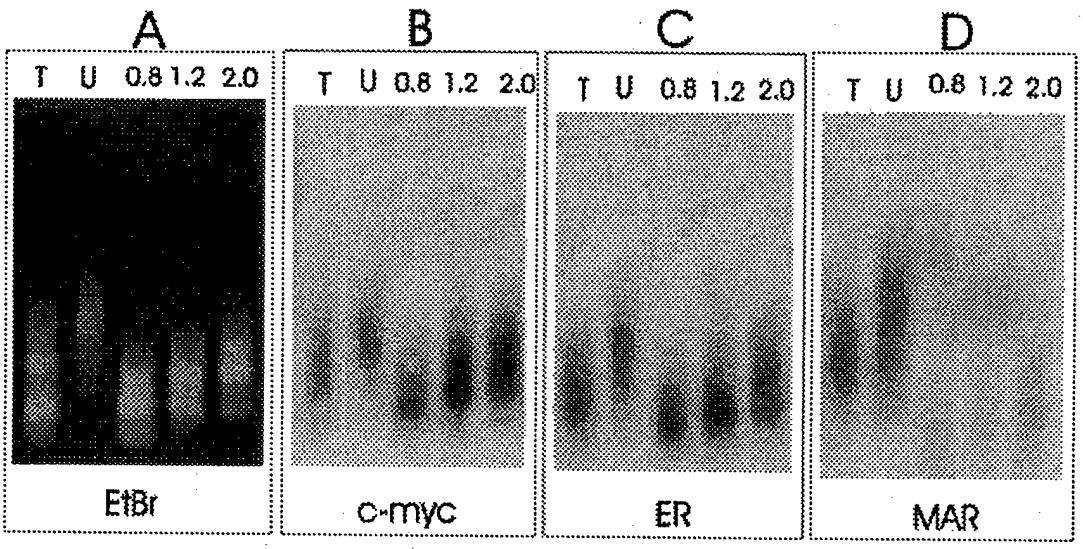

Fig. 3. Association of unfolded nucleosomes with transcribed estrogen receptor and c-*myc* DNA. SE chromatin from T5 human breast cancer cells was fractionated by Sulfolink column chromatography. **Panel A:** Each lane had 10 μg of DNA fragments extracted from the input (T), unbound (U), 0.8 M NaCl fraction (0.8), 1.2 M NaCl fraction (1.2), and 2 M NaCl fraction (2.0), which were electrophoretically resolved on 0.8% agarose gel and then visualised by ethidium bromide staining. **Panels B–D:** The DNA fragments were transferred to membranes, which were hybridised to a genomic c-*myc* probe (panel B), genomic ER probe (panel C), or apolipoprotein A1 5′ MAR (MAR) genomic probe (panel D). The autoradiograms are shown in panels B–D.

acetylated histone. The input DNA and DNA isolated by ChIPs with anti-acetylated H3 and anti-acetylated H4 antibodies were amplified by PCR with specific primer sets and analyzed on agarose gels. The primer sets chosen monitored the human ERα exon 1 and c-*myc* exon 1. Figure 4 shows that the 171-bp ERα exon 1 and 279-bp c-*myc* exon 1 were found in DNA isolated by ChIPs from T5 cells. Using slot blot hybridisation rather than PCR analyses of the immunoprecipitated DNA, we found that apolipoprotein 5′ MAR sequences were not enriched in the immunoprecipitated DNA. In control studies, we detected the c-*myc* exon 1, but not the ERα1, fragment in DNA immunoprecipitated from ERα negative MDA MB 231 human breast cancer cells (Fig. 4). These results demonstrate that in T5 cells the coding regions of ERα and c-*myc* are bound to highly acetylated H3 and H4, which would maintain the unfolded nucleosome structure once formed by transcription of the gene.

DISCUSSION

Mercury affinity chromatography has been used to isolate and characterise active nucleosomes and to identify differentially expressed genes [Allfrey and Chen, 1991; Cui et al., 1999]. The unavailability of the commercial mercury affinity matrix, however, necessitated an alternate methodology. This study presents a novel method to isolate transcriptionally active unfolded nucleosomes by sulfolink coupling gel chromatography. Using this strategy, we show that the transcribed ERα and c-*myc* genes, but not the transcriptionally inert apolipoprotein MAR DNA, in human breast cancer T5 cells are associated with unfolded nucleosomes. Consistent with previous studies, the thiol reactive unfolded nucleosomes were enriched in highly acetylated H3 and H4.

There is considerable interest in acetylation status of histones at promoters [Chen et al., 1999; Davie and Moniwa, 2000; Davie and Spencer, 2001; Shang et al., 2000]. However, dynamic acetylation occurs along the coding region of the gene and may occur throughout an entire active gene domain [Vogelauer et al., 2000; Myers et al., 2001]. Histone acetylation is not sufficient to establish the unfolded nucleosome state, but highly acetylated histones have a role in maintaining the unfolded nucleosome structure once it is formed by transcription [Walia et al., 1998]. Our studies with chicken immature erythrocyte chromatin showed that the longevity of the unfolded transcribing nucleosome was dependent upon time that the histones were maintained in highly acetylated status [Walia et al., 1998]. The inability to

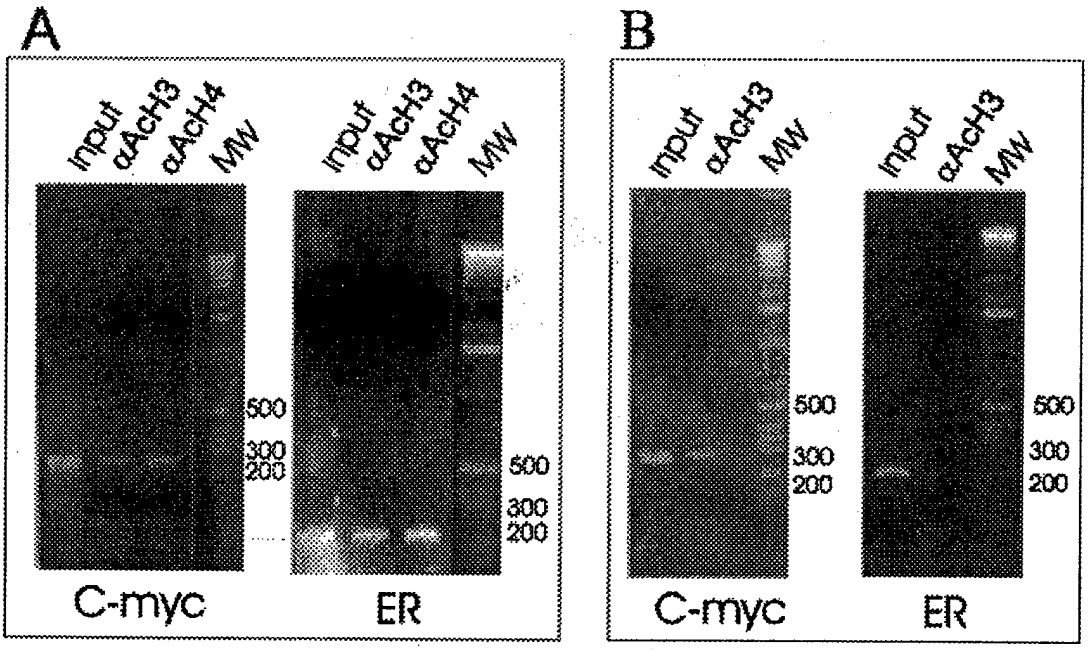

Fig. 4. Association of highly acetylated H3 and H4 isoforms with transcribed estrogen receptor and c-*myc* coding regions. DNA fragments isolated by ChIPs from T5 cells (**panel A**) and MDA MB 231 cell (**panel B**) with anti-acetylated H3 (αAcH3) or H4 (αAcH4) antibodies were analyzed by PCR. One hundred nanograms of DNA isolated from total cell lysate (input) and immunoprecipitated DNA from T5 and MDA MB 231 cells were used as templates in PCR. The primers designed from human ERα exon I and human c-*myc* exon I were used in PCR. The PCR products were electrophoresed on a 1% agarose gel. MW is the DNA molecular marker.

isolate unfolded nucleosomes from avian erythroid cells not treated with butyrate suggested that the steady state of acetylation of histones associated with transcribed chromatin in avian immature erythrocytes is low. As the balance of histone acetyltransferases and deacetylases along the transcribed region of genes decides the steady state level of histone acetylation, our results argue that the activity of histone deacetylases is in excess of that of the histone acetyltransferases at transcriptionally active loci in avian immature erythrocytes. The situation in cultured human breast cancer cells is different in that the steady state of acetylated histones along transcribed DNA is high. This is shown indirectly in that unfolded transcribing nucleosomes are isolated from cultured cells without blocking histone deacetylase activity and shown directly in ChIPs studies. The later studies showed that the exons of ERα and c-*myc* are bound to highly acetylated H3 and H4 in T5 cells. These observations suggest that the coding regions of these genes have a greater level of histone acetyltransferases relative to that of histone deacetylases, maintaining the histones in highly acetylated states. Thus, once a nucleosome was unfolded, the highly acetylated histones would maintain this state, facilitating subsequent rounds of elongation.

ACKNOWLEDGMENTS

A CIHR Senior Scientist to J.R.D. is gratefully acknowledged.

REFERENCES

Allegra P, Sterner R, Clayton DF, Allfrey VG. 1987. Affinity chromatographic purification of nucleosomes containing transcriptionally active DNA sequences. J Mol Biol 196:379–388.

Allfrey VG, Chen TA. 1991. Nucleosomes of transcriptionally active chromatin: isolation of template-active nucleosomes by affinity chromatography. Methods Cell Biol 35:315–335.

Bazett-Jones DP, Mendez E, Czarnota GJ, Ottensmeyer FP, Allfrey VG. 1996. Visualization and analysis of unfolded nucleosomes associated with transcribing chromatin. Nucleic Acids Res 24:321–329.

Chadee DN, Hendzel MJ, Tylipski CP, Allis CD, Bazett-Jones DP, Wright JA, Davie JR. 1999. Increased Ser-10 phosphorylation of histone H3 in mitogen-stimulated and oncogene-transformed mouse fibroblasts. J Biol Chem 274:24914–24920.

Chen TA, Allfrey VG. 1987. Rapid and reversible changes in nucleosome structure accompany the activation, repression, and superinduction of murine fibroblast

protooncogenes c-fos and c-myc. Proc Natl Acad Sci USA 84:5252–5256.

Chen H, Lin RJ, Xie W, Wilpitz D, Evans RM. 1999. Regulation of hormone-induced histone hyperacetylation and gene activation via acetylation of an acetylase. Cell 98:675–686.

Coutts AS, Davie JR, Dotzlaw H, Murphy LC. 1996. Estrogen regulation of nuclear matrix-intermediate filament proteins in human breast cancer cells. J Cell Biochem 63:174–184.

Cui K, Feldman L, Sytkowski AJ. 1999. Isolation of differentially expressed genes by cloning transcriptionally active DNA fragments. Methods 17:265–271.

Davie JR, Moniwa M. 2000. Control of chromatin remodeling. Crit Rev Eukaryot Gene Expr 10:303–325.

Davie JR, Spencer VA. 2001. Signal transduction pathways and the modification of chromatin structure. Prog Nucleic Acid Res Mol Biol 65:299–340.

Delcuve GP, Davie JR. 1989. Chromatin structure of erythroid-specific genes of immature and mature chicken erythrocytes. Biochem J 263:179–186.

Delcuve GP, Davie JR. 1992. Western blotting and immunochemical detection of histones electrophoretically resolved on acid-urea-triton- and sodium dodecyl sulfate-polyacrylamide gels. Anal Biochem 200: 339–341.

Guo C, Davis AT, Ahmed K. 1998. Dynamics of protein kinase CK2 association with nucleosomes in relation to transcriptional activity. J Biol Chem 273:13675–13680.

Li W, Nagaraja S, Delcuve GP, Hendzel MJ, Davie JR. 1993. Effects of histone acetylation, ubiquitination and variants on nucleosome stability. Biochem J 296:737–744.

Myers FA, Evans DR, Clayton AL, Thome AW, Crane-Robinson C. 2001. Targeted and extended acetylation of histones H4 and H3 at active and inactive genes in chicken embryo erythrocytes. J Biol Chem 276:20197–20205.

Risdale JA, Rattner JB, Davie JR. 1988. Erythroid-specific gene chromatin has an altered association with linker histones. Nucleic Acids Res 16:5915–5926.

Shang Y, Hu X, DiRenzo J, Lazar MA, Brown M. 2000. Cofactor dynamics and sufficiency in estrogen receptor-regulated transcription. Cell 103:843–852.

Sun J-M, Chen HY, Moniwa M, Samuel S, Davie JR. 1999. Purification and characterization of chicken erythrocyte histone deacetylase 1. Biochemistry 38:5939–5947.

Vogelauer M, Wu J, Suka N, Grunstein M. 2000. Global histone acetylation and deacetylation in yeast. Nature 408:495–498.

Walia H, Chen HY, Sun J-M, Holth LT, Davie JR. 1998. Histone acetylation is required to maintain the unfolded nucleosome structure associated with transcribing DNA. J Biol Chem 273:14516–24522.

THE JOURNAL OF BIOLOGICAL CHEMISTRY

Vol. 276, No. 52, Issue of December 28, pp. 49435–49442, 2001
Printed in U.S.A.

Effect of Estradiol on Histone Acetylation Dynamics in Human Breast Cancer Cells*

Received for publication, August 30, 2001, and in revised form, October 22, 2001
Published, JBC Papers in Press, October 26, 2001, DOI 10.1074/jbc.M108364200

Jian-Min Sun, Hou Yu Chen, and James R. Davie‡

From the Manitoba Institute of Cell Biology, Winnipeg, Manitoba R3E 0V9, Canada

Histone acetylation plays an important role in remodeling chromatin structure, facilitating nuclear processes such as transcription. We investigated the effect of estradiol on global histone acetylation in hormone-responsive human breast cancer cells. Pulse-chase experiments and immunoblot analyses of dynamically acetylated histones show that estradiol rapidly increases histone acetylation in estrogen receptor (ER)-positive, hormone-dependent T5, but not in ER-negative, hormone-independent MDA MB 231 breast cancer cells. The effect of estradiol on the rates of histone acetylation and deacetylation in T5 cells was determined. We found that estradiol increased the level of acetylated histones by reducing the rate of histone deacetylation, whereas the rate of histone acetylation was not altered. Enzymatic assays and immunoblot analyses of cell fractions showed that estradiol did not affect the level, subnuclear distribution, or activity of class I and II histone deacetylases. However, estradiol did alter the intranuclear distribution of ER and histone acetyltransferases, with both becoming tightly bound in the nucleus and associated with the nuclear matrix. We propose that, following the association of ER with nuclear matrix sites, ER alters the balance of histone acetyltransferases and histone deacetylases at these sites and the dynamics of acetylation of histones associated with transcriptionally active and competent chromatin.

Histone acetylation is a dynamic process directed by histone acetyltransferases (HATs)[1] and histone deacetylases (HDACs). Transcription factors recruit coactivators with HAT activity to regulatory DNA sites, whereas transcriptional repressors recruit corepressors with HDAC activity (1). Nucleosomal histones at or near regulatory elements associated with coactivators with HAT activity become highly acetylated, resulting in the remodeling of chromatin structure (1). These highly acetylated histones are rapidly deacetylated by HDACs accessing these sites. Dynamically acetylated histones, however, are not confined to regulatory regions but are located along the coding region of genes and, in some cases, with a chromatin domain (2–4).

Studies on histone acetylation rates have revealed that in animal cells there are different populations of dynamically acetylated histones. One population is rapidly modified to highly acetylated isoforms (*e.g.* tetra-acetylated H4) and rapidly deacetylated. This population of dynamically acetylated histones is bound to transcriptionally active and competent DNA (5). Another larger population of acetylated histones is slowly modified to highly acetylated states and slowly deacetylated (6).

We have demonstrated that HAT and HDAC activities are associated with the nuclear matrix of avian erythrocytes (7). Further, avian HDAC1 and mammalian HDAC1 are bound to the nuclear matrix, a nuclear substructure that has a critical role in chromatin organization and function (8–12). We proposed a model where nuclear matrix-associated HATs and HDACs mediate a dynamic attachment between transcriptionally active chromatin domains and the nuclear matrix.

Estrogen plays an important role in the cell proliferation and stimulation of DNA synthesis in hormone-responsible breast cancer cells. The estrogen receptor α (ER), when bound to estradiol, recruits the coactivator/HATs CBP, PCAF, steroid receptor cofactor (SRC) 1, and SRC-3 to estrogen-responsive elements, resulting in acetylation of histones at and near the site of ER binding (13, 14). Immediately following the addition of estradiol to hormone-responsive breast cancer cells, ER undergoes a rapid intranuclear redistribution to punctate nuclear foci that are associated with the nuclear matrix (10, 15). This alteration in ER intranuclear trafficking is accompanied with the recruitment of the coactivator/HAT SRC-1 to nuclear matrix-associated sites containing ER.

In this study we investigated the effect of estradiol on global histone acetylation in hormone-responsive breast cancer cells. A previous study demonstrated that estradiol decreased the level of acetylated histones (16). In contrast to these observations, we found that estradiol rapidly increased the level of acetylated histones. An analysis of the rates of histone acetylation and deacetylation in breast cancer cells cultured in estradiol-depleted and -replete conditions revealed that estradiol decreased the rates of histone deacetylation, but had no effect on the rates of histone acetylation. Evidence is presented that estradiol does not affect the levels or nuclear distribution of HDACs, but it does alter the nuclear distribution of HATs.

MATERIALS AND METHODS

Cell Lines and Culture Conditions—Human breast cancer cell line T5 (ER-positive and estrogen-dependent) and MDA MB 231 (ER-negative and estrogen-independent) were grown in DMEM (Invitrogen) supplemented with 5% fetal bovine serum, penicillin (100 units/ml), streptomycin (100 mg/ml), and 5% glucose. Under estrogen-depleted conditions, cells were grown in estrogen-depleted medium, consisting of phenol red-free DMEM (Invitrogen), 7% charcoal-stripped fetal bovine

* This work was supported in part by United States Army Medical and Materiel Command Breast Cancer Research Program Grant DAM17-97-1-7175 and Canadian Institutes of Health Research (CIHR) Grant MT-9186. The costs of publication of this article were defrayed in part by the payment of page charges. This article must therefore be hereby marked "*advertisement*" in accordance with 18 U.S.C. Section 1734 solely to indicate this fact.

‡ Recipient of a CIHR Senior Scientist award. To whom correspondence should be addressed: Manitoba Inst. of Cell Biology, 675 McDermot Ave., Winnipeg, Manitoba R3E 0V9, Canada. Tel.: 204-787-2391; Fax: 204-787-2190; E-mail: davie@cc.umanitoba.ca.

[1] The abbreviations used are: HAT, histone acetyltransferase; HDAC, histone deacetylase; ER, estrogen receptor; ERE, estrogen response element; E_2, estradiol; PBS, phosphate-buffered saline; SRC, steroid receptor cofactor; AUT, acetic acid-urea-Triton X-100; DMEM, Dulbecco's modified Eagle's medium; ABR, Affinity Bioreagents Inc.

serum, penicillin (100 units/ml), streptomycin (100 mg/ml), and 5% glucose as described previously (17). Cells were grown in a 37 °C humidified incubator with 5% CO_2.

Pulse-Chase Labeling Cells for Analyses of Histone Acetylation Rates—To study the effect of estradiol on histone acetylation, T5 cells were grown in estrogen-depleted medium. After 3 days of incubation, T5 cells were grown in the same medium containing cycloheximide (10 μg/ml) for 30 min. Cells were incubated in the same medium containing cycloheximide (10 μg/ml) and [^{3}H]acetate (0.1 mCi/ml; ICN) in the absence (ethanol vehicle only) or presence of 10 nM estradiol for 20 min. After labeling, the cells were washed twice with ice-cold PBS containing 10 mM butyrate and then harvested.

Rates of histone acetylation were determined as described previously (6, 18). T5 cells were grown to a confluence of 70–80%. The medium was removed and cells were washed with pre-warmed PBS. The cells were grown in the same medium containing cycloheximide (10 μg/ml) for 30 min. Cycloheximide was present throughout the labeling period. The cells were incubated at 37 °C for various times with fresh medium containing [^{3}H]acetate in the absence or presence of 10 nM estradiol. After labeling, the cells were washed twice with DMEM containing 10 mM sodium butyrate and 0.1 mM nonradioactive acetate. The cells were chased in the same buffer at 37 °C for various times.

Pulse-Chase Labeling Cells for Analyses of Histone Deacetylation Rates—Rates of histone deacetylation were determined as described previously (6, 19). T5 cells were grown in estrogen-depleted medium for at least 3 days. After two washes with PBS, T5 cells were grown in the same medium containing cycloheximide (10 μg/ml) for 30 min. The cells were incubated for 120 min in the same medium containing 10 mM butyrate, 10 μg/ml cycloheximide, and [^{3}H]acetate in the presence or absence of 10 nM estradiol. After labeling, the cells were washed three times with pre-warmed PBS, and incubated in the same medium without butyrate and radioactive acetate, and with or without estradiol for various times. The cells were then washed and harvested.

Cellular Fractionation—T5 cells were resuspended in TNM buffer (100 mM NaCl, 300 mM sucrose, 10 mM Tris-HCl, pH 7.4, 2 mM $MgCl_2$, 1% thiodiglycol) containing 1 mM phenylmethylsulfonyl fluoride and protease inhibitor mixture (Roche). The cells were lysed by being passed through a syringe with 22-gauge needle. The cytosol and nuclei were isolated from lysed cells after centrifugation at 4500 × *g*. Nuclei preparations were inspected by microscopic analyses. The nuclei were resuspended in TNM buffer. The nuclei were extracted by adding Triton X-100 to a final concentration of 0.5% and incubated on ice for 5 min. After centrifugation at 4500 × *g* for 10 min, the supernatant, named the Triton X-100 supernatant fraction, or Triton-S, was saved. The nuclei pellet was resuspended in an equal volume of TNM buffer with 0.5% Triton X-100; this fraction was named the Triton X-100 pellet fraction, or Triton-P.

Immunoprecipitation and Immunoblotting—Immunoblot analyses was carried out as described previously (9). Polyclonal antibodies against human HDAC1 (Affinity Bioreagents Inc. (ABR)), human HDAC2 (ABR), human HDAC3 (ABR), human HDAC4 (Santa Cruz), human SRC-1 (ABR), and mouse monoclonal antibodies against human ERα (Novocastra Laboratories Ltd.) and SRC-3 (AIB1/RAC3) (Upstate Biotechnology, Inc.) were used. Antibodies against PCAF-A and PCAF-B were a kind gift from Dr. Yoshihiro Nakatani. Acetylated isoforms of H3 and H4 were detected with polyclonal antibodies to di-acetylated H3 and penta-acetylated H4 (Upstate Biotechnology, Inc.).

Histone Acetyltransferase and Deacetylase Assays—Histone acetyltransferase and deacetylase assays were performed as described previously (7, 20).

RESULTS

Estradiol Increases Histone Acetylation in Human Breast Cancer ER-positive T5 Cells—To determine the immediate effect of estradiol (E_2) on histone acetylation, T5 cells (ER-positive and hormone-dependent) grown under E_2-depleted conditions were incubated with or without E_2 and [^{3}H]acetate for 20 min to label dynamically acetylated histones. Comparison of the Coomassie Blue-stained AUT gel patterns shows that histones from E_2-incubated cells had slightly increased levels of highly acetylated (di-, tri-, and tetra-acetylated) isoforms of H4 (Fig. 1*A*). Relative to the di-, tri-, and tetra-acetylated H4 isoforms from cells cultured under E_2-depleted conditions, the level of these acetylated H4 isoforms increased by 2.5% in the E_2-incubated cells. Analyses of the fluorogram revealed a greater change in the levels of the acetylated histones with the labeled highly acetylated isoforms of H3.2, H2B, and H4 being increased in the E_2-incubated cells (Fig. 1*A*). After scanning the fluorogram, the ratios of the level of labeled highly acetylated histone isoforms (Ac3 and Ac4) to total labeled acetylated H4, H3.2, and H2B were calculated. The percentage of acetylated H4 that was highly acetylated was 9 and 12.5% in histones from cells incubated without and with E_2, respectively. The highly acetylated H3 isoforms was 18 and 23% of acetylated H3 in preparations from cells grown without and with E_2. The acetylated H2B that was highly acetylated increased to 17%, while being 15% in cells grown without E_2.

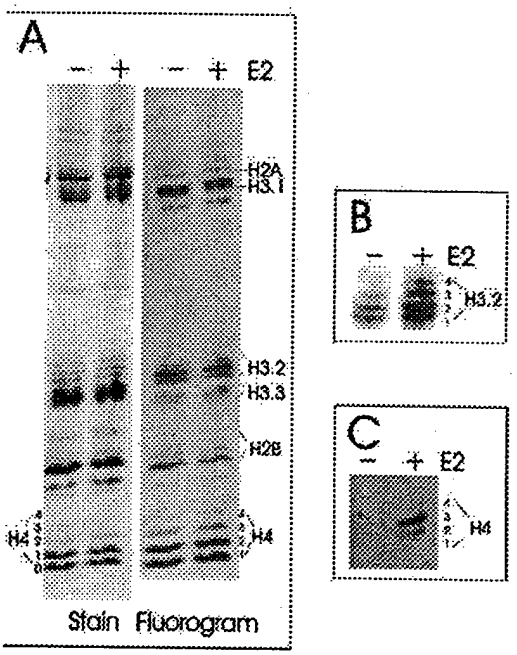

FIG. 1. **Estradiol increases acetylated histone levels in hormone-responsive, human breast cancer T5 cells.** T5 (ER-positive and hormone-dependent) cells were cultured in estrogen-depleted conditions for 3 days, and then incubated in the presence or absence of 10 nM E_2 for 20 min. The histones were resolved by 15% AUT-PAGE (40 μg of protein/lane). *Panel A, left*, Coomassie Blue-stained gel pattern; *right*, accompanying fluorogram. *Panels B* and *C*, the histones from cells incubated in the presence or absence of 10 nM E_2 for 30 min were resolved by 15% AUT-PAGE, transferred to nitrocellulose membranes and immunochemically stained with anti-acetylated H3 (*panel B*) and anti-acetylated H4 (*panel C*) antibodies. The acetylated isoforms of H3.2 and H4 are indicated. *0*, *1*, *2*, *3*, and *4* correspond to un-, mono-, di-, tri-, and tetra-acetylated isoforms, respectively.

To further illustrate the increase in the level of highly acetylated histones in T5 cells incubated with E_2 for 30 min, the histones were analyzed by immunoblot analyses with antibodies recognizing highly acetylated isoforms of H3 (Fig. 1*B*) and H4 (Fig. 1*C*). Fig. 1*B* shows that E_2 incubation increased the levels of highly acetylated isoforms of H3.2. Similarly, Fig. 1*C* shows that E_2 incubation elevated the levels of highly acetylated H4 isoforms. Together, these results demonstrate that E_2 rapidly increases the level of highly acetylated histone isoforms.

This study was repeated with the human breast cancer cell line MDA MB 231 (ER-negative and hormone-independent). Analyses of Coomassie Blue-stained AUT gels and accompanying fluorograms demonstrated that incubation of MDA MB 231 cells with E_2 did not affect acetylated histone levels (data not shown). The ratio of labeled highly acetylated H4 isoforms to total acetylated H4 in E_2-treated MDA MB 231 cells was ~17.5%, which was very similar to the observed 18% for cells cultured without E_2. Immunoblot analyses of histones from

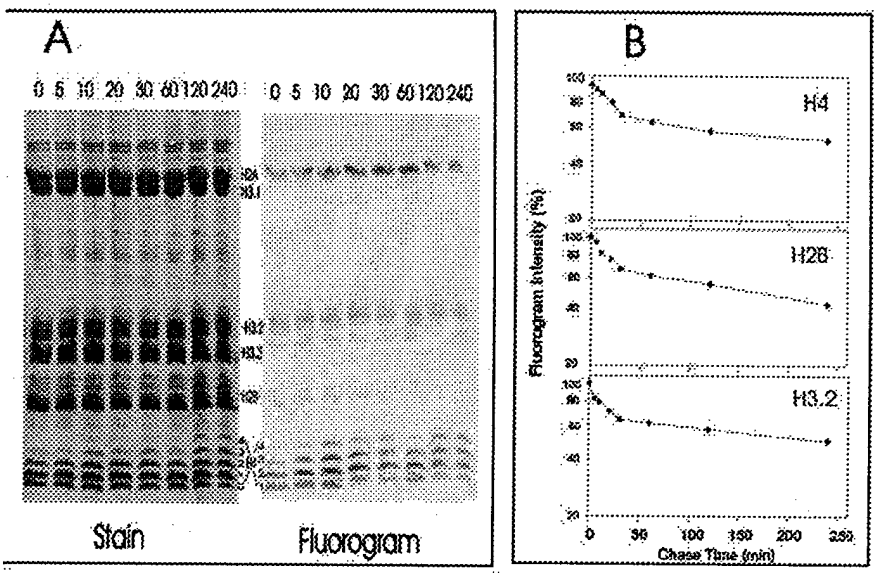

FIG. 2. **Rates of histone acetylation in T5 cells cultured under estrogen-replete conditions.** T5 cells were pulse-labeled with [^{3}H]acetate for 15 min and then chased for 0–240 min in the presence of 10 mM sodium butyrate. The histones were resolved by 15% AUT-PAGE (60 μg of protein in each lane). *Panel A, left*, Coomassie Blue-stained gel; *right*, accompanying fluorogram. The proportions of total radiolabeled H4, H2B, and H3 associated with monoacetylated form were determined by scanning the fluorograms. The proportion of labeled monoacetylated isoforms (H4-Ac1, H3.2-Ac1, and H2B-Ac1) present in total labeled H4, H3 and H2B at zero time was arbitrarily set at 100. The rapid rate of acetylation was determined using the data obtained from the 0–20-min butyrate chase period, whereas the slower rate of acetylation was determined using data from the 60–240-min butyrate chase period (*panel B*).

cells incubated with and without E_2 with antibodies against highly acetylated H4 isoforms showed that E_2 did not affect the levels of highly acetylated H4 isoforms in MDA MB 231 (data not shown). These observations suggest that the E_2-induced increase in histone acetylation in T5 cells involves the ER.

Estradiol Does Not Affect the Rate of Histone Acetylation in T5 Cells—The E_2-induced increase in histone acetylation in T5 cells may be a consequence of an increase in histone acetylation rates, a decrease in histone deacetylation rates, or a combination of both. To determine rates of acetylation, T5 cells were pulse-labeled with [^{3}H]acetate for 5 or 15 min. After labeling, the cells were washed and incubated at 37 °C in medium containing sodium butyrate and cold acetate for various times, chasing label into highly acetylated histone isoforms. It should be noted that the cells were grown in E_2-replete conditions (DMEM with fetal bovine serum). The AUT gel was stained with Coomassie Blue, and the labeled acetylated histone isoforms were detected by fluorography (Fig. 2*A*). Long AUT polyacrylamide gels were used in these experiments to achieve high resolution of the acetylated histone isoforms.

A population of the acetylated histones is engaged in dynamic acetylation, whereas the remainder is "frozen" at various acetylation states. To determine the percentage of histones that were being rapidly acetylated, the loss of unacetylated H4 was plotted as a function of time that the cells were incubated with sodium butyrate as determined by scanning the Coomassie Blue-stained gels (data not shown). The results showed that ~10% of H4 were rapidly acetylated, whereas the bulk of H4 was acetylated at a slow rate.

The intensities of labeled H4, H3, and H2B acetylated isoforms in the fluorograms were scanned. Fig. 2*B* shows the plots of the ratio of monoacetylated H4, H3.2, and H2B isoforms to the total acetylated H4, H3, and H2B, respectively, as a function of time in sodium butyrate. The loss of fluorographic intensity from the monoacetylated histone as a function of time determines the rates of histone acetylation (6). Two rates of acetylation were observed for H4, a fast rate with a $t_{1/2}$ = 8 min and slow rate with a $t_{1/2}$ = 200–350 min. H3.2 also had two rates of acetylation: a fast rate with a $t_{1/2}$ = 8 min and a slow rate with a $t_{1/2}$ = 400 min. The two acetylated rates for H2B were $t_{1/2}$ = 10 and 350 min. These rates of acetylation are comparable with those observed in rat hepatoma cells, human fibroblasts, and avian erythrocytes (6, 18, 21).

To decide whether E_2 affects histone acetylation rates, the pulse-chase experiment was repeated with T5 cells grown under E_2-replete (10 nM E_2) and -depleted conditions. The cells grown under E_2-depleted conditions were incubated with [^{3}H]acetate and ethanol or E_2 at 37 °C for 15 min, and chased in the same medium containing 10 mM butyrate with ethanol or E_2 for various times. Electrophoresis and fluorography were performed as described previously.

The loss of unacetylated H4 was plotted as a function of time that the cells were cultured with sodium butyrate and with or without E_2, as determined by scanning the Coomassie Blue-stained gels (data not shown). The results showed that 14.0 ± 2.0 and 11.0 ± 1.0% of H4 (n = 3) was rapidly acetylated in cells incubated without and with E_2, respectively.

The fluorograms were scanned, and the loss of fluorographic intensity from the monoacetylated histone as a function of time was plotted (Fig. 3). The fast rates of acetylation of monoacetylated H4 were similar in cells grown in the presence or absence of E_2 ($t_{1/2}$ = 8 *versus* 7 min, respectively). Additionally, the slow rates of acetylation of monoacetylated H4 were similar for cells grown under E_2-replete and -depleted conditions ($t_{1/2}$ = 380 *versus* 320 min, respectively). Similar results were obtained for H3.2 and H2B. These results show that E_2 does not affect the rates of histone acetylation in T5 cells.

Estradiol Affects the Rate of Histone Deacetylation in T5 Cells—The effect of E_2 on histone deacetylation rates was determined. T5 cells were grown in E_2-depleted conditions for 3 days. Thirty min following the addition of cycloheximide, T5 cells were incubated with 10 mM butyrate, [^{3}H]acetate, and with or without 10 nM E_2 at 37 °C for 2 h. After removal of butyrate, cells were incubated in fresh medium replaced with or without E_2 for 0–240 min to monitor histone deacetylation. A comparison of the fluorograms shown in Fig. 4 (*A* and *B*) revealed that E_2-incubated cells had a slower rate of deacetylation for the core histones. The fluorograms were scanned, and the loss of fluorographic intensity from the tetra-acetylated H4 (Fig. 4*C*) and acetylated H3.2 (Fig. 4*D*) as a function of time was plotted. The rate of deacetylation of tetra-acetylated H4 was rapid, with the intensity of hyperacetylated H4 decreasing significantly after 20 min following the removal of sodium butyrate. The rate of H4-Ac4 deacetylation was appreciably slower in E_2-incubated cells. The rates of H4-Ac4 deacetylation were $t_{1/2}$ = 8 and 3 min for cells cultured with and without E_2,

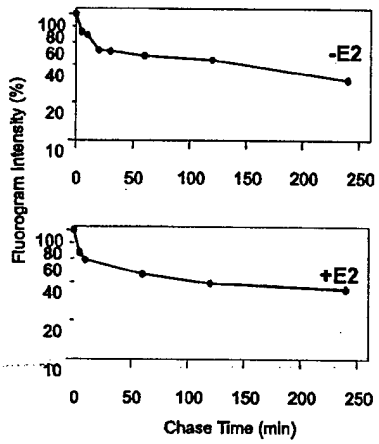

FIG. 3. **Estradiol does not affect the rate of H4 acetylation in T5 cells.** The cells were grown in estrogen-depleted condition for 3 days. T5 cells were pulse-labeled with [^{3}H]acetate for 15 min in the presence or absence of 10 nM E_2 and then chased for 0–240 min in the presence of 10 mM sodium butyrate. The histones were resolved by 15% AUT-PAGE, subsequently stained with Coomassie Blue, and fluorographed. The proportions of total radiolabeled H4 associated with monoacetylated forms (H4-Ac1) were determined from scanning of the fluorograms and plotted as function of chase time in the absence of E_2 (*−E2*) and in the presence of 10 nM E_2 (*+E2*). The proportion of H4-Ac1 label present in total labeled H4 at zero time was arbitrarily set at 100.

respectively. The rate of deacetylation of H3.2 was also significantly reduced in E_2-incubated cells ($t_{1/2}$ = 6 *versus* 3 min in cells without E_2) (Fig. 4*D*).

T5 cells were grown under E_2-replete conditions for 20 min with or without E_2, [^{3}H]acetate, and sodium butyrate to compare the effect of E_2 on the hyperacetylation state of histones in the absence of HDAC activity. Analysis of the fluorogram showed that the levels of hyperacetylated histones were similar in cells grown with and without E_2 (data not shown). These results show that E_2 has an effect on histone deacetylation, but not on histone acetylation, in T5 breast cancer cells.

Estradiol Does Not Affect HDAC Levels or Activity in T5 Cells—The addition of E_2 to T5 cells may result in a decline in HDAC levels and/or HDAC activity. The levels of ER and HDAC in cells incubated with or without E_2 for different times were analyzed by immunoblotting. The conditions for treating the cells were the same as those used in the deacetylation pulse-chase experiments. Fig. 5 shows the immunoblot analyses of cell lysates with antibodies to ER and HDAC1. After 2 h of incubation with E_2 and in the absence of butyrate, ER levels declined. Note that this time period corresponds to cells being incubated for 4 h with E_2 and 4.5 h with cycloheximide. This result is consistent with previous studies reporting that E_2 increases ER degradation rates (22, 23). However, HDAC1 levels were not altered. Identical results were obtained with HDAC2, HDAC3, and HDAC4 (see Fig. 6). Thus, the decrease in histone deacetylation rates is not a consequence of a decline in HDAC levels.

Next we measured HDAC activity in T5 cells incubated with or without E_2. The cells were grown in E_2-depleted medium for 3 days and incubated in the presence or absence of 10 nM E_2 for 20 min. The HDAC activity in the lysates from cells incubated with and without E_2 were identical (data not shown). Thus, E_2 does not have an effect on the HDAC levels and activity in T5 cells.

Estradiol Affects the Subcellular Distribution of ER, but Not HDAC, in T5 Cells—Our studies presented above demonstrated that the E_2-induced reduction in histone deacetylation rates was not a consequence of an alteration in HDAC levels or activity. We tested the idea that E_2 altered the subcellular distribution of HDAC. Cells were lysed in TNM buffer without any detergents to minimize loosely bound nuclear proteins from leaking out of the nuclei. The nuclei were resuspended in TNM buffer with 0.5% Triton X-100 and incubated on ice to release loosely bound nuclear proteins (Triton-S fraction). The resulting pellet contained the tightly bound nuclear proteins, which includes proteins associated with the nuclear matrix (Triton-P).

The distribution of ER in the cell fractions from the cells treated with or without E_2 for 20 min was determined by immunoblot analyses. ER levels in the lysates from cells incubated with and without E_2 did not change (Fig. 6*A*, compare *lane 1* with *lane 6*). Most ER was in the nuclear fraction. However, the cytosol fraction from cells incubated without E_2 had higher levels of ER than did the corresponding fraction from cells incubated with E_2. As ER is located primarily in the nucleus, the ER in cytosol represents ER that was loosely bound in the nucleus. Fractionation of the nuclear proteins into those that were loosely bound from those that were tightly bound revealed a shift in the intranuclear partitioning of ER following the addition of E_2. Comparison of the ER levels in the Triton-S and Triton-P fractions showed that, after 20 min E_2, ER became tightly bound to the nucleus. This observation is agreement with previous reports (10, 15). Further, others and we have demonstrated that the tightly bound form of ER is associated with the nuclear matrix (10, 15).

The distribution of class I HDACs among the cellular fractions was determined by immunoblot analyses with antibodies against human HDAC1, HDAC2, and HDAC3. Fig. 6*A* shows that E_2 had little affect on the fractionation of these HDACs. Most HDAC1 and HDAC2 were present in the nuclei. Triton X-100 released only a small amount of HDAC1 and HDAC2 from the nuclei. In low stringency immunoprecipitation experiments, we found that most HDAC2 was in complex with HDAC1. However, HDAC1 was in excess of HDAC2; thus, a population of HDAC1 is not in complex with HDAC2. Further, we found that both HDAC1 and HDAC2 were associated with the nuclear matrix (data not shown). HDAC3 was also in the nuclear fraction, and approximately half of HDAC3 was associated with the tightly bound nuclear protein fraction. This result agrees with the findings that HDAC1 and -2 exist in different complexes than those that contain HDAC3 (1). HDAC3 was associated with the nuclear matrix (data not shown). In contrast to the class I HDACs, the class II HDAC4 was found exclusively in the loosely bound nuclear protein fraction (Fig. 6). It is possible that the HDAC3 in this fraction is in complex with HDAC4 (24). As expected from the lack of HDAC4 in the Triton-P fraction, HDAC4 was not associated with the nuclear matrix (data not shown). However, as with the class I HDACs, E_2 did not have an effect on the fractionation of HDAC4.

The immunoblot analyses showed the fractionation of several known HDACs. However, the HDAC family of proteins is complex (1). Thus, we measured HDAC activities in the nuclei and nuclear fractions, Triton-S and Triton-P. Fig. 6*B* shows that most nuclear HDAC activity was present in the tightly bound nuclear fraction and that E_2 did not affect the distribution of nuclear HDAC activity.

Estradiol Affects the Subcellular Distribution of Histone Acetyltransferases in T5 Cells—An E_2-induced alteration in the subcellular trafficking of HATs may also change the histone deacetylase rates (see "Discussion"). HAT activity assays were done with cell lysate, cytosol, nuclei, loosely bound, and tightly bound nuclear fractions from T5 cells incubated with and without E_2. Fig. 7*A* shows that the HAT activity in the lysed cell

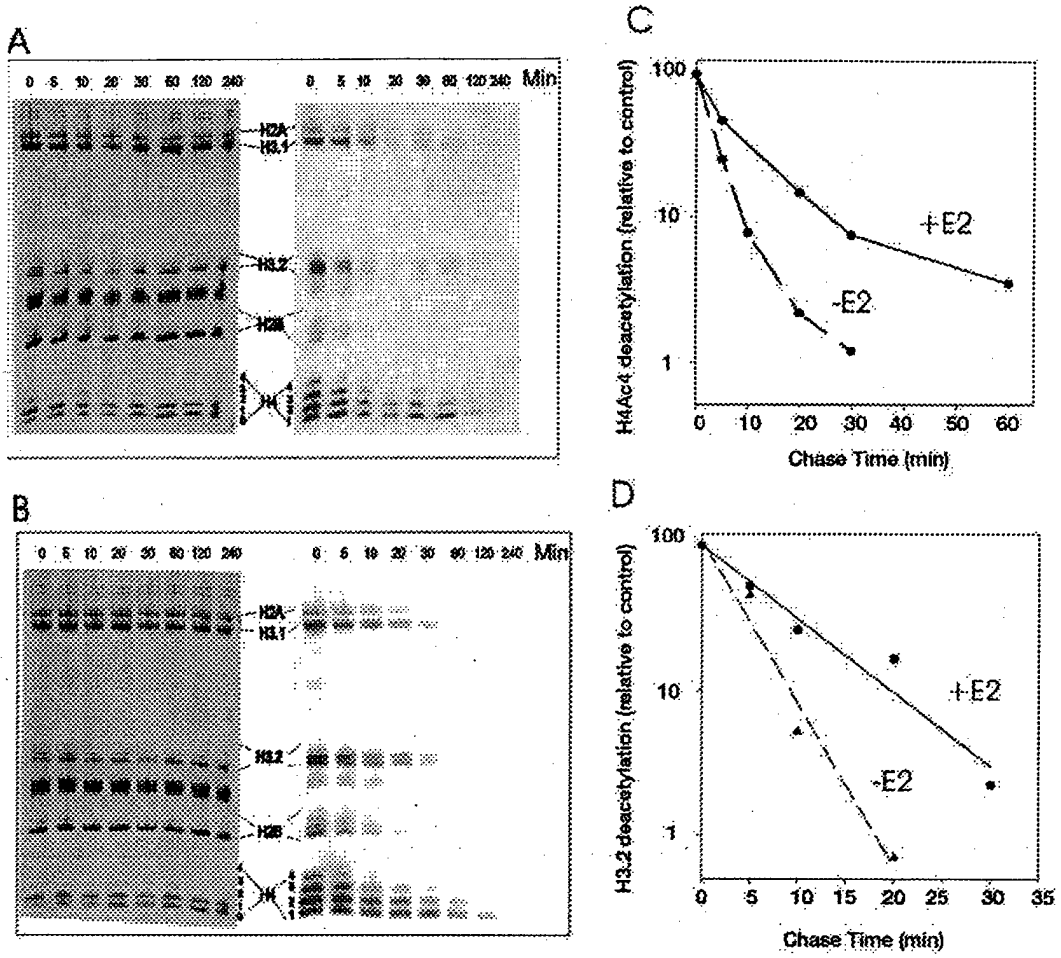

FIG. 4. **Estradiol affects the rate of histone deacetylation in T5 cells.** The cells were incubated with 10 mM sodium butyrate and [^{3}H]acetate in the presence or absence of 10 nM E_2 for 120 min, and then chased for 0–240 min in the absence of butyrate. The histones were resolved by AUT 15% PAGE, subsequently stained with Coomassie Blue, and fluorographed (*−E2, panel A*; *+E2, panel B*). The proportions of total radiolabeled H4 associated with the tetra-acetylated form (H4-Ac4) were determined from scanning of the fluorograms, and plotted as function of chase time in the absence of E_2 (*−E2*) and in the presence of 10 nM E_2 (*+E2*) (*panel C*). The proportion of H4-Ac4 label present in total H4 at zero time was arbitrarily set at 100. *Panel D* shows the total fluorographic intensity of labeled H3.2 as a function of time that cells were chased in the presence or absence of 10 nM E_2. The intensity of H3.2 at zero time was arbitrarily set at 100. The acetylated isoforms of H4 are indicated. *0, 1, 2, 3,* and *4* correspond to un-, mono-, di-, tri-, and tetra-acetylated isoforms, respectively.

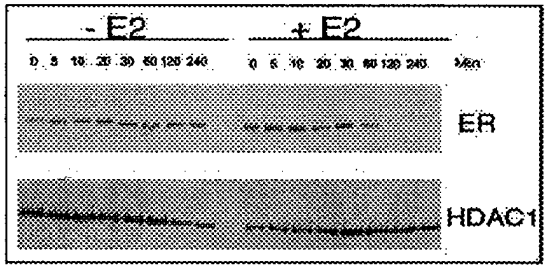

FIG. 5. **Estradiol affects the degradation of the estrogen receptor but not HDAC1 in T5 cells.** T5 cells previously incubated with cycloheximide for 30 min were incubated with 10 mM sodium butyrate, cycloheximide and with or without 10 nM E_2 for 2 h. After butyrate removal, the cells were incubated in the same medium without butyrate for 0–240 min. The cells (0.5×10^6) were lysed in SDS lysis buffer. Equal volumes of cell lysates were loaded on 10% SDS-polyacrylamide gels. The resolved proteins were transferred onto nitrocellulose membranes and immunochemically stained with anti-ERα and anti-HDAC1 antibodies.

fractions from cells treated with or without E_2 did not significantly change. However, the HAT activity of nuclei from cells incubated with E_2 was greater than that of nuclei from cells grown without E_2 (Fig. 7*B*). Fractionation of the nuclear fraction showed both the loosely bound and tightly bound nuclear proteins had HAT activity. However, the tightly bound nuclear proteins demonstrated a differential HAT activity with preparations isolated from cells grown with and without E_2. After 20 min of E_2 incubation, there was an increase in the HAT activity associated with the Triton-P, tightly bound nuclear protein fraction.

Immunoblot analysis with antibodies to known HATs was done with the intent to identify the HAT responsible for the increased activity in the Triton-P fraction of E_2-incubated cells. SRC-1 was located primarily in the nuclear fraction (Fig. 7*C*). Triton X-100 released less SRC-1 from nuclei in cells treated with E_2 than from nuclei of cells treated without E_2 (Fig. 7*C*, compare *lane 4* with *lane 5*, and *lane 9* with *lane 10*). These results with SRC-1 are in agreement with those of Mancini and colleagues (10), who analyzed the effect of E_2 and ER on the subnuclear trafficking of a bioluminescent derivative of SRC-1 in HeLa cells.

The partitioning of SRC-3 (AIB1/RAC3/ACTR) was similar to that of SRC-1, except that SRC-3 was also detected in the cytosol fraction (Fig. 7*C*). Following 20 min of incubation with

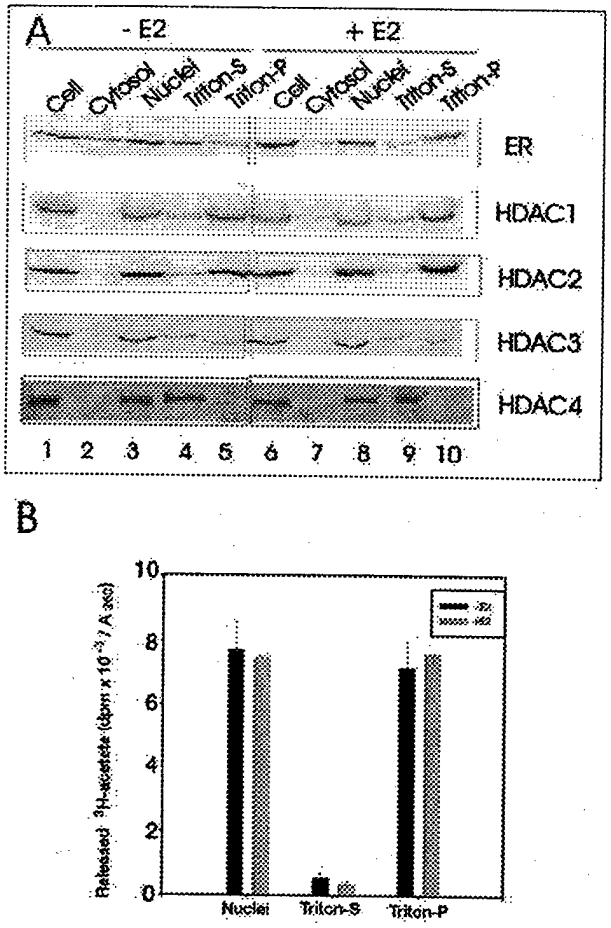

FIG. 6. **Estradiol affects the intranuclear distribution of ER, but not HDAC, in T5 cells.** T5 cells were cultured with or without 10 nM E_2 at 37 °C for 20 min. Equal volumes (10 μl) of cell fractions: cell lysate (*lanes 1* and *6*), cytosol (*lanes 2* and *7*), nuclei (*lanes 3* and *8*), Triton-S (*lanes 4* and *9*), and Triton-P (*lanes 5* and *10*), were loaded onto SDS 10% polyacrylamide gels and transferred to nitrocellulose membranes. Anti-ERα, anti-HDAC1, anti-HDAC2, anti-HDAC3, and anti-HDAC4 antibodies immunochemically stained membranes are shown in *panel A*. Equal volumes (20 μl) of cell fractions were used to do the HDAC enzyme activity assays. *Panel B* shows the HDAC activity in the nuclei, Triton-S, and Triton-P fractions.

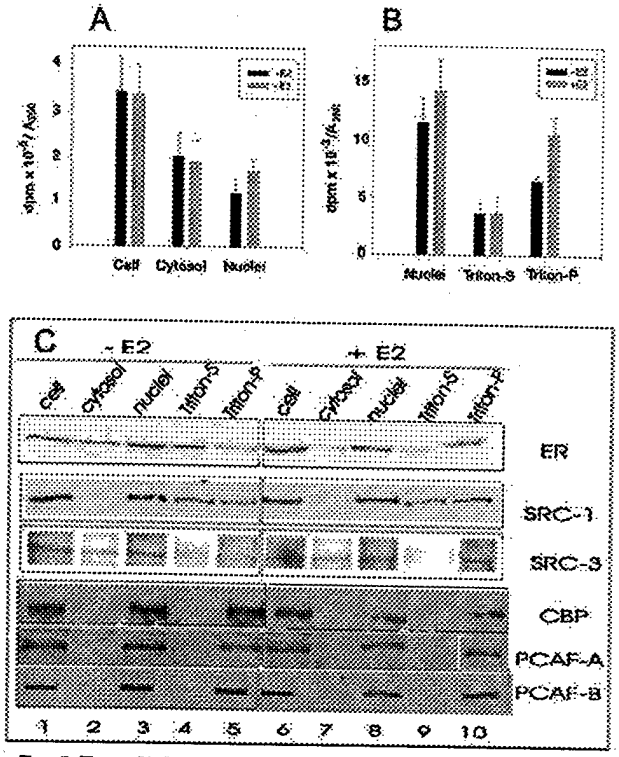

FIG. 7. **Estradiol affects the subcellular distribution of histone acetyltransferases in T5 cells.** Cell fractions were obtained from T5 cells cultured with or without E_2 (37 °C for 20 min). *Panels A* and *B*, equal volumes (20 μl) of cellular fractions were used in the HAT activity assay. *Panel A* shows the HAT activity in cell, cytosol and nuclei fractions. The distribution of HAT activity in nuclei, Triton-S, and Triton-P fractions is shown in *panel B*. *Panel C*, equal volumes (10 μl) of cell fractions, cell lysate (*lanes 1* and *6*), cytosol (*lanes 2* and *7*), nuclei (*lanes 3* and *8*), Triton-S (*lanes 4* and *9*), and Triton-P (*lanes 5* and *10*), were loaded onto 10% SDS-polyacrylamide gels and transferred to nitrocellulose membranes. Antibodies against human ERα, SRC-1, SRC-3, CBP, PCAF-A, and PCAF-B were used to immunochemically stain the membranes.

E_2, there was an increased amount of SRC-3 in the Triton-P fraction.

The effect of E_2 on the subcellular distribution of the HATs CBP, PCAF-A, and PCAF-B (long form of Gcn5; Ref. 25) was also determined. Fig. 7*C* shows that E_2 did not affect the distribution of these HATs among the cellular fractions. Most CBP, PCAF-A, and PCAF-B were present in the tightly bound nuclear protein fraction, suggesting that these transcriptional coactivators/HATs are predominantly associated with the nuclear matrix. Indeed, we observed that these HATs were associated with the nuclear matrix (data not shown). These studies show that E_2 has an effect on the intranuclear distribution of SRC-1 and SRC-3, but not CBP, PCAF-A, and PCAF-B, in T5 cells.

DISCUSSION

Estradiol rapidly elevates the level of acetylated histones in ER-positive, hormone-dependent, but not in ER-negative, hormone-independent breast cancer cells. Our results are in striking contrast to those of Pasqualini *et al.* (16), who observed a decrease in histone acetylation following a 20-min incubation of MCF-7 cells with estradiol. Differences in media conditions, histone isolation procedure, and the addition of a protein synthesis inhibitor during the labeling period may explain the discrepancy in results.

Approximately 60–70% of H4 and H3 were acetylated in human breast cancer T5 cells. These acetylated histones fall into at least three groups: those that are "frozen" in an acetylated state, those that are rapidly acetylated and deacetylated, and those that are slowly acetylated and deacetylated. The latter group comprises the bulk of the dynamically acetylated histones. The rapidly acetylated and deacetylated histones represent ~10% of the dynamically acetylated histones in T5 cells. The rapidity of the effect of E_2 on histone acetylation suggests that histones undergoing rapid acetylation and deacetylation are the population of dynamically acetylated histones being most affected (4).

Our results suggest that E_2 decreased the rates of histone deacetylation, but had no effect on histone acetylation rates, in T5 cells. Analyses of the activities of HDACs and HATs showed that the net activities of either group of enzymes were not affected by E_2. However, biochemical fractionation studies indicated that the intranuclear distribution of HATs, including SRC-1 and SRC-3, were affected by E_2. When presented with E_2, ER rapidly locates to specific nuclear matrix sites, binds to estrogen response elements (EREs), and recruits with it SRC-1 and SRC-3 (10, 12–15) (Fig. 8). As SRC-1 and SRC-3 acetylate primarily H3, other HATs that acetylate the other core histones would also be recruited by ER bound to E_2 to account for

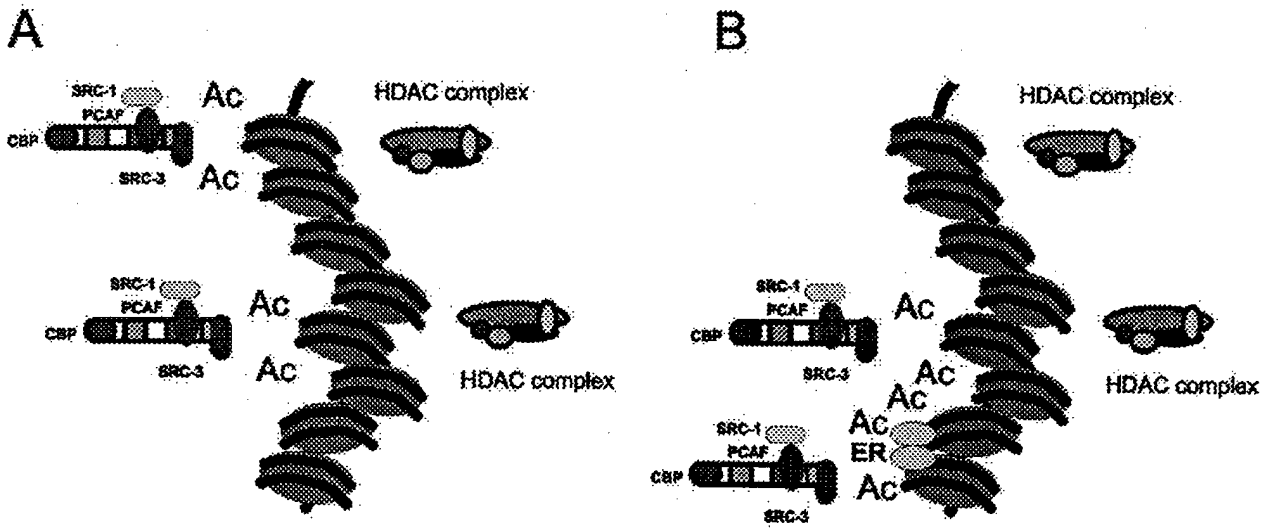

FIG. 8. **Model effect of ER in altering distribution of HATs and histone acetylation in human breast cancer cells.** *A*, in the absence of estradiol, histone acetyltransferases (CBP, SRC-1, SRC-3, PCAF) are located in chromatin regions that also have histone deacetylases (*e.g.* complexes with HDAC1 and 2). Upon addition of estradiol, ER is recruited to nuclear matrix sites and associates with estrogen response elements. Ligand-bound ER recruits histone acetyltransferases away from other nuclear regions and alters the balance of histone acetyltransferases and deacetylases in chromatin regions associated with ER.

the increased acetylation of H2B and H4 that we observe. Elegant studies by the Evans and Brown groups (13, 14) demonstrate that CBP is recruited to EREs. CBP will acetylate the four core histones (3, 26). However, our biochemical fractionation studies were unable to detect E_2-induced intranuclear redistribution of CBP. Possibly, ER and the EREs are recruited to the nuclear matrix sites containing CBP (27).

It is interesting to note that most characterized EREs of breast cancer estrogen-responsive genes have the ERE (½) $(N)_x$ Sp1 (a half-site ERE positioned next to a Sp1 site) motif ERE (28). It has been determined experimentally that there are 1.86×10^5 ER molecules/cell in T5 cells (29). Thus, ER is in far excess to estrogen-responsive genes. The association of Sp1 with ER presents the possibility that Sp1 will recruit ER to Sp1 sites in promoters and enhancers (30). Further, we have found that, as with ER-E_2, Sp1 is associated with the nuclear matrix of T5 cells. It is conceivable that by binding to nuclear matrix site ER when bound to E_2, ER alters the balance of HATs and HDACs and the dynamics of acetylation of histones associated with transcriptionally active and competent chromatin domains.

We have shown previously that HAT and HDAC activities are associated with the nuclear matrix (7, 9, 20). In this study we found that HDAC1, -2, and -3, but not HDAC4, are bound to the nuclear matrix of human breast cancer T5 cells. Further, we observed that the HATs CBP, PCAF-A, and PCAF-B are nuclear matrix-associated, and Mancini and colleagues (10) reported that SRC-1 is bound to this nuclear substructure. We have proposed a model in which nuclear matrix-associated HATs and HDACs mediate a dynamic attachment between transcriptionally active chromatin domains and the nuclear matrix. In support of this model, we recently reported that the dynamically rapidly acetylated and deacetylated histones, referred to as class 1 acetylated histones, are bound to nuclear matrix-associated coding regions of transcriptionally active and competent genes in avian immature erythrocytes (5). Further, we have shown that highly acetylated H3 and H4 are bound to the coding regions of E_2-inducible ER and c-*myc* genes (31). Although the dynamics of the histones associated with these genes were not determined, our work and that of Grunstein's group suggest that these histones are dynamically acetylated by HATs and HDACs (2, 5, 7, 20). We propose that ER bound to E_2 alters the balance of HATs and HDACs at specific nuclear matrix sites, which are associated with transcriptionally active and competent chromatin regions in T5 cells. When bound to E_2, ER would recruit HATs altering the balance of HATs and HDACs at those sites. The HDACs at these sites would be confronted with greater amounts of acetylated histone substrates, requiring a longer time to deacetylate the acetylated histones (Fig. 8). Hence, this may explain the slower rates of deacetylation in cells incubated with E_2 and the increase in the level of dynamically acetylated histones.

Acknowledgment—We are grateful to Dr. Yoshihiro Nakatani (National Institutes of Health, Bethesda, MD) for anti-PCAF A and B antibodies.

REFERENCES

1. Davie, J. R., and Moniwa, M. (2000) *Crit. Rev. Eukaryotic Gene Expression* **10,** 303–325
2. Vogelauer, M., Wu, J., Suka, N., and Grunstein, M. (2000) *Nature* **408,** 495–498
3. Davie, J. R., and Spencer, V. A. (1999) *J. Cell. Biochem.* **32/33,** 141–148
4. Clayton, A. L., Rose, S., Barratt, M. J., and Mahadevan, L. C. (2000) *EMBO J.* **19,** 3714–3726
5. Spencer, V. A., and Davie, J. R. (2001) *J. Biol. Chem.* **276,** 34810–34815
6. Covault, J., and Chalkley, R. (1980) *J. Biol. Chem.* **255,** 9110–9116
7. Hendzel, M. J., Sun, J.-M., Chen, H. Y., Rattner, J. B., and Davie, J. R. (1994) *J. Biol. Chem.* **269,** 22894–22901
8. Sun, J.-M., Chen, H. Y., Moniwa, M., Samuel, S., and Davie, J. R. (1999) *Biochemistry* **38,** 5939–5947
9. Samuel, S. K., Spencer, V. A., Bajno, L., Sun, J.-M., Holth, L. T., Oesterreich, S., and Davie, J. R. (1998) *Cancer Res.* **58,** 3004–3008
10. Stenoien, D. L., Mancini, M. G., Patel, K., Allegretto, E. A., Smith, C. L., and Mancini, M. A. (2000) *Mol. Endocrinol.* **14,** 518–534
11. Stein, G. S., van Wijnen, A. J., Stein, J. L., Lian, J. B., Montecino, M., Choi, J., Zaidi, K., and Javed, A. (2000) *J. Cell Sci.* **113,** 2527–2533
12. Stenoien, D. L., Patel, K., Mancini, M. G., Dutertre, M., Smith, C. L., O'Malley, B. W., and Mancini, M. A. (2001) *Nat. Cell Biol.* **3,** 15–23
13. Chen, H., Lin, R. J., Xie, W., Wilpitz, D., and Evans, R. M. (1999) *Cell* **98,** 675–686
14. Shang, Y., Hu, X., DiRenzo, J., Lazar, M. A., and Brown, M. (2000) *Cell* **103,** 843–852
15. Htun, H., Holth, L. T., Walker, D., Davie, J. R., and Hager, G. L. (1999) *Mol. Biol. Cell* **10,** 471–486
16. Pasqualini, J. R., Mercat, P., and Giambiagi, N. (1989) *Breast Cancer Res. Treat.* **14,** 101–105
17. Spencer, V. A., Coutts, A. S., Samuel, S. K., Murphy, L. C., and Davie, J. R. (1998) *J. Biol. Chem.* **273,** 29093–29097
18. Zhang, D.-E., and Nelson, D. A. (1988) *Biochem. J.* **250,** 233–240
19. Zhang, D.-E., and Nelson, D. A. (1988) *Biochem. J.* **250,** 241–245
20. Hendzel, M. J., Delcuve, G. P., and Davie, J. R. (1991) *J. Biol. Chem.* **266,** 21936–21942
21. Horiuchi, K., Fujimoto, D., Fukushima, M., and Kanai, K. (1981) *Cancer Res.* **41,** 1488–1491

22. Eckert, R. L., Mullick, A., Rorke, E. A., and Katzenellenbogen, B. S. (1984) *Endocrinology* **114**, 629–637
23. Nawaz, Z., Lonard, D. M., Dennis, A. P., Smith, C. L., and O'Malley, B. W. (1999) *Proc. Natl. Acad. Sci. U. S. A.* **96**, 1858–1862
24. Grozinger, C. M., and Schreiber, S. L. (2000) *Proc. Natl. Acad. Sci. U. S. A.* **97**, 7835–7840
25. Schiltz, R. L., and Nakatani, Y. (2000) *Biochim. Biophys. Acta* **1470**, M37–M53
26. Sterner, D. E., and Berger, S. L. (2000) *Microbiol. Mol. Biol. Rev.* **64**, 435–459
27. Thorburn, A., and Knowland, J. (1993) *Biochem. Biophys. Res. Commun.* **191**, 308–313
28. Samudio, I., Vyhlidal, C., Wang, F., Stoner, M., Chen, I., Kladde, M., Barhoumi, R., Burghardt, R., and Safe, S. (2001) *Endocrinology* **142**, 1000–1008
29. Coutts, A. S., Davie, J. R., Dotzlaw, H., and Murphy, L. C. (1996) *J. Cell. Biochem.* **63**, 174–184
30. Porter, W., Saville, B., Hoivik, D., and Safe, S. (1997) *Mol. Endocrinol.* **11**, 1569–1580
31. Sun, J.-M., Chen, H. Y., and Davie, J. R. (2001) *J. Cell. Biochem.* in press

102

Isolation of Proteins Cross-linked to DNA by Cisplatin

Virginia A. Spencer and James R. Davie

1. Introduction

One way of identifying and further characterizing transcription factors is to study their association with DNA *in situ*. Many studies have performed this task using agents such as formaldehyde that crosslink proteins to DNA. However, the treatment of cells with agents such as formaldehyde results in the cross-linking of protein to DNA, and protein to protein. Thus, proteins cross-linked to DNA binding proteins may be misinterpreted as DNA binding proteins. To overcome this obstacle, researchers have focussed their attention on cisplatin (*cis*-DDP; *cis*-platinum (II)diamminedichloride), a cross-linking agent shown to crosslink protein to DNA and not to protein *(1)*. Recent studies have shown that the majority of proteins cross-linked to DNA by cisplatin *in situ* are nuclear matrix proteins *(2–4)*. We have also shown that cisplatin cross-links nuclear matrix-associated transcription factors and cofactors to DNA in the MCF-7 human breast cancer cell line *(5)*. Thus, cisplatin appears to be an effective cross-linking agent for studying the role of transcription factors and nuclear matrix proteins in transcription. In support of this, we have discovered cisplatin DNA-cross-linked nuclear matrix (NM) proteins whose levels vary between well and poorly differentiated human breast cancer cell lines *(6)*. Such changes in protein levels indicate that breast cancer development most likely involves changes in DNA organization, and, likely, changes in transcriptional events. Currently used nuclear matrix protein extraction protocols have been effective in identifying diagnostic NM protein markers for bladder cancer detection *(7)*. Thus, the isolation of cisplatin DNA-cross-linked proteins is a complementary approach to these nuclear matrix extraction protocols, which may also be useful in the detection of additional nuclear matrix proteins for cancer diagnosis.

This chapter provides a detailed description of the isolation of proteins cross-linked to DNA by cisplatin. The method is similar to that previously published by Ferraro and colleagues *(8)*. In addition, this method has been successfully performed on human breast cancer cells and avian erythrocytes. (*See* **Fig. 1**).

2. Materials

All solutions are prepared fresh from analytical grade reagents dissolved in double-distilled water. 1 m*M* Phenylmethylsulfonyl flouride (PMSF) was added to all solu-

From: *The Protein Protocols Handbook, 2nd Edition*
Edited by: J. M. Walker © Humana Press Inc., Totowa, NJ

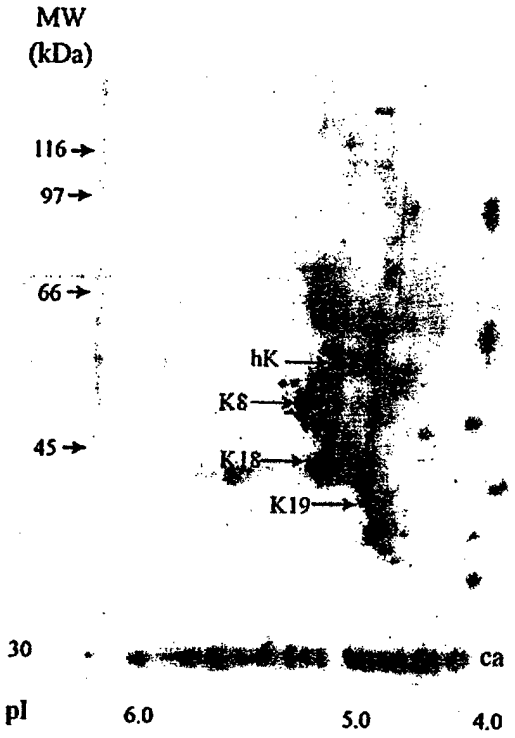

Fig. 1. Two-dimension gel electrophoresis profile of cisplatin DNA-cross-linked proteins. Thirty micrograms of proteins cross-linked to DNA in situ by cisplatin in MCF-7 human breast cancer cells were electrophoretically resolved on a two-dimensional gel, and the gel was stained with silver. K8, K18, and K19 represent cytokeratins 8, 18, and 19, respectively. The transcription factor hnRNPK is designated as hK. The position of the carbamylated forms of carbonic anhydrase is indicated by ca. The position of the molecular weight standards (in thousands) is shown to the left of the gel pattern.

tions immediately before use. With the exception of the cisplatin solution, all solutions are cooled on ice before use.

1. Hanks buffer: 0.2 g KCl (5.4 m*M*), 0.025 g Na_2HPO_4 (0.3 m*M*), 0.03 g KH_2PO_4 (0.4 m*M*), 0.175 g $NaHCO_3$ (4.2 m*M*), 0.07 g $CaCl_2$ (Ann) (1.3 m*M*), 62.5 µL 4 *M* $MgCl_2$ (0.5 m*M*), 0.075 g $MgSO_4$ (0.6 m*M*), 4 g NaCl (137 m*M*), and 0.5 g D-glucose (5.6 m*M*) in 500 mL of double distilled water.
2. Hanks buffer with Na acetate instead of NaCl: Refer to recipe for Hanks buffer except replace the NaCl with 9.3 g sodium acetate (137 m*M*).
3. 1 m*M* Cisplatin Cross-linking Solution: Add 0.003 g of cisplatin (*cis*-platinum (II)-diammine dichloride; Sigma) to 10 mL of Hanks buffer containing sodium acetate instead of NaCl. Cover the solution with foil to protect the cisplatin from the light and stir over gentle heat (approx 40°C) to dissolve the cisplatin. Once the cisplatin is dissolved, keep the solution at room temperature in a foil-covered or amber bottle (*see* **Notes 1–3**).
4. Lysis buffer: Add 150 g urea (5 *M*), 95.5 g guanidine hydrochloride (2 *M*), and 58.5 g NaCl (2 *M*) to 16 mL of 1 *M* KH_2PO_4 and 84 mL of 1 *M* K_2HPO_4 (200 m*M* potassium phosphate buffer, pH 7.5). Stir while heating solution to approx. 50°C to speed up solubi-

lization, make up to 500 mL with double distilled water, and filter solution with 1 *M* Whatman filter (*see* **Note 4**).

5. Hydroxyapatite preparation: Weigh out 1 g of hydroxyapatite Bio-Gel® HTP Gel (Bio-Rad, CA) for every 4 mg of total cellular DNA in the cell lysate, as determined by A_{260} measurements. Place hydroxyapatite into a 30 mL polypropylene tube and pre-equilibrate the hydroxyapatite by suspending the resin in 6 vol of lysis buffer. Gently invert the resin in the lysis buffer to mix, let the resin settle for approx 20 min on ice, then decant the lysis buffer off the hydroxyapatite (*see* **Notes 5,6**).
6. Reverse lysis buffer: Add 3.8 g Thiourea (1 *M*), 9.55 g guanidine hydrochloride (2 *M*), and 5.85 g NaCl (2 *M*), to 1.6 mL 1 *M* KH_2PO_4 and 8.4 mL 1 *M* K_2HPO_4 (200 m*M* potassium phosphate buffer, pH 7.5). Stir while heating solution to approx. 50°C, make up to 50 mL with double distilled water.

3. Methods

3.1. Isolation of Cisplatin DNA-Cross-linked Proteins

1. Rinse 1×10^7 cells in 30 mL of cold Hank's buffer.
2. Centrifuge at 50*g* for 5 min at room temperature.
3. Repeat the rinse two more times.
4. Decant the Hank's buffer from the cell pellet and add 10 mL of 1 m*M* cisplatin solution to the pellet.
5. Incubate at 37°C for 2 h with shaking.
6. Centrifuge at 50*g* for 5 min at room temperature.
7. Resuspend the cell pellet in 10 mL of cold lysis buffer, and store on ice.
8. Measure the A_{260} of 10 µL of the cell lysate and use this value to determine the grams of hydroxyapatite required for DNA isolation (*see* **Notes 6**, **8**, and **9**).
9. Preequilibrate the hydroxyapatite in a 30-mL tube.
10. Transfer the cell lysate into the tube containing the preequilibrated hydroxyapatite, and mix by gentle inversion until all the hydroxyapatite is resuspended.
11. Incubate 1 h at 4°C on an orbitron.
12. Centrifuge at 5000*g* for 5 min at 4°C.
13. Remove the supernatant that contains proteins not cross-linked to DNA.
14. Wash the hydroxyapatite resin with 20 mL of ice-cold lysis buffer by gentle inversion until the resin is completely resuspended.
15. Centrifuge the washed resin at 5000*g* for 5 min at 4°C.
16. Repeat this wash two more times.
17. Add 10 mL of cold reverse lysis buffer to the hydroxyapatite resin.
18. Incubate at 4°C for 2 h on the orbitron to reverse the crosslink between the protein and resin-bound DNA.
19. Centrifuge the hydroxyapatite resin at 5000*g* for 5 min at 4°C.
20. Carefully remove the supernatant and place it in dialysis tubing that has been soaked in distilled water for at least 30 min.
21. Dialyze the protein sample at 4°C against four 2-L changes of double-distilled water over a 24-h period. Include 0.5 m*M* PMSF in the first change of double-distilled water (*see* **Notes 10** and **11**).
22. Transfer the dialyzed solution from the dialysis tubing to a 13-mL centrifuge tube, and freeze at –80°C until the solution is completely frozen.
23. Lyophilize the solution to a dry powder.
24. Resuspend the dry powder in 100 µL of 8 *M* urea and store at –20°C (**Fig. 1**).

4. Notes

1. The conditions for cisplatin cross-linking and protein isolation may vary for other cell types.
2. NaCl is excluded from the cross-linking solution because chloride ions impair the efficiency of the cross-linking reaction by competing with cisplatin for cellular proteins *(9)*.
3. Human breast cancer cells treated with 1 μM cisplatin display a drastic decrease in cell number after 2 h. Thus, a prolonged incubation time (i.e., > 2 h) in the presence of cisplatin may result in the activation of pro-apoptotic proteins involved in protein degradation *(5)*.
4. Filtering the lysis solution with 1M Whatman filter paper will remove particulates that may interfere with A_{260} measurements.
5. Hydroxyapatite is a calcium phosphate resin that binds to the phosphate backbone of DNA.
6. One gram of hydroxyapatite is used for every 4 mg of genomic DNA in the cell lysate, as determined by A_{260} measurements, as this ratio has been shown previously in our laboratory to bind all cellular DNA with approx 100% efficiency (data not shown).
7. Gentle inversion of the hydroxyapatite resin is important to avoid damaging the integrity of the resin.
8. For measuring the A_{260} of the cell lysate, transfer 10 µL of cell lysate into a tube containing 990 µL of lysis buffer.
9. For determining an approximate amount of total cellular DNA within the lysate, the following equation is used.
10. The porosity of the dialysis tubing will depend on the size of the protein of interest.
11. Dialysis tubing should be soaked in distilled water for at least 30 min before use.

$$A_{260} \times 50\ \mu g/mL \times 100 \times 10\ mL/1000\ \mu g/mg\ of\ DNA$$

One A_{260} unit represents 50 mg of DNA/mL of cell lysate; thus the absorbance reading is first multiplied by 50 and then by the dilution factor (i.e., 100) to determine the micrograms of DNA in 1 mL of cell lysate. The resulting value is multiplied by the total volume of cell lysate (i.e., 10 mL) to determine the total micrograms of DNA in the cell lysate and then divided by 1000 to convert this value into milligrams of DNA. The determined amount of cellular DNA is considered only an approximation, as the cell lysate contains some proteins with a peak absorption at 260 nm.

Acknowledgments

Our research was supported by grants from the Medical Research Council of Canada (MT-9186, RO-15183), CancerCare Manitoba, U.S. Army Medical and Materiel Command Breast Cancer Research Program (DAMD17-001-10319), and the National Cancer Institute of Canada (NCIC) with funds from the Canadian Cancer Society. A Medical Research Council of Canada Senior Scientist to J. R. D. and a NCIC Studentship to V. A. S. are gratefully acknowledged.

References

1. Foka, M. and Paoletti, J. (1986) Interaction of *cis*-diamminedichloroplatinum (II) to chromatin. *Biochem. Pharmacol.* **35,** 3283–3291.
2. Davie, J. R., Samuel, S. K., Spencer, V. A., Bajno, L., Sun, J. M., Chen, H. Y., and Holth, L. T. (1998) Nuclear matrix: application to diagnosis of cancer and role in transcription and modulation of chromatin structure. *Gene Ther. Mol. Biol.* **1,** 509–528.

3. Ferraro, A., Eufemi, M., Cervoni, L., Altieri, F., and Turano, C. (1995) DNA–nuclear matrix interactions analyzed by crosslinking reactions in intact nuclei from avian liver. *Acta Biochim. Pol.* **42,** 145–151.
4. Ferraro, A., Cervoni, L., Eufemi, M., Altieri, F., and Turano, C. (1996) A comparison of DNA–protein interactions in intact nuclei from avian liver and erythrocytes: a crosslinking study. *J. Cell. Biochem.* **62,** 495–505.
5. Samuel, S. K., Spencer, V. A., Bajno, L., Sun, J. M., Holth, L. T., Oesterreich, S., and Davie, J. R. (1998) *In situ* crosslinking by cisplatin of nuclear matrix-bound transcription factors to nuclear DNA of human breast cancer cells. *Cancer Res.* **58,** 3004–3008.
6. Spencer, V. A., Samuel, S. K., and Davie, J. R. (2000) Nuclear matrix proteins associated with DNA *in situ* in hormone-dependent and hormone-independent human breast cancer cell lines. *Cancer Res.* **60,** 288–292.
7. Konety, B. R., Nguyen, T. S., Brenes, G., Sholder, A., Lewis, N., Bastacky, S., et al. (2000) Clinical usefulness of the novel marker BLCA-4 for the detection of bladder cancer. *J. Urol.* **164,** 634–639.
8. Ferraro, A., Grandi, P., Eufemi, M., Altieri, F., Cervoni, L., and Turano, C. (1991) The presence of *N*-glycosylated proteins in cell nuclei. *Biochem. Biophys. Res. Commun.* **178,** 1365–1370.
9. Lippard, S. J. (1982) New chemistry of an old molecule: *cis*-$[Pt(NH_3)_2Cl_2]$. *Science* **218,** 1075–1082.

103

Isolation of Proteins Cross-linked to DNA by Formaldehyde

Virginia A. Spencer and James R. Davie

1. Introduction

Formaldehyde is a reversible cross-linker that will cross-link protein to DNA, RNA, or protein *(1)*. Because of its high-resolution (2 Å) cross-linking, formaldehyde is a useful agent to cross-link a DNA binding protein of interest to DNA. For example, formaldehyde has been used to cross-link proteins to DNA in studies fine-mapping the distribution of particular DNA binding proteins along specific DNA sequences *(1,2)*.

When applied to a cell, formaldehyde will initially begin to cross-link protein to DNA. As the time of exposure to formaldehyde increases, proteins become cross-linked to one another. Soluble cellular components become more insoluble as they become cross-linked to one another and to the insoluble cellular material. Sonication is most commonly used to release cross-linked DNA–protein complexes from the insoluble nuclear material. Excessively cross-linking a cell with formaldehyde will cause nuclear DNA cross-linked to protein to become trapped within the insoluble nuclear material. Such an event will protect this cross-linked DNA from breakage by sonication. Moreover, the efficiency of formaldehyde DNA–protein cross-linking varies with cell type *(3)*. Therefore, two parameters must be considered when using formaldehyde as an agent for cross-linking DNA to a protein of interest: the release of DNA from the insoluble nuclear material after cross-linking and the extent of sonication of cross-linked cells. This chapter describes an approach for determining the optimal formaldehyde cross-linking conditions of a cell and for isolating proteins cross-linked to DNA by formaldehyde. (*See* **Fig. 1**).

2. Materials

All solutions are prepared from analytical grade reagents dissolved in double-distilled water. 1 m*M* phenylmethylsulfonyl fluoride (PMSF) was added to all solutions immediately before use. All solutions were cooled on ice before use.

1. RSB buffer: Add 10 mL of 1 *M* Tris-HCl, pH 7.5 (10 m*M*), and 2.5 mL of 4 *M* NaCl (10 m*M*) to approx 800 mL of double-distilled water. Adjust the pH to 7.5 with NaOH then add 0.75 mL of 4 *M* $MgCl_2$ (3 m*M*). Readjust the pH if necessary, then make volume up to 1 L with double-distilled water.

From: *The Protein Protocols Handbook, 2nd Edition*
Edited by: J. M. Walker © Humana Press Inc., Totowa, NJ

2. Hepes buffer: Add 2.38 g of Hepes (10 m*M*), and 2.5 mL of 4 *M* NaCl (10 m*M*) to 800 mL of double-distilled water. Adjust the pH to 7.5 with NaOH then add 0.75 mL of 4 *M* $MgCl_2$ (3 m*M*). Re-adjust the pH if necessary, then make volume up to 1 L with double-distilled water.
3. Lysis buffer: Add 150 g urea (5 *M*), 95.5 g guanidine hydrochloride (2 *M*), and 58.5 g NaCl (2 *M*) to 16 mL of 1 *M* KH_2PO_4 and 84 mL of 1 *M* K_2HPO_4 (200 m*M* potassium phosphate buffer, pH 7.5). Stir while heating solution to approx. 50°C to speed up solubilization, make up to 500 mL with double distilled water, and filter solution with 1 *M* Whatman filter.
4. Dounce homogenizer (for 20-mL sample volume).
5. Hydroxyapatite preparation: Weigh out 1 g of hydroxyapatite Bio-Gel® HTP Gel (Bio-Rad, CA) for every 4 mg of total cellular DNA in the cell lysate, as determined by A_{260} measurements. Place hydroxyapatite into a 30-mL polypropylene tube and preequilibrate the hydroxyapatite by suspending the resin in six volumes of lysis buffer. Gently invert the resin in the lysis buffer to mix, let the resin settle for approx 20 min on ice, and then decant the lysis buffer off the hydroxyapatite.

3. Methods

3.1. Formaldehyde Cross-linking of Immature Chicken Erythrocyte Nuclei

This procedure was performed on immature chicken erythrocytes isolated from adult white Leghorn chickens treated with phenylhydrazine.

1. 2 mL of packed erythrocytes are resuspended in 15 mL of RSB buffer containing 0.25% Nonidet P-40 (NP-40).
2. The cells are homogenized 5× in a Dounce homogenizer and centrifuged at 1500*g* for 10 min at 4°C.
3. **Steps 1** and **2** are performed two more times, leaving a pellet of nuclei.
4. The nuclei are resuspended in HEPES buffer to an A_{260} of 20 U/mL (*see* **Note 1**).
5. Formaldehyde is then added to the suspension of nuclei to a final concentration of 1% (v/v).
6. The nuclei are mixed gently by inversion, and incubated for up to 15 min at room temperature.
7. After 0, 5, 10, and 15 min of formaldehyde cross-linking, 4-mL aliquots of nuclei are collected and made up to 125 m*M* glycine on ice to stop the cross-linking reaction.
8. The aliquots of nuclei are then centrifuged at 1500*g* for 10 min at 4°C (*see* **Note 2**).
9. The nuclear pellets are then washed in 10 mL of RSB buffer and centrifuged at 1500*g* for 10 min at 4°C.
10. The nuclear pellets are resuspended in 10 mL of ice-cold lysis buffer.

3.2. Sonication of Formaldehyde-Cross-linked Cells

For each formaldehyde-cross-linked sample from **Subheading 3.1.**:

1. The 4 mL of the lysed nuclei are transferred to a 50-mL Falcon tube and sonicated under 170 W for ten 30-s pulses with a Braun-sonic 1510 Sonicator. The sample is cooled on ice for 1-min waiting intervals between each pulse (*see* **Notes 3–5**).
2. A 100-µL aliquot of nuclei is dialyzed against double-distilled water (without PMSF) overnight at 4°C to remove excess urea and salt that may interfere with proteinase K digestion. The dialyzed sample is made to 0.5% sodium dodecyl sulfate (SDS) and 0.4 mg/mL of proteinase K and incubated for 2 h at 55°C to digest the protein.
3. The sample is then incubated at 65°C for 6 h to reverse the formaldehyde cross-links between the DNA and protein.

4. The digested mixture is extracted 3× with an equal volume of solution composed of phenol–chloroform–isoamyl alcohol in a 25:24:1 ratio, respectively.
5. To precipitate the DNA from the sample, 1/10th the sample volume of 3 *M* sodium acetate, pH 5.5, along with three volumes of absolute ethanol is added to the sample and the sample is incubated at –80°C for 20 min.
6. The sample is centrifuged at 12,000*g* for 10 min at 4°C to pellet the DNA.
7. The DNA pellet is washed with 1 mL of ice-cold 70% ethanol, and centrifuged at 12,000*g* for 10 min at 4°C.
8. The resulting DNA pellet is resuspended in 30 µL of double-distilled water, and 4 µL of this pellet is electrophoresed on a 0.8% agarose gel to identify high molecular weight DNA bands indicative of extensive cross-linking.

3.3. Efficiency of Solubilization of Formaldehyde-Cross-linked Cells

For each formaldehyde-cross-linked sample from **Subheading 3.1.**:

1. Transfer the 4 mL of cross-linked, lysed, and sonicated nuclei to a 15-mL tube.
2. Determine the A_{260} of 10 µL of the total nuclear lysate.
3. Centrifuge the sample at 9000*g* for 10 min at 4°C.
4. The supernatant contains solubilized DNA and protein. Transfer the supernatant to a clean 15-mL tube.
5. Determine the A_{260} of 10 µL of the supernatant in 990 µL of lysis buffer.
6. Divide the A_{260} of the supernatant by the A_{260} of the total nuclear lysate and multiply this value by 100 to determine the percent of DNA released from the nuclei following formaldehyde cross-link and sonication.

3.4. Isolation of Proteins Cross-linked to DNA by Formaldehyde

For each formaldehyde-cross-linked sample from **Subheading 3.1.**:

1. Determine the approximate amount of DNA present in the 4 mL of lysed nuclei suspension from **Subheading 3.3.**
2. Add the lysed nuclei suspension to preequilibrated hydroxyapatite (*see* **Notes 6–8**) and mix by gentle inversion.
3. Incubate at 4°C for 1 h on an orbitron.
4. Centrifuge the hydroxyapatite at 5000*g* for 5 min at 4°C.
5. Wash the hydroxyapatite with 10 mL of lysis buffer, mix by gentle inversion, and centrifuge at 5000*g* for 5 min at 4°C.
6. Repeat **step 4** an additional two times.
7. Add 2 mL of lysis buffer to the washed hydroxyapatite and mix by gentle inversion.
8. Incubate this suspension at 68°C for 6 h to reverse the formaldehyde cross-links between the DNA and protein.
9. Centrifuge the sample at 4°C or room temperature for 5 min at 5000*g*.
10. Place the supernatant containing protein that was cross-linked to DNA into presoaked dialysis tubing (*see* **Notes 10** and **11**).
11. Dialyze the sample overnight at 4°C against 2–3-L changes of double-distilled water (include 0.5 m*M* PMSF in the first change).
12. Lyophilize the sample to a powder form.
13. Resuspend the powder in double distilled water and store at –20°C (*see* **Fig. 1**).

4. Notes

1. Sonication conditions will vary for different cell types.
2. Perform sonication on ice to avoid protein denaturation.

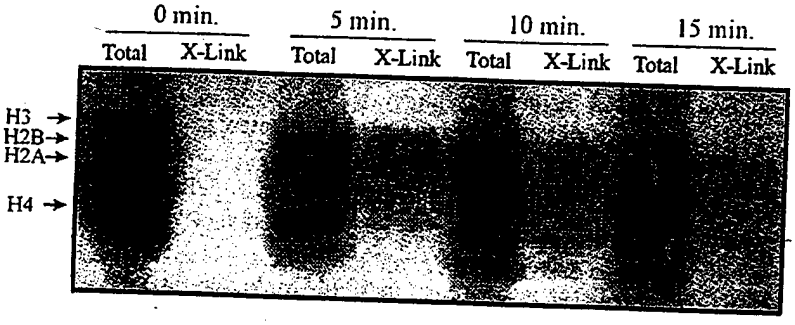

Fig. 1. Sodium dodecyl sulfate-polyacrylamide gel electrophoresis (SDS-PAGE) of total cellular proteins and formaldehyde-DNA-crosslinked proteins. Formaldehyde-crosslinked nuclei were separated into two fractions of equal volume. One fraction was crosslinked with formaldehyde for 0, 5, 10, and 15 min, and the DNA-crosslinked proteins were isolated by hydroxyapatite chromatography, dialyzed against double-distilled water, lyophilized to a powder form, and made up to a final volume of 200 µL with double-distilled water. The other fraction was lysed, dialyzed, lyophilized to a powder form, and made up to a final volume of 1 mL with double-distilled water. Equal volumes of total nuclear protein were loaded onto a 15% SDS-PAGE gel for each treatment. In addition, equal volumes of DNA-crosslinked proteins were loaded onto the same gel for each treatment. The gel was electrophoresed at 170 V for 70 min at room temperature, stained with Coomassie Blue overnight, and then destained. H3, H2B, H2A, and H4 represent histones H3, H2B, H2A, and H4, respectively.

3. The extent of sonication depends on the length of the target DNA sequence. For example, if the association of a protein with a specific 1000-basepair region needs to be determined, then the DNA should be sonicated to 500 basepairs to avoid the immunoprecipitation of DNA sequences surrounding the target region (*see* **ref. 4** for further explanation). However, if one is simply trying to determine if a protein of interest is associated with DNA, then the formaldehyde-cross-linked cells need only be sonicated to an extent that allows the efficient release of nuclear DNA from the insoluble nuclear material (*see* **Note 5**).
4. Formaldehyde reacts with amine groups of proteins. Thus, to ensure a high efficiency of cross-linking, it is important to resuspend the nuclei in a HEPES buffer before treatment with formaldehyde.
5. The duration of formaldehyde cross-linking will vary according to cell type, cell treatment, and the degree to which the DNA associated with the nuclear material can be solubilized. For example, the sonication and subsequent centrifugation of a nuclear lysate may result in the solubilization of only 80% of total nuclear DNA. The acceptability of this percentage of DNA release from the nucleus depends on the location of the protein of interest. If the target protein is tightly associated with DNA that is associated with the nuclear matrix, the fraction of solubilized DNA–protein complexes may be somewhat depleted of the target protein even though as much as 80% of the nuclear DNA is released from the insoluble material.
6. Hydroxyapatite is a calcium phosphate resin that binds to the phosphate backbone of DNA.
7. A ratio of 1 g of hydroxyapatite for every 4 mg of genomic DNA has been shown in our lab to bind all cellular DNA with 100% efficiency (data not shown).
8. The following equation can be used to determine the approximate amount of DNA within the cell lysate:

$$A_{260} \times 50\ \mu g/mL \times 100 \times (\text{volume of cell lysate})/1000\ \mu g/mg \text{ of DNA}$$

One A_{260} unit represents 50 mg of DNA/mL of cell lysate. To determine the micrograms of DNA in 1 mL of cell lysate, multiply the absorbance reading by 50 and then by the dilution factor (i.e., 100). Multiply the resulting concentration by the total volume of cell lysate to determine the total mg of DNA in the cell lysate. Divide the total micrograms by 1000 to convert this value into milligrams of DNA. The resulting amount of cellular DNA is only an approximation, as some proteins within the cell lysate will have a peak absorption at 260 nm.

9. Gently inverting the hydroxyapatite resin when mixing avoids damaging the integrity of the resin.
10. The porosity of the dialysis tubing will depend on the size of the protein of interest.
11. Dialysis tubing should be soaked in distilled water for at least 30 min before use.

Acknowledgments

Our research was supported by grants from the Medical Research Council of Canada (MT-9186, RO-15183), CancerCare Manitoba, U.S. Army Medical and Materiel Command Breast Cancer Research Program (DAMD17-001-10319), and the National Cancer Institute of Canada (NCIC) with funds from the Canadian Cancer Society. A Medical Research Council of Canada Senior Scientist to J. R. D. and a NCIC Studentship to V. A. S. are gratefully acknowledged.

References

1. Orlando, V. (2000) Mapping chromosomal proteins by in vivo formaldehyde-crosslinked-chromatin immunoprecipitation. *Trends Biochem. Sci.* **25,** 99–104.
2. Dedon, P. C., Soults, J. A., Allis, C. D., and Gorovsky, M. A. (1991) A simplified formaldehyde fixation and immunoprecipitation technique for studying protein-DNA interactions. *Analyt. Biochem.* **197,** 83–90.
3. Orlando, V., Strutt H., and Paro, R. (1997) Analysis of chromatin structure by in vivo formaldehyde crosslinking. *Methods* **11,** 205–214.
4. Kadosh, D. and Struhl, K. (1998) Targeted recruitment of the Sin3-Rpd3 histone deacetylase complex generates a highly localized domain of repressed chromatin in vivo. *Mol. Cell. Biol.* **18,** 5121–5127.